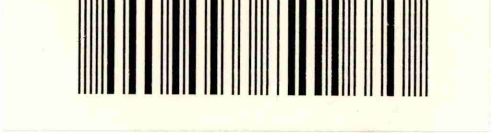

15/4 19:01
16/4 18:50

Evaluation of Solvatochromic Materials as Sensor Components

Xiaoming Liu

A thesis submitted in partial fulfilment of the
requirements of
Sheffield Hallam University
for the degree of Doctor of Philosophy

June 1994

Collaborating Organisation: Health and Safety Executive

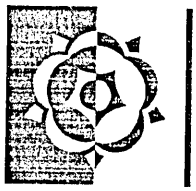

Sheffield Hallam University

Abstract

Sensors play an important role in industry and in academic research for measurement of various chemical and physical parameters in a variety of environments.

Optical materials, whose properties (e.g. absorption, colour) change on interaction with a target analyte, are very useful for sensor applications. Among organic optical materials, there is a class showing electrochromic or solvatochromic properties, which have potential to be used as sensor materials.

Normally, organic compounds, with electrochromic or solvatochromic properties, have a conjugated system linking donor and acceptor groups in the molecule. During excitation by a field (electric or light), an intramolecular charge transfer takes place resulting in an excited state with different dipole moment to the ground state. A number of such dye compounds have been synthesised in this work, some of them show considerable electrochromism or solvatochromism, such as 3-ethyl-5-{[1-dodecyl-2(1H)-pyridylidene]-ethylidene}-rhodanine. Its absorption maxima are 524 nm in acetonitrile and 584 nm in ether, having a 60 nm shift. It was found that solvatochromism of such compounds was increased with the increase of the chain length of their conjugated system.

The conjugated compounds synthesised were deposited onto a transparent substrate either by solution evaporation or by Langmuir-Blodgett film technology. The films formed did respond to some toxic gases such as NO_2, resulting in an absorption wavelength shift in their uv-vis spectra.

Pyridinium N-phenoxide betaine dyes are known as good probes for solvent polarity. The best example is ET(30). ET(30) values have been widely used for polarity measurement of solvents.

In order to covalently link these betaine dyes to a solid support for convenience of use, a number of dyes with a functional amino group have been synthesised. This amino group forms the basis for linkage. Additionally, modifications were made to the phenoxide end of the molecule to reduce the phenolate pKa. Dichloro and difluoro variations from the parent diphenyl structure were made.

Several methods have been used to try to covalently immobilise the betaine dyes synthesised onto a solid support. Some of them have been successfully immobilised onto a silica sorbent by a thiourea linkage or an amide linkage. Immobilised dyes showed reduced but still good solvatochromism. Their ET values demonstrated linear correlation with standard ET(30) values.

I would like to dedicate this thesis to my wife, Yi Zhao

and my daughter, Jingmei Liu

Acknowledgements

I would like to express my many thanks to Dr. D. Crowther, the director of my PhD study, for his help and encouragement throughout the course of this research work.

I should thank Dr. A. Hewson, the supervisor of my PhD study, too. He gave me a lot of advice and helpful suggestions in my synthesis work.

Many thank to the technicians and secretaries in the Division of Chemistry of this university. They gave me help and encouragement during the period of my study.

Finally, I should thank the School of Science of this university for awarding me a scholarship to undertake this research programme.

Contents

Chapter 5

Immobilisation of the conjugated compounds synthesised on solid surface by physical adsorption or by Langmuir-Blodgett film technology and investigation of their optical response to some toxic gases

1.1 Sensors

A sensor is an element which can provide information about our physical, chemical, and biological environment.[1] Sensors have a wide range of applications to the measurement of physical, chemical and biological quantities. For example, some interesting applications are a). pH measurement, b). the measurement of liquid ionic species, c). hazardous gas detection, and d). the measurement of temperature, pressure and other physical quantities.[2]

From the viewpoint of chemistry, a chemical sensor can be thought of as "a transducer which provides direct information about the chemical composition of its environment".[3] Chemical sensors have been classified through four fundamental transduction modes,[3] i.e., thermal, mass, electrochemical and optical.

1. Thermal sensors

Heat is a general property of any chemical reaction. As such it should be an ideal physical parameter to use for sensing. A thermal sensor for humidity based on the changes of heat conductivity of TaN thin film was studied by Shioyama[4] and an integrated thermal sensor for glucose using the temperature dependence of the output of the Darlington amplifier has been constructed.[5]

2. Mass sensors

The measurement of change of mass as the means of chemical sensing is almost as universal as is the measurement of reaction heat. In principle, it is applicable to any reactions in which there is a net change of mass which, by

definition, leaves out most of the selective catalytic reactions including the enzymatic ones.[3]

There are two types of mass change chemical sensors: those based on piezoelectric bulk oscillators (quartz is the most common material used for the bulk oscillators, e.g. quartz crystal microbalance QCM), and those based on surface acoustic wave (SAW). Two stories have dominated the development of mass sensors: the possibility of their use for general chemical sensing in the liquid phase, and immunochemically produced selectivity in the gas phase. The focus of development of mass sensors for gas applications is on the selective layer. Coatings on SAW or QCM devices aimed at sensing individual gas species which have been studied, include those for carbon dioxide,[6] hydrogen sulphide,[7] sulphur dioxide,[8] and nitrogen dioxide.[9] The QCM devices have been extensively used as supplementary tools in several areas of solution physical chemistry.[10]

3. Electrochemical sensors

In electrochemical sensors the response is derived from the interaction between chemistry and electricity. Thus potentiometric sensors are based on measurement of cell voltage, amperometric sensors on measurement of cell current, and conductometric sensors on measurement of cell admittance. Some reviews which compare potentiometric and amperometric sensors in terms of their performance and limitations have been published.[11,12] Advantages of gas-membrane electrochemical sensors[13] and high temperature oxygen sensors[14] using either of the three modes of measurement have also been discussed.

4. Optical sensors

Optical sensors have become a very active research area recently. Janata thought that "the most overwhelming immediate impression that one gets when

browsing through the file on optical sensors is that they can do anything and everything".[15] Three principal reasons for the recent enthusiasm for optical sensors were suggested by Janata and Bezegh.[3] The first is the availability of optical hardware which in most cases can be readily adopted for chemical sensing. The second is that they can draw on an enormous amount of knowledge which exists in optical spectroscopy and which is usually readily transformable to remote optical sensing. The third is the safety of their operation.

There are many types of optical sensors, including ionic sensors, gas sensors, and biosensors. In the liquid phase, there are a growing number of reports of optical sensors for sensing of ionic species. They are based either on measurement of absorbance,[16] fluorescence,[17] or reflectance.[18] A number of papers describe development of an optical pH sensor for the normal pH range,[19,20] for high acidities,[21] and for measurement of pH in gastric juices.[22] Optical sensors for detection of water in organic solvents based on measurement of absorbance have been developed.[23] The detection of organic solvents (above 30 ppm) in water is possible with a triphenylmethane dye optical sensor.[24] Many papers have been published describing the applications of optical sensors in gas sensing, for example, reviews[25,26] of fluorescence sensors for oxygen, optical sensors for nitrogen oxides based on phthalocyanine,[27] and measurement of multiple species, O_2 and CO_2[28] or O_2 and NH_3[29] by using of different wavelengths.

1.2 Organic Materials for sensors

No matter what types of sensor is used, or what equipment is used with the device, they all have a sensing element. This sensing element is in most cases, some kind of organic material.

There are many types of organic molecules which can be used as a sensor element, one useful class being those which also show nonlinear optical properties.

1.2.1. Organic materials with nonlinear optical properties

When a molecule is placed in an external electromagnetic field, the electron density in different parts of the molecule will be changed. In this case, the molecule is known as being polarised, which results in a redistribution of molecular electron density. This redistribution of molecular electron density will result in changing its dipole moment, μ. The dipole moment μ can be expressed in terms of the permanent, ground-state dipole moment (in the absence of a field), μ_g, and the applied field E by equation (1) in one dimension case.[30,31]

$$\mu = \mu_g + \alpha E + \beta E^2 + \gamma E^3 + \ldots\ldots \qquad (1)$$

$$\text{or} \qquad \mu - \mu_g = \alpha E + \beta E^2 + \gamma E^3 + \ldots\ldots$$

$\mu - \mu_g$ is known as induced dipole moment. The coefficients of E, --- α, β, γ etc. are in turn called the first-order (or linear), second-order, third-order, and higher polarisabilities of the molecule. It is these second-order and higher terms, or called "nonlinear" terms, that give rise to a number of interesting optical effects in the field of "nonlinear optics." For example, second harmonic generation (SHG; i.e., doubling the frequency of laser radiation) is related to second-order polarisabilities β.

In practice, the situation is not one-dimension, thus, equation (1) becomes tensorial and α_{ij} is a first-rank tensor, β_{ijk} is a second-rank tensor, etc.:

$$\mu_i = (\mu_g)_i + \alpha_{ij}E_j + \beta_{ijk}E_jE_k + \gamma_{ijkl}E_jE_kE_l + \ldots \qquad (2)$$

Organic molecular materials which possess nonlinear optical properties (NLO) are attracting considerable interest due to their potential applications in many fields of modern technology, such as optical communications and optical signal processing, certainly including sensors.

Historically, inorganic single crystals, such as potassium dihydrogen phosphate (KDP) and lithium niobate ($LiNbO_3$), played a significant role in nonlinear optical (NLO) applications. Although many nonlinear optical effects have been found in inorganic compounds, such as frequency doubling in KDP, they have a serious drawback. Inorganic single crystals are comprised of positive and negative ions which can be considered as building blocks for NLO materials. These ions have relatively large masses and are bound to a particular region of the crystal, therefore, ionic lattice deformation are relatively slow and restricted to definite distance when they respond to certain field changes. However, organic materials, consisting of molecular building blocks incorporating conjugated π electron systems, could provide better nonlinear properties than the inorganic compounds. Firstly, the charges to be displaced in such organic systems are electrons with very small masses; secondly, the conjugated π electron system would allow large electron displacements. Combining these two features, large polarisation are expected, being able to follow very rapidly oscillating electric (optical) fields. Thirdly, organic chemistry allows the synthesis of molecules optimised for nonlinear applications.[32]

Mohlmann[32] studied NLO (second order) organic materials and suggested that they could be divided into the following forms:

1) Single crystal

A number of organic single crystals which exhibit considerable optical nonlinear effects have been found, such as urea and 2-methyl-4-nitro-aniline (MNA). As only those organic single crystals which have a non-centrosymmetric (n.c.s) structure can exhibit this feature,[33] so the number of organic crystals which have useful NLO properties are limited. Also, single crystals are not easily processed, as well as which the growth and shaping of crystals of sufficient optical quality is difficult.

2) Langmuir-Blodgett (L-B) films

The Langmuir-Blodgett technique enables us to orientate molecules in a non-centrosymmetric (n.c.s) fashion, therefore relatively large areas of NLO materials can be achieved by transferring monolayers of suitable organic molecules from the surface of a liquid onto a suitable substrate. A high degree of polar order (n.c.s) can be obtained spontaneously in the deposited layer by means of using appropriately substituted molecules.

However, the main limitation on the Langmuir-Blodgett technique at the moment is the difficulty of building up thick multilayers of sufficient quality. If the L-B film is used as the waveguide, even for monomode waveguide, guiding layers of the order of 1 micron thickness are required, corresponding to about 500 or more monolayers.[32]

3) Polymeric solid solution

In order to overcome the drawback of Langmuir-Blodgett technique mentioned above, nonlinear polymers can be deposited via spincoating or dipping

techniques, when the required thickness can be easily obtained. One of methods used is to dissolve a polymer host , together with optically nonlinear guest polymer, in a proper solvent, then the solution is deposited onto a suitable substrate. The solvent is evaporated by the spinning or dipping step and a smooth film is obtained. The film thickness generated depends on the speed of spinning or dipping, on the concentration of the solution, as well as on the type of substrate.

Conjugated organic molecules show a very large optical response in an external field.[34] Virtually, all organic nonlinear optical (NLO) molecules contain π bonds such as the single short polar π bond of the carbonyl as in the urea or a more extended series of π bonds as in the benzene and substituted benzene derivatives. Many of these conjugated organic molecules with π electron systems have solvatochromic or electrochromic properties, which are very useful in sensor applications.

1.2.2. Electrochromism and solvatochromism

The position and the intensity of absorption and emission spectra of conjugated organic molecules can be influenced greatly upon application of a strong electric field.[35] Significant changes in the position of electronic bands (chromatic effects) are mainly due to the dipole moment of the molecule in the ground state and the change in the dipole moment during the excitation process. Pronounced changes in intensity of electronic bands are due to the electric field dependence of the transition moment.

This effect of an external electric field on the optical absorption or emission spectra of some organic compounds could be called "electrochromism",

in a similar way to "thermochromism" and "photochromism" which describe changes of absorption or emission spectra produced by heat and by light.

The solvent, as a medium for chemical and physical processes, has always played a very important role in chemistry. It has been found that the absorption and emission spectra of some substances, especially some organic dyes, can be shifted significantly by certain solvents. Liptay[36] studied these phenomena and suggested the following viewpoints.

In any solution, molecules having a permanent dipole moment are located in an electric field, the reaction field of the dissolved molecule, as showed in Fig. 1-1.

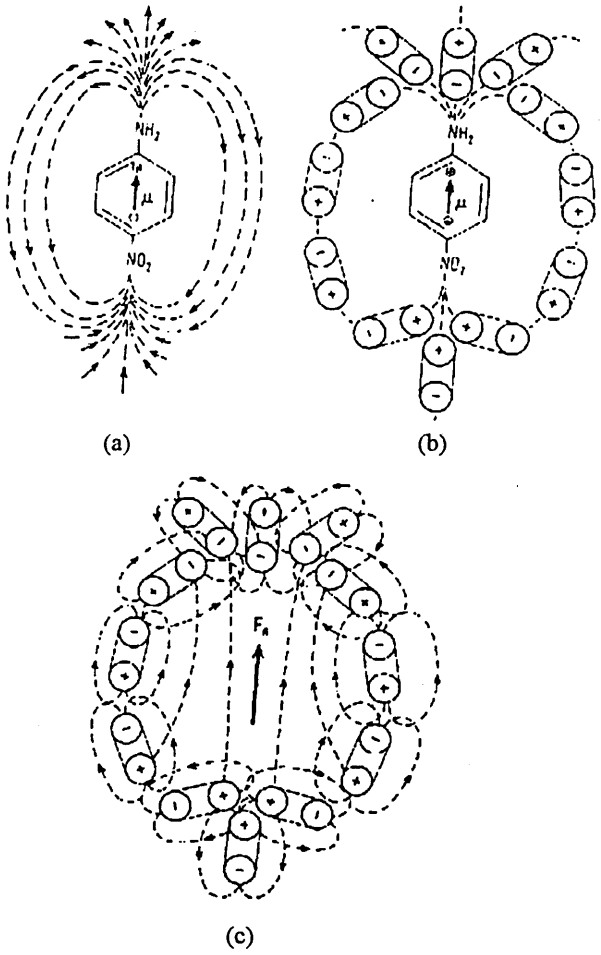

Fig. 1-1. Reaction field of a dissolved molecule

(a) A gas state molecule such as p-nitroaniline, with a dipole moment μ, causes an electric dipole field in its environment, the field lines of which are showed broken.

(b) In solution, this dipole field acts on the surrounding solvent molecules. If the solvent molecules have a permanent dipole moment, they orient themselves with their dipole moment as nearly as possible parallel to the field lines. The orientation is opposed by thermal motion, so that only some of the solvent molecules are ideally oriented at any time. If solvent molecules have no permanent dipole moment, an induced dipole moment is produced by the dipole field of the dissolved molecule. In the case of solvent molecules having a permanent dipole moment, the polarizability effect is superimposed on the orientation effect.

(c) If the electronic and nuclear configurations of all the solvent molecules are imagined to be frozen and the dissolved molecule then removed, a cavity surrounded by solvent molecules remains. Each of these solvent molecules has a dipole moment, which is made up from the permanent and the induced dipole moment. Each of the dipole moments of the solvent molecules produces a dipole field in its environment, the field lines of which are showed broken. In the cavity, at the position of the dissolved molecule, the dipole field of the solvent molecules superimpose and produce a field having the same direction as the dipole moment of the original dissolved molecule; this field is known as the reaction field FR. If the dissolved molecule is now imagined to be back in the cavity, it is clearly in an electric field.

The reaction field acts on the dissolved molecule in the same way as an external electric field, that is, it is capable of causing a band shift and a change in the transition moment, and hence in the intensity of the band.

This effect (solvent-dependence of the position and intensity of electronic bands) could be called "solvatochromism". Actually, it is a particular electrochromic phenomenon.

In analogy to solvatochromism, all gases can be thought of as gaseous solvent. They also can produce more or less the same effect on a conjugated organic molecule as solvents. Gas molecules having a permanent dipole moment should have a stronger such effect than those having no permanent dipole moment.

On the basis of these considerations, it is proposed to study the properties of some electrochromic or solvatochromic materials as possible components for gas phase and liquid phase chemical sensors.

1.2.3. Electrochromic materials and their applications

Electrochromic and solvatochromic effects are expected in conjugated organic compounds of the dipolar linear-chain type. Three types of organic dyes with good electrochromism and solvatochromism are introduced here. They have been used for this work.

1. Organic dye materials

a). Merocyanine dyes

This class of organic dyes was firstly studied by Brooker and his co-workers.[37] Their spectra and excited states can often be shifted significantly by solvent and polarisation effects.

Since a portion of the molecule of one of these dyes is identical with that present in a cyanine, the general name "merocyanine" was used for them. Normally, the structures of the merocyanine compounds may be expressed by two extreme resonance structures. One is the following uncharged type:

$$O{=}CH{-}CH{=}CH{-}\cdots{-}CH{=}CH{-}NH_2 \qquad (I)$$

The other can be written with a dipolar-ionic zwitterionic structure,

$$^{-}O{-}CH{=}CH{-}CH{=}\cdots{=}CH{-}CH{=}NH_2^{+} \qquad (II)$$

Generally, it is thought that the dipolar structure (II) is of higher energy because of charge separation, which has been confirmed from experiments by Brooker, et al..[37]

Platt[35] studied this type of organic dyes and proposed that in a given solvent, the formula for the spectral energy E of the maximum wavelength absorption peak (first absorption peak) of the organic dyes is

$$E^2=E_I^2+(b_L-b_R)^2 \qquad (3)$$

Where E_I is the spectral energy of the isoenergetic wavelength of a given chain length, and b_L and b_R are the basicities of the terminal groups on the left and right ends of the chain, expressed in energy units. The difference (b_L-b_R) measures quantitatively the stabilisation of one of the two extreme resonance structures relative to the other.

In a series of different solvents having different polarities, the (b_L-b_R) value of some of these dyes can be changed essentially and continuously from a negative value in a nonpolar solvent through a zero value to a positive value in a

polar solvent. As showed by Eq.(3), the peak wavelength of a absorption or emission is then shifted from a short wavelength (high energy) in nonpolar solvents to progressively longer wavelength until it reaches the isoenergetic wavelength and energy E_I where (b_L-b_R) is zero, and then it is shifted back toward short wavelength again in the polar solvents. In those molecules that are fluorescent, the emission peak should be at slightly longer wavelength than the absorption peak and should shift correspondingly.

b). Betaine dyes

Another important class of organic dyes is so-called Reichardt's betaine dyes. Their basic structure is shown in Fig. 1-2 as below.

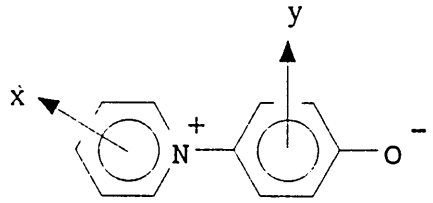

Fig. 1-2 Basic structure of the betaine dyes

The best known example among these dyes is 2,6-diphenyl-4-(2,4,6-triphenyl-N-pyridinio)-phenolate (known as ET-30).[38,39,40] Its structure is shown in Fig. 1-3.

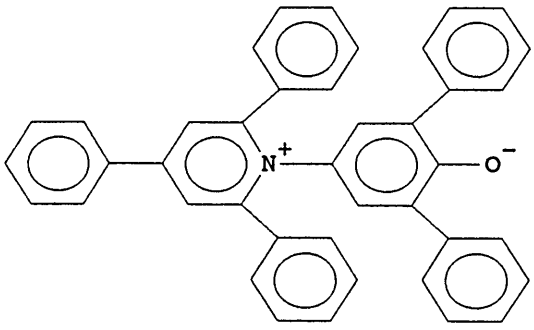

Fig. 1-3 The structure of ET-30

This dye possesses a number of unique features, such as a 44 π-electron aromatic ring system (including the oxygen lone pair), a negatively charged phenoxide group, and a positively charged pyridinium ring nitrogen system. This molecule undergoes one of the largest known solvent-induced shifts in λ_{max}, amounting to some 357 nm in going from water (453 nm) to diphenyl ether (810 nm).[38] Since this dye absorbs within the visible region, it is possible to estimate visually the polarity of a solvent. For example, in methanol, the solution of the dye is wine-red, while in acetonitrile the solution becomes deep blue in colour. A set of E_T scale of solvent polarity was developed in the early 1960's by Dimroth and Reichardt, who reported on the solvatochromism of a series of pyridinium betaine dye molecules.[38]

The E_T scale (also call ET value) of solvent polarity is based on the intramolecular charge transfer absorption of the betaine dyes (actually it is a scale of the molar transition energies of the dye concerned in different solvents). ET values are calculated (Equation 4) in the same manner as are z-values, which are an empirical parameter for measuring the polarity of solvents, and have been reported for more than 50 pure solvents and solvent mixtures.[41]

$$ET(kcal/mol) = 28592/\lambda_{max}\,(nm) \quad or$$
$$ET(kJ/mol) = 1.1959 \times 10^{-2}\,\nu\,(cm^{-1}) \qquad (4)$$

ET polarity values of the dye ET-30 have been reported for over 200 solvents.[42]

c). Adducts of 7,7,8,8-tetracyanoquinodimethane (TCNQ)

Solvatochromism requires an intramolecular charge transfer on excitation by light. A series of N-alkylquinolinium adducts of 7,7,8,8-tetracyanoquino-

dimethane (TCNQ) were found to show such charge transfer. TCNQ is a powerful electron acceptor and can form charge transfer compounds with a variety of electron donors. Most of these TCNQ charge transfer compounds were found to show electrochromic and solvatochromic properties, such as the series[43,44,45,46] of compounds showed in Fig. 1-4:

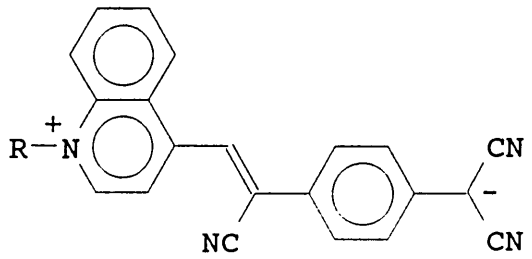

R(4)Q3CNQ

Fig. 1-4 Structure of adducts of TCNQ

R - refers to the alkyl chain.

(4) - refers to substitution ion in the '4' - position of the quinolinium ring.

Q - refers to quinolinium donor.

3CN - shows 3 cyano groups present.

Q - refers to TCNQ as the acceptor.

2. Applications of organic dye materials

Electrochromic and solvatochromic materials have been found to be of considerable value in the study of chemical and biological systems.

a. Applications in chemical systems

Many organic molecules with electrochromic or solvatochromic properties are used as a polarity indicator of solvent.

It is well known that, apart from reaction agents, reaction temperature, and reaction time etc. for a given chemical reaction, an appropriate solvent for the planned reaction is very important too. Usually, one of the significant solvent effects for a given reaction is the so-called solvent polarity which chemists must carefully consider so that they can select a proper solvent when they carry out a reaction. There are many ways to characterise the polarity of a solvent. Bulk physical properties, such as dielectric constant, viscosity, or refractive index represent the simplest measures of solvent properties. However, no single physical property can adequately characterise the 'polarity' of a solvent. It is extremely difficult to define, and represents the sum total of many possible interactions that a solute may experience when dissolved in a particular medium. Therefore, bulk or macroscopic properties will only provide information about the interaction between the solvent molecules themselves. Interactions that a solute may experience include dispersion, dipole-dipole, dipole-induced dipole, and hydrogen-bond forces, etc.. Because of the difficulty of characterising the polarity of a solvent through bulk physical properties, a number of empirical values of solvent polarity have been developed in the past 50 years.[47] They have been reviewed by Reichardt,[48] Griffiths and Pugh.[49] These empirical values are based on the properties of particular solutes dissolved in the solvent of interest. In this way, specific microscopic interactions with the solvent are probed, since the test solute is able to 'see' these better than bulk macroscopic properties can. Some examples among them are the Y-values based on a kinetic measurement of some reaction carried out in the solvent of interest,[50] and the Z-values based on the intramolecular charge-transfer absorption of a dye.[41]

Kamlet et al.[51,52,53] have developed an approach based on hydrogen bonding, referred to as the Solvatochromic Comparison Method. They devised three scales to describe the essential properties of a solvent: a β scale of solvent hydrogen bond acceptor basicity; an α scale of solvent hydrogen bond donor

acidity; and a π^* scale of solvent dipolarity/polarisability. In their method, solvents are classified as three groups according to their hydrogen bonding capacities. They are i) non hydrogen bonding solvents such as benzene and hexane; ii) hydrogen bonding acceptor solvents such as anisole and pyridine; iii) amphiprotic solvents such as alcohols which play dual roles, i.e. as both hydrogen bond donors and acceptors.

More recently, ET-values based on the use of Reichardt's betaine dyes, have been used for solvent polarity measurement, and have been applied in many binary solvent systems.[54-60] For example, Langhals et al. have found[61] that the presence of small amount of water in many organic solvents changes the apparent solution colour from blue (λ_{max} = 575 nm) to red (λ_{max} = 532 nm). Thus, the colour of the solution serves as a visual indicator of the water content, and measurement of λ_{max} for ET-30 dissolved in a given solvent can be a rapid and precise method for water detection. In their recent work, the water content of organic solvents is calculated by a two parameter equation from λ_{max} of the dye ET-30.[62]

The change in absorption intensity of a ET-30 solution at a fixed wavelength has been used to determine mixture composition. Water concentrations of about 60 μg/ml can be detected in acetonitrile.[63]

ET-30 has also been used in the examination of the polarity of aqueous micellar media. For examples, Zachariasse et al. used ET-30 as a polarity probe for micelles, microemulsions, and phospholipid bilayers and found that changes in micelle conformation (e.g. sphere-to-rod transition) were easily detected by the discontinuity in measured ET(30) polarity as the concentration of sodium chloride was increased.[64] Plieninger and Baumgartel also studied the NMR

spectrum of ET-30 in various surfactant media to determine the position in which the molecule resides in the micelles.[65,66]

ET(30) values have been used in chromatographic systems in a number of ways to provide information about either the mobile phase (solvent polarity) or the stationary phase (surface polarity). For example, the ET(30) polarity of mobile phases used in supercritical fluid chromatography (SFC) have been reported by Hyatt[67] (typical mobile phases used in SFC are compressed gases such as carbon dioxide or ammonia, at a temperature greater than their critical point). The polarity of silica surfaces in normal liquid chromatography was examined by Lindley et al.,[68] who measured the diffuse reflectance spectrum of the betaine adsorbed onto chromatographic silica.

b. Applications in biological systems

Many organic dye materials have been applied in biological systems; some examples are described here.

Loew and his co-workers[69,70,71] studied the p-aminostyryl-pyridinium (ASP) chromophore and found that this chromophore can be incorporated into membrane probes whose absorption and emission spectra may respond to membrane potential by an electrochromic mechanism. These probes were designed according to Loew's theoretical model[72] which predicted a large charge shift down the length of the chromophore upon photoexcitation. Side chains of appropriate polarity can be appended to the chromophore at points that will ensure that any transmembrane electric field is parallel to the charge displacement vector,[70,73] thus maximizing an electrochromic effect. Therefore, electrochromism permits a theoretical approach to the development of potential sensitive probes.

The characteristics of transmittance and fluorescence changes of 4-(p-aminostyryl)-1-pyridinium dyes (the dye structures studied are showed in Fig.1-5) in response to voltage-clamp pulses on the squid giant axon were also examined by Loew et al.[74]

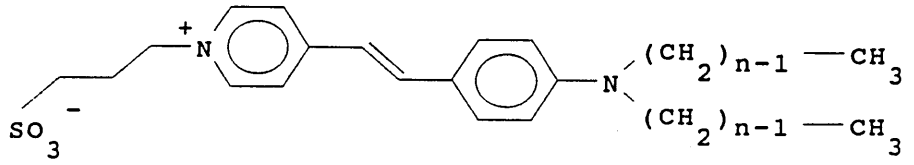

di-n-ASPPS n=4,6,10

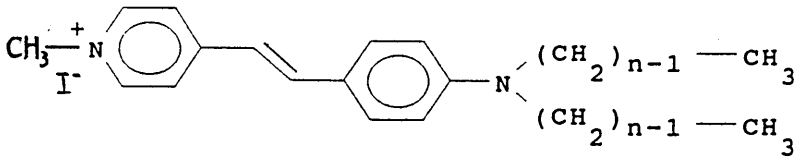

di-n-ASP n=1,4,5,6,10

ASPPS - aminostyrylpyridinium propylsulfonate.

ASP - aminostyrylpyridinium.

Fig.1-5 Structures of p-aminostyrylpyridinium probes

The transmittance and emission spectra of the zwitterionic styryl dye on the voltage-clamped squid axon had the same shapes as those measured on a model membrane system and were consistent with a postulated electrochromic mechanism. The speed of the transmittance response is faster than 1.2μs. The size of the fluorescence change is a factor of 40 lower than on the model membrane, however, this diminution was rationalised in terms of the background fluorescence from the nonoptimal geometric arrangement of the axon membrane. It was found that the cationic ASP series of dyes (e.g., di-4-ASP [Fig.1-5]) had the same response characteristics as the zwitterionic ASPPS dyes while the axon was bathed in a solution of ASP dye.

The cyanine class of dyes have been employed extensively as probes in biological systems, especially in mitochondria and sarcoplasmic reticulum vesicles. The 3,3'-diethylthiodicarbocyanine [diS-C_2-(5)] and 3,3'-dipropylthio-dicarbocyanine [diS-C_3-(5)] have been used most widely. A detailed review about the studies of these probes is provided by Smith.[75] One example is the use of diS-C_3-(5) as a probe in hamster liver mitochondria preparations.[76]

A number of oxonol dyes, such as Bis[3-phenyl-5-oxoisoxazol-4-yl]penta-methineoxonol (oxonol V) and Bis[3-propyl-5-oxoisoxazol-4-yl]pentamethine-oxonol (oxonol VI), have been extensively used as indicators of charge separation in systems that generate inside-positive potentials such as submitochondrial particles, chloroplasts, sarcoplasmic reticulum vesicles under certain conditions, and several reconstituted preparations.[77,78,79,80]

Merocyanine dyes as probes of action potential in the squid giant axon have extensively investigated by Cohen et al.[81,82] For example, it was found that fluorescence response of 5-[(3-sulfopropyl-2(3H)-benzoxazolylidene)-2-butenylidene]-1,3-dibutyl-2-thiobarbituric acid (called Merocyanine-540) to the action potential was coincident with the signal from electrodes and, as subsequently demonstrated by Ross et al.[83] An increase in the signal-to-noise ratio over that obtained from fluorescence measurements was possible using absorption spectroscopy to follow the probe response to this potential. Merocyanine-540 emission has also been found to accurately follow the time-course of the action potential in frog heart muscle strips.[84] Binding studies indicated that the origin of the merocyanine-540 energy-dependent signals in submitochondrial particles is enhanced association of the probe with the particle membrane.[85]

A review about potential-sensitive molecular probes has been provided by Smith.[79] The classification, applications and mechanism of these molecular probes are discussed in detail.

1.3 Aim of the present work

On the basis of their response to electric field change, electrochromic and solvatochromic materials have been extensively used as probes to detect a wide range of events in biological systems where a suitable membrane system exists. These probe molecules are often introduced at an interface and, if they interact with the adjoining phases, small changes in surface potential or transmembrane potential can be monitored non-invasively by spectroscopic techniques.

In chemical systems, solvatochromic materials have been used to examine both solvent polarity and surface charge.

The aims of the present work are to produce and characterise novel electrochromic and solvatochromic materials that can be used as sensors for toxic gases such as NO_2, and as sensors for analytes in liquid phases. The research project is divided into three main parts.

1). Synthesis of new organic materials with electrochromic and solvatochromic properties and structural modification of established materials. Synthesis of electrochromic compounds already described in the literature was the beginning of this work because few of the candidate molecular species for the project are commercially available. Structural modification of these compounds was then carried out in order to obtain a more pronounced solvatochromism, or in order to link the compound covalently onto solid supports.

2). Deposition of these materials at interfaces using physical adsorption or covalent binding. In both methods, it is important that the binding should not affect the solvatochromic property of the materials of interest. Orientated layers (monolayer or multilayers) of suitable molecular materials were obtained by means of L-B technology in order to construct a sensor for gas phase applications, while covalent bonding to chromatographic silica and to glass slide was attempted for production of liquid phase sensors.

3). Investigation and evaluation of the spectral responses of the L-B film orientated materials to toxic gases such as NO_2, Cl_2 and NH_3. Investigation and evaluation of the sensing effects of the covalently bonded materials in liquid systems as a sensor of solvent polarity.

References:

1. Janata Jiri, Principles of Chemical Sensors, Plenum Press, New York, 1989.

2. Robert Bogue and Partners, Sensor Review, April 1990, p. 64.

3. Jiri Janata and Andras Bezegh, Anal. Chem. Vol. 60, No. 12, 1988, 62 R - 74R.

4.Shioyama, T. Mem. fac. Eng. Des., Kyoto Inst. Technol., Ser. Sci. T Technol. 1985, 34, 50. CA105(2): 839 1k.

5. H. Muramatsu, J. M. Dicks, I. Karube, Anal. Chim. Acta 1987, 197, 347. CA108(2): 15546e.

6. O. Fatlbello-Fllho, J. F. De Andrade, A. A. Suieiman, G. G. Guilbault, Anal. Chem. 1989, 61 (7), 746-8.

7. J. F. De Andrade, A. A. Suieiman, G. G. Guilbault, Anal. Chim. Acta 1989, 217 (1), 187-92.

8. R. L. CooK, R. C. Macduff, A. F. Sammells, Anal. Chim. Acta 1989, 217 (1), 101-9.

9. T. E. Edmonds, M. J. Hepher, T. S. West, Anal. Chim. Acta 1988, 207 (1-2), 67-75.

10. D. O. Orata, D. A. Buttry, J. Am. Chem. Soc. 1988, 110, 6258-6261.

11. W. J. Albery, P. N. Bartlett, A. E G. Cass, D. H. Craston, B. G. D. Haggett, J. Chem. Soc., Faraday Trans. 1, 1986, 82(4), 1033. CA105(16): 141901t.

12. C. D. Van, C. Laane, and C. Veeger, Recl. Trav. Chim. Pays-Bas 1985, 104, 245. CA103(25): 210064v.

13. S. Bruckenstein, J. S. Symanski, J. Chem. Soc., Faraday Trans. 1 1986, 82(4), 1105. CA105(16): 145084b.

14. E. M. Logothetis, Proc.-Electrochem. Soc. 1987, 87-9 (Proc. Symp. Chem. Sens.), 142. CA107(24): 222248d.

15. Jiri Janata, Anal. Chem. Vol. 62, No. 12, 1990, 33 R - 44R.

16. R. Narayanaswamy, D. A. Russell, Sens. Actuators 1988, 13 (3), 293-8.

17. A. J. Bryan, D. S. A. Prasanna, A. Sallya De Silva, R. A. D. D. Repusinghe, K. R. A. Sandanayake, Samanakumara Biosensors 1989, 4 (3), 169-79.

18. A. J. Guthrie, R. Narayanaswamy, D. A. Russell, Analyst (London) 1988, 113 (3), 457-61.

19. T. P. Jones, M. D. Porter, Anal. Chem. 1988, 60 (5), 404-6.

20. S. Luo, D. R. Walt, Anal. Chem. 1989, 61 (2), 174-7.

21. W. P. Carey, M. D. DeGrandpre, B. S. Jorgensen, Anal. Chem. 1989, 61 (15), 1674-8.

22. H. E. Posch, M. J. P. Leiner, Otto S. Wolfbeis, Fresenius' Z. Anal. Chem. 1989, 334 (2), 162-5.

23. E. Smela, J. J. Santiago-Aviles, Sens. Actuators 1988, 13 (2), 117-29.

24. F. L. Dickert, S. K. Schreiner, G.R. Mages, H. Kimmel, Anal. Chem. 1989, 61 (20), 2306-9.

25. Optiz, N.; Luebbers, Dietrich W. Int. Anesthesiol. Clin. 1987, 25 (3), 177-97.

26. Wolfbeis, Otto S.; Leiner, Marc J. P. Proc. SPIE-Int. Opt. Eng. 1988, 906 (Opt. Fibers Med. 3), 42-8.

27. T. A. Temofonte, K. F. Schoch, J Appl. Phys. 1989, 65 (3), 1350-5.

28. Wolfbeis, Otto S.; Weis, Leonie J.; Leiner, Marc J. P.; Ziegier, Werner E. Anal. Chem. 1988, 60 (19), 2028-30.

29. Blyler, L. L. Jr.; Lieberman, R. A.; Cohen, L. G.; Ferrara, J. A.; Macchesney, J. B. Polym. Eng. Sci. 1989, 29 (17), 1215-18.

30. D. Pugh and J.O. Morley, Molecular Hyperpolarizabilities of Organic Materials, in Nonlinear Optical Properties of Organic Molecules and Crystals, Vol.1, p193, edited by D.S. Chemla and J. Zyss, published by Academic Press Inc. (London) Ltd., 1987.

31. M. S. Paley and J. M. Harris, J. Org. Chem. 1989, 54, 3773-3778.

32. G.R. Mohlmann, Perspectives for Optically Non-linear Polymers in Electro-optic Applications, in Organic Materials for Non-linear Optics, p275, edited by R.A.Hann and D.Bloor, published by the Royal Society of Chemistry, 1989.

33. J. Zyss, J.F. Nicoud and M. Coquillay, J. Chem. Phys., 81, p4160, 1984.

34. J.O. Morley, V.J. Docherty and D. Pugh, J. CHEM. SOC. PERKIN TRANS. II, p1351, 1987.

35. J.R. Platt, J. Chem. Phys., 34, 862(1961).

36. W. Liptay, Angew. Chem. internat. Edit./Vol.8, 177 (1969)/No.3.

37. (a) L.G.S. Brooker, G.H. Keyes, R.H. Sprague, R.H. VanDyke, E.VanLare, G. VanZandt, and F.L. White, J. Am. Chem. Soc. 73, 5326 (1951); (b) L.G.S. Brooker, G.H. Keyes, R.H. Sprague, R.H. VanDyke, E.VanLare, G. VanZandt, F.L. White, H.W.J. Cressman, and S.G. Dent, Jr., ibid. 73,5332 (1951); (c) L.G.S. Brooker, G.H. Keyes and D.W. Heseltine, ibid. 73,5350 (1951).

38. Dimroth, K.; Reichardt, C.; Siepmann, T.; Bohlmann, F. Justus Liebigs Ann. Chem. 1963, 661, 1-37.

39. Reichardt, C. Angew. Chem., Int. Ed. Engl. 1965, 4(1), 29-40.

40. Reichardt, C. Solvent Effects in Organic Chemistry; Verlag Chemie: New York, 1979.

41. E. M. Kosower, J. Am. Chem. Soc., 80, 3253-3260 (1958).

42. C. Reichardt and E. Harbusch-Gornert, Justus Liebigs Ann. Chem., 721-743 (1983).

43. G.J. Ashwell, Emma J.C. Dawnay, A.P. Kuczynskl, M. Szablewskl and Ian M. Sandy, Martin R. Bryce, Andrew M. Grainger and Masihul Hasan, J. CHEM. SOC. FARADY TRANS., 1990, 86(7), 1117-1121.

44. Norman A. Bell, Richard A. Broughton, John S. Brooks, T. Alwyn Jones, Stephen C. Thorpe and Geoffrey J. Ashwell, J. CHEM. SOC., CHEM. COMMUN., 1990, 325-326.

45. P. Carr, May, 1990, Gas detection using adducts of TCNQ, A report on the final year project, Sheffield City polytechnic.

46. R.A. Broughton, July, 1987, Transfer report, Sheffield City Polytechnic.

47. B. P. Johnson, B. Gabrielsen, M. Matulenko and J. G. Dorsey, Analytical Letters, 19 (9&10), 939-962 (1986).

48. C. Reichardt, "Solvent Effects in Organic Chemistry", Verlag Chemie, New York, 1979.

49. T. R. Griffiths and D. C. Pugh, Coord. Chem. Rev., 29, 129-211 (1979).

50. E. Grunwald and S. Winstein, J. Am. Chem. Soc., 70, 846-854 (1948).

51. M. J. Kamlet, J. L. M. Abboud, and R. W. Taft, J. Am. Chem. Soc. 1976, 98, 377, 2886.

52. M. J. Kamlet, J. L. M. Abboud, and R. W. Taft, J. Am. Chem. Soc. 1977, 99, 6027.

53. M. J. Kamlet, J. L. M. Abboud, M. H. Abraham, and R. W. Taft, J. Org. Chem. 1983, 48, 2877.

54. S. Balakrishnan and A. J. Easteal, Aust. J. Chem., 34, 933-941 (1981).

55. S. Balakrishnan and A. J. Easteal, Aust. J. Chem., 34, 943-947 (1981).

56. I. A. Koppel and J. B. Koppel, Org. React. (Tartu), 20, 523-546 (1983). CA 101:110180v (1984).

57. I. A. Koppel and J. B. Koppel, Org. React. (Tartu), 20, 547-560 (1983). CA 101:110274d (1984).

58. T. M. Krygowski, P. K. Wrona, U. Zielkowska, and C. Reichardt, Tetrahedron, 41, 4519-4527 (1985).

59. P. Nagy and R. Herzfeld, Acta Phys. Chem., 31, 735-742 (1985).

60. H. Langhals, Angew. Chem. Int. Ed. Engl., 21, 724-733 (1982).

61. H. Langhals, E. Fritz, and I. Mergelsberg, Chem. Ber., 113, 3662-3665 (1980).

62. H. Langhals, Analytical Letters, 23(12), 2243-2258 (1990).

63. S. Kumoi, K. Oyama, T. Yano, H. Kobayashi, and K. Ueno, Talanta, 17, 319-327 (1970).

64. K. A. Zachariasse, N. Van Phuc, and B. Kozankiewicz, J. Phys. Chem., 85, 2676-2683 (1981).

65. P. Plieninger and H. Baumgartel, Liebigs Ann. Chem., 860-875 (1983).

66. P. Plieninger and H. Baumgartel, Ber. Bunsen-Ges. Phys. Chem., 86, 161-167 (1982).

67. J. A. Hyatt, J. Org. Chem., 49, 5097-5101 (1984).

68. S. M. Lindley, G. C. Flowers, and J. E. Leffler, J. Org. Chem., 50, 607-610 (1985).

69. L.M. Loew, S. Scully, L. Simpson and A.S. Waggoner, Evidence for a charge shift electrochromic mechanism in a probe of membrane potential., Nature. (Lond.). 281:497-499, (1979).

70. L.M. Loew and L. Simpson, charge shift probes of membrane potential. A probable electrochromic mechanism for ASP probes on a hemispherical lipid bilayer. Biophys. J., 34:353-365, (1981).

71. L.M. Loew, Design and characterization of electrochromic membrane probes, J. Biochem. Biophys. Meth., 6:243-260, (1982).

72. L.M. Loew, G.W. Bonneville and J. Surow, Charge shift probes of membrane potential. Theory, Biochemistry, 17:4065-4071, (1978).

73. L.M. Loew, L. Simpson, A. Hassner and V. Alexanian, An unexpected blue shift caused by differential solvation of a chromophore oriented in a lipid bilayer, J. Am. Chem. Soc., 101:5439-5440, (1979).

74. L.M. Loew, L.B. Cohen, B.M. Salzberg, A.L. Obaid and F. Bezanilla, Characterization of aminostyrylpyridinium dyes on the squid giant axon, Biophys. J., 47:71-76, (1985).

75. J.C. Smith, (1988) in Spectroscopic Membrane Probes (L.M. Loew, ed.), Vol.3, pp153-157, CRC Press, Boca Raton.

76. P.C. Laris, D.P. Bahr and R.R.J. Chaffee, BioChim. Biophys. Acta 376, 415, (1975).

77. C.L. Bashford and W.S. Thayer, J. Biol. Chem., 252, 8459, (1977).

78. S. Krab, H.S. Van Walraven, M.J.C. Scholts and R. Kraayenhof, Biochim. Biophys. Acta 809, 228-235, (1985).

79. J.C. Smith, Biochim. Biophys. Acta, 1016, 1-28, (1990).

80. J.C. Smith, P. Russ, B.S. Cooperman and B. Chance, Biochemistry 15, 5094, (1976).

81. L.B. Cohen and B.M. Salzberg, Rev. Physiol. Biochem. Pharmacol, 83, 35, (1978).

82. L.B. Cohen, B.M. Salzberg, H.V. Davila, W.N. Ross, D. Landowne, A.S. Waggoner and C. H. Wang, J. Membr. Biol., 19, 1, (1974).

83. W.N. Ross, B. M. Salzberg, L.B. Cohen and H.V. Davila, Biophys. J., 14, 983, (1974).

84. G. Salama and M. Morad, J. Physiol., (London) 292, 267, (1979).

85. J.C. Smith, J.M. Graves and M. Williamson, Arch. Biochem. Biophys., 231, 430, (1984).

A number of modern techniques were used in this work. A brief introduction to each is given below.

2.1 Infrared spectroscopy

Infrared spectroscopy is one of the most important analytical tools used to investigate a wide variety of molecules in the solid, liquid, and gas states. It yields useful information about molecular structure and molecular bonds, and also can probe molecular orientation in ordered systems.

A molecule will absorb infrared radiation if it vibrates in such a way that its electric dipole moment changes during vibration.[1]

The IR region of the electromagnetic spectrum corresponds to wavenumber in the range, 200-10 cm^{-1} (far infrared), 4000-200 cm^{-1} (medium infrared) and 14,285-4000 cm^{-1} (near infrared).[1,2] The energies associated with IR radiation cause vibrations, either of the whole molecule, or of individual bonds or functional groups within the molecule.

The majority of functional groups relevant to organic chemistry absorb radiation within a fairly narrow range of the IR region, 600-4000 cm^{-1}, and therefore most simple spectrometers operate only within this range. In the present work, for most samples of the compounds prepared, their IR spectra were recorded by means of a simple dispersive spectrometer, a Philips PU9706. The samples were presented as a KBr disc.

In the past decade, a new type of IR spectroscopy, known as Fourier transform IR (FTIR) spectroscopy, has been developed. Although the spectrum obtained from FTIR looks identical to one that is obtained from normal IR

method, the spectrometer operates on an entirely different principle. Fourier transforms involve complicated mathematics, which will not be discussed here. However, it must be stated that FTIR has many advantages over the traditional IR method: sensitivity (very small samples can be examined), resolution (not dependent on optical properties of gratings, slits and prisms), and the flexibility that comes with the on-board computer (allows subtraction of one spectrum from another, digital plots of data and so on).

2.2. FTIR microspectroscopy

FTIR microspectroscopy is based on the same concepts and principles as in normal FTIR spectroscopy. However, because the sample is very small, some additional problems appear, which result in the requirement of special skills for sample preparation, sample mounting, data acquisition and data processing.[3]

FTIR microspectroscopies have a wide range of applications,[4] and can operate in transmission or reflection modes.

In reflectance mode, there are three classifications of reflectance measurements: reflection-absorption, diffuse reflectance, and specular reflectance. Reflection-absorption spectra are obtained from thin films on reflecting surfaces.[5] Reflection-absorption occurs when a thin absorbing layer of a material is on the surface of a more reflecting substrate. The ideal case is a thin absorbing layer on a polished metallic substrate. The incident radiation passing through the absorbing layer is reflected at the metal's surface, and then passes through the absorbing layer a second time before emerging as reflected radiation.[6] Diffuse reflectance spectra are obtained from irregular surfaces or aggregates of fine particles, and specular reflectance spectra are obtained from mirror-like reflections from the flat surfaces of dielectric materials.[5,6]

In the present work, reflection mode was used to detect the Langmuir-Blodgett films deposited on a glass slide with gold deposition. The IR-Plan Analytical Microscope produced by Spectra-Tech Inc. was used.

2.3 Mass spectrometry

Mass spectrometry is used to determine the molecular mass of the sample in question ------ a particularly useful piece of information for the organic chemist which the other spectroscopic techniques cannot provide. The basic principle by which the individual molecules are 'weighed' is very simple and was first demonstrated by Wien in 1898.[2] The sample is first converted into positive ions by being bombarded with high energy electrons which remove an electron from the molecule on impact. The positive ions are then accelerated by an electrical potential and pass through a magnetic field which cause them to be deflected from their initial straight line of flight. The degree of deviation depends on the magnetic field strength, the charge on the ion and its momentum. It is not difficult to appreciate intuitively that lighter ions will be deflected more than heavier ions for a given magnetic field strength and ionic charge, and very simple application of classical mechanics permits the following relationship to be derived:

$$m/z = H^2R^2/2V$$

where m = mass of the ion, z = charge on the ion, H = applied magnetic field strength, R = radius of arc of deflection and V = applied accelerating voltage.

In addition to giving the molecular weight of the substance under examination (molecular ion), mass spectrometry also provides information about

molecular structure. It is now being applied routinely to the investigation of organic structures.[7] Under the fairly brutal conditions of electron impact ionisation, the molecules tend to undergo cleavage either at weak bonds or to give particularly stable fragments in very predictable ways. Consequently, it is usually possible to infer molecular structure by analysis of the breakdown pattern in the mass spectrum of an unknown.

A VG Micromass 30F Spectrometer was used to record mass spectra of the samples in the present work. The samples were introduced using a direct insertion probe.

2.4 Nuclear magnetic resonance (NMR) spectroscopy[1,2,8]

NMR spectroscopy is one of the most powerful techniques for structural analysis. With the aid of NMR it is possible to define the environment of practically all commonly occurring functional groups, as well as of fragments (such as hydrogen atoms attached to carbon) which are not otherwise accessible to spectroscopic or analytical techniques.

Nuclear resonance comes about because the nuclei of at least one of the isotopes of most elements posses magnetic moments (in other words, they behave like small bar magnets). The magnetic moment arises because the nucleus may have 'spin', and is also charged, so that it can be considered as a tiny loop of electric current. When placed in a constant magnetic field, the energy of the nuclear magnetic moment depends on the orientation of the nucleus with respect to that field (just as bar magnets attract or repel according to their relative orientation), and on the microscopic nuclear scale only certain energies are permitted (that is, the energy is quantized).

The fundamental property of a nucleus of significance for NMR is its spin, characterised by a quantum number I. The spin quantum number, I, can have values 0, 1/2, 3/2, and so on. There are three principal groups of nuclei:

1. I = 0 (nonspinning nuclei). These have no magnetic moment and are composed of even protons and neutrons, e.g., $^{12}_{6}C$, $^{16}_{8}O$.

2. I = 1/2 (spherical spinning charges). These nuclei have a magnetic moment but no electric quadrupole. This group is by far the most important from the chemical point of view. For example, $^{1}_{1}H$, $^{13}_{6}C$ and $^{19}_{9}F$.

3. I > 1/2 (nonspherical spinning charges). These nuclei have both magnetic dipoles and electric quadrupoles; examples are I = 1: $^{2}_{1}H$; I = 3/2: $^{11}_{5}B$, $^{35}_{17}Cl$; I = 2: $^{58}_{27}Co$.

A fundamental quantum law is that: In a uniform magnetic field, a nucleus of spin I may assume 2I+1 orientations. Thus, for a proton I is 1/2, there are 2(1/2) + 1 = 2 permissible orientations. This makes a nucleus of I = 1/2 analogous to a bar magnet in a magnetic field (Fig. 2-1).

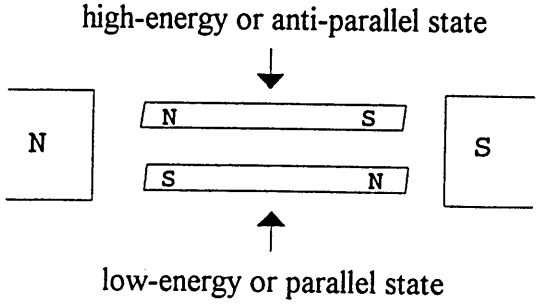

Fig. 2-1 The bar-magnet analogy for nuclei with I = 1/2

As with the bar magnet, the two orientations of the nuclear magnet in the magnetic field (of strength H_0) have different energies, and it is possible to induce a nuclear transition, analogous to the flipping of the bar magnet, by applying electromagnetic radiation of an appropriate frequency ν given by

$$\nu = \gamma H_0/2\pi \qquad (2.1)$$

where γ = a fundamental constant known as the gyromagnetic ratio or magnetogyric ratio, and is characteristic of the particular nucleus concerned.

Equation 2.1 can be reduced to

$$\nu = \text{constant} \times H_0 \qquad (2.2)$$

Equation 2.2 is known as the Larmor equation; it shows that one could observe a nuclear transition (spin flip) by keeping the magnetic field constant and varying the applied frequency (or vice versa) until the combination of field strength and irradiating frequency characteristic of the nucleus concerned is reached. This condition is often described as resonance and is the origin of the term "resonance" in nuclear magnetic resonance. The term resonance frequency is also sometimes used, but it must be remembered that the term would be meaningless without specifying the field strength H_0.

To summarise: some nuclei, notably protons, have magnetic moments. "Spin-flip" nuclear-magnetic transitions of these nuclei can be observed at frequencies predicted by the Larmor equation. The strength of the signal is directly proportional to the number of nuclei involved.

The amount of structural information given by a nmr spectrum is greatly enhanced by the two factors. Firstly, the exact position of resonance is determined by the chemical environment of the nucleus. The proton magnetic resonance (pmr) spectrum of an organic compound may therefore show several absorption bands, each corresponding to a particular proton or group of protons. Secondly, a given band may be split into several peaks as a result of interactions between neighbouring nuclei. The two effects give rise to what are termed the chemical shift and spin-spin coupling or splitting. A third useful feature of the spectrum is that the integrated area of a absorption peak is directly proportional to the number of nuclei responsible for the signal.

According to Larmor equation 2.2, at a given frequency all protons (or nuclei) will absorb energy at the same value of the magnetic field H0. However, the field experienced by a particular nucleus differs in magnitude from that of the applied field because of shielding effects by neighbouring electrons. It is because of varying degrees of shielding that protons (or nuclei) in different chemical environments absorb at different values of the applied field. Difference between such absorptions are referred to as chemical shifts. Quantitatively, chemical shifts are measured in frequency (Hz) relative to a standard, the universally accepted reference compound being tetramethylsilane $(CH_3)_4Si$ (TMS). The desirable properties of this compound are that it has twelve highly shielded protons in identical chemical and magnetic environments thereby producing a single sharp resonance peak at a higher field than most other organic protons. Furthermore it is chemically inert, soluble in organic solvents and boils at 27 °C. In practice chemical shifts are expressed in dimensionless units δ (equation 2.3) by dividing them by the operating frequency of the instrument, thus facilitating comparisons between spectra run on different instruments.

$$\delta = \{[\nu(\text{sample}) - f(\text{TMS})]/\nu(\text{instrument})\} \times 10^6 \text{ ppm} \qquad (2.3)$$

By including a factor of 10^6, δ values fall within the range 0 - 15 for most organic protons, the values then being expressed in parts per million (ppm).

Many signals in pmr spectra exhibit fine structure (or multiplets) because of the splitting of spin-state energy levels of the protons by other magnetic nuclei in the neighbourhood. The fine structure or the multiplets of pmr spectra can be analysed by direct measurement in a large number of cases. Such spectra are known as first-order spectra. The rules for interpreting first-order spectra are as follows:

1. When a proton (or a group of magnetically equivalent protons) is spin-spin coupled to n equivalent protons with a coupling constant of J Hz, its NMR signal is split into n + 1 lines separated by J Hz. The relative intensities of the lines are in the ration of the binomial coefficients of $(x + y)^n$. The true chemical shift of the protons concerned lies at the centre of the multiplets.

2. If there are more than two interacting groups of protons ($A_nM_mX_p$.....), the multiplicity of the signal due to the A protons is given by (m + 1)(p + 1).....;

3. In first-order spectra, equivalent protons appear not to split one another; in other word, the transitions corresponding to such interactions are forbidden, or of zero probability.

In the present work, only first-order spectra of pmr were met and interpreted. Two NMR spectrometers were used to recorded nmr spectra, a PMX 60 SI model and a Bruker AC 250 model.

2.5 Ultraviolet and visible spectroscopy[1,2,8]

Ultraviolet and visible spectroscopy was the first method of spectroscopic analysis to make an impact on organic chemistry and it is still very useful tool to provide qualitative and quantitative information for chemists.

Absorption of ultraviolet or visible light by an organic molecule involves electronic transitions between molecular orbitals. The energy changes in the transitions are relative large, corresponding to about 10^5 J mol^{-1}. This corresponds to a wavelength range of 200 to 800 nm.

Beer's law describes the relationship among absorption, concentration, and pathlength, that is

$$A = \varepsilon bc \qquad (2.4)$$

where A = absorption; b = pathlength (cm); c = concentration (mol. dm^{-3}); ε = molar absorption coefficient (dm^3. mol^{-1}. cm^{-1})

According to molecular orbital theory, the interaction of atomic orbitals leads to the formation of bonding and antibonding molecular orbitals. Depending on the nature of the overlapping atomic orbitals, molecular orbitals may be of the σ (bonding) or σ^* (antibonding) type where the electron density is concentrated along the internuclear axis, or of the π (bonding) or π^* (antibonding) type where the electron density is concentrated on either side of the internuclear axis. Those occupied by electrons not participating in bonding are known as n non-bonding orbitals.

In most organic compounds the bonding and non-bonding orbitals are filled and the antibonding orbitals are vacant. The electronic transitions that concern organic chemists are those involving the excitation (promotion) of an electron from a bonding or non-bonding to an antibonding orbital. The energy, and hence the wavelength of radiation required, to cause the promotion of an electron, depends on the energy difference between the two relevant orbitals, which in turn depends on the type of electrons involved. In addition to matching the requirement of the energy, a second requirement must be met for the transition, i.e., the energy transition in the molecule must be accompanied by a change in the electronic configuration so that transition can be carried out on the molecule by the electromagnetic radiation. Requirements for the absorption of radiation are decided by quantum-mechanical selection rules, which determine which transitions may take place. These rules, based on considerations of the symmetry of the system in the upper and lower states, point out that some transitions are more probable than others. The first selection rule is related to all molecules with centres of symmetry and deals with the parity-forbidden transitions. The second rule states that singlet-triplet transitions are forbidden. The third rule applies to forbidden transitions that arise from the symmetry of states.

However, forbidden transitions are still observed in many molecules, because intramolecular or intermolecular perturbations cause the rules to relax considerably.

The most common electronic transitions relevant to uv-vis spectroscopy are $\pi \rightarrow \pi^*$ transitions with intense bands, and $n \rightarrow \sigma^*$ or $n \rightarrow \pi^*$ transitions with weak bands because of unfavourable selection rules.

2.5.1. Charge-transfer spectra:[1,8]

Many systems exhibit spectra generally considered to be charge-transfer spectra. Absorptions of this type are characterised by high intensity and are fully allowed transitions. Charge-transfer transitions involve an intramolecular or an intermolecular (or interionic) redistribution of charge whereby an electron or a fraction of an electron is transferred from one ion or molecule to another ion or molecule in the same species. For example, the betaine dyes studied in this work all have the structure showed in Fig. 1-2.

One electron is transferred from oxygen atom to nitrogen atom by either intermolecular or intramolecular transition to produce a charge-transfer band in the uv-vis spectrum.

2.5.2. Reflectance spectroscopy[1]

The most reliable method of spectroscopy is transmission, where light is passed through optically clear sample. For opaque samples, however, reflectance spectroscopy must be used.

In reflectance spectroscopy, one measures the amount of radiant energy reflected from a sample surface. These data are generally reported as percent reflectance

$$R\% = I/I_o \times 100 \qquad (2.5)$$

where I = the intensity of reflected radiation; I_o = the intensity of radiation reflected from some "standard" reflecting surface.

There are two types of reflectance, specular and diffuse. Specular reflectance is simply mirrorlike reflectance from a surface and is sometimes called regular reflectance; it has a well-defined reflectance angle. Diffuse reflectance is defined as reflected radiant energy that has been partially absorbed and partially scattered by a surface with no defined angle of reflectance. The diffuse reflectance technique is widely used for industrial applications involving textiles, plastics, paints, dyestuffs, inks, paper, food, and building materials. A common design feature of all commercial diffuse-reflectance instruments is the integrating sphere, which permits the collection of reflected light. Many of the commercial ultraviolet-visible spectrophotometers offer this mode of operation as an accessory.

In the present work, ultraviolet-visible transmission spectra were recorded using a Hitachi U2000 spectrophotometer and reflectance spectra were recorded by means of a PYE UNICAM SP 800 spectrophotometer with a reflectance unit.

2.6 Langmuir-Blodgett films[9]

The technology of Langmuir-Blodgett films (LB films) has become a very active area of research in the last fifteen years. Langmuir and Blodgett developed the techniques and theory which led to the modern understanding of monolayers and their transference to a suitable substrate.

In this technique, amphiphilic molecules (those having both a hydrophilic and hydrophobic portions) are dissolved in a suitable volatile solvent before being deposited on an ultra-clean subphase in a so-called Langmuir trough. Subphase is virtually always pure water since it is relatively cheap and easily obtained.

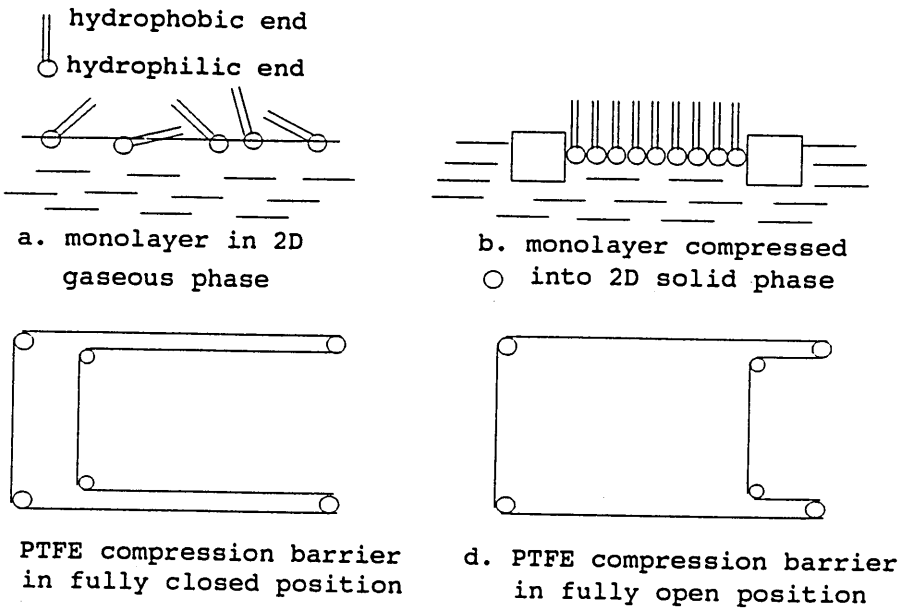

Fig. 2-2 Diagram of monolayer and PTFE barrier

When the solvent is evaporated, a loosely packed monomolecular layer (Fig. 2-2 a) is left at the water-air interface. This monomolecular layer acts, effectively, as a two-dimensional gas, and by compressing this layer, it passes through the corresponding liquid phase until it becomes a two-dimensional solid (Fig. 2-2 b). Further compression eventually leads to the breakdown of the monolayer. This compression was achieved in this case by using a PTFE coated, constant perimeter glass fibre barrier. The area contained was adjusted via computer control (Fig. 2-2 c and d).

A sensitive microbalance linked to a sensor monitors the surface pressure. Typically, this sensor is a piece of Whatman grade I chromatography paper. This Wilhelmy plate technique is very reliable and enables surface pressure to be measured over a wide range.

Dipping and raising a suitably prepared substrate through the compressed layer results in the successive build-up of monolayers onto the substrate. There

are three types of depositions, i.e. so-called 'X', 'Y' and 'Z' types. In x type, deposition is on down stroke only; in y type, deposition is on both up and down strokes, and in z type, deposition is on up stroke only.

In the present work, a Joyce Loebl Langmuir Trough 4 was used.

References:

1. H. H. Bauer, G. D. Christian, and J. E. O'Reilly, Instrumental Analysis, Allyn and Bacon, Inc. Boston, London, Sydney, Toronto, 1978, p201.

2. L. M. Harwood & C. J. Moody, Experimental Organic Chemistry, Principles and Practice, Blackwell Scientific Publications, Oxford, London, 1989.

3. D. Crowther, Practical FTIR Spectroscopy, on the notes, Sheffield Hallam University, 1993.

4. R. G. Messerschmidi and M. A. Harthcock, Infrared Microscopy Theory and Applications (Marcel Dekker Inc., New York, NY, 1988).

5. W. G. Golden, Fourier Transform Infrared Spectroscopy, vol. 4 (Academic Press. Inc., New York, NY, 1985), p. 315.

6. J. A. Reffner and W. T. Wihlborg, International Laboratory, July/August, 1990, p. 20.

7. William Kemp, Qualitative Organic Analysis, Spectrochemical Techniques, second edition, McGraw-Hill Book Company (UK) Limited, 1986, p. 169.

8. F. W. Fifield and D. Kealey, Principles and Practice of Analytical Chemistry, Third Edition, Published by Blackie and Son Ltd., 1990.

9. M. Sugi, J. Mol. Electronics, 1, 3 (1985).

3.1 Introduction

Many molecules with solvatochromic and electrochromic properties are used as probes in biological systems. One class of these materials is the merocyanine and cyanine dyes studied by Brooker and co-workers.[1,2,3] It was decided to study some of Brooker's dyes for possible optical response to some toxic gases.

N-alkylquinolinium adducts of TCNQ (7,7,8,8-tetracyanoquino-dimethane) are known to be zwitterionic optically non-linear materials.[4,5] These TCNQ adducts were found to show electrochromic and solvatochromic properties.[6] Some of the TCNQ adducts were also studied for possible optical response to toxic gases.

Because none of the molecular species mentioned above are commercially available, synthesis of some of these compounds, as described in the literature, was the beginning of this work.

The technology of Langmuir-Blodgett (L-B) films has become an active area of study. The orientated layers (monolayer or multilayers) of solvatochromic molecule materials can be obtained by means of L-B technology in order to construct a gas sensor. However, materials suitable for producing L-B film typically possess both hydrophobic and hydrophilic end groups. The hydrophobic end groups often are a long alkyl chain. In order to produce a L-B film of monolayer or multilayers from the solvatochromic materials used in the present work, modification by attachment of a long alkyl chain to the compounds studied was necessary.

3.2 Preparation of 3,3'-dihexyloxacarbocyanine

3,3'-dihexyloxacarbocyanine is one of the cyanine dyes, and has been used as a molecular probe of membrane potential.[7] The dye was prepared according to the procedures described by Cohen et al.[7] A simple reaction scheme is showed in Fig. 3-1.

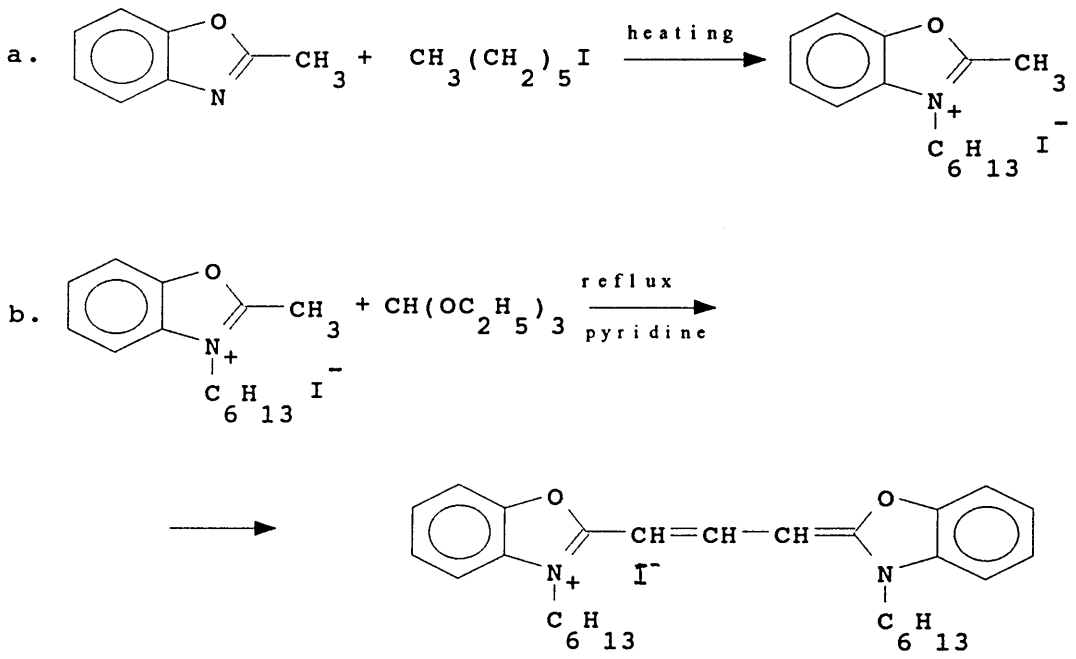

Fig. 3-1 Reaction scheme for the preparation of 3,3'-dihexyloxacarbocyanine

2-methylbenzoxazole (Aldrich, 6.7 g, 50 mmoles) was mixed with n-hexyl iodide (Aldrich, 11.6 g, 50 mmoles), and then the mixture was heated at 130 °C for 48 hours. The resulting brown oil was treated with 40 ml of pyridine, and the fine crystals generated were collected and rinsed thoroughly with ether. 9.13 g (yield: 53%) white product was obtained. The crude 3-hexyl-2-methyl benzoxazolium iodide was used for the next step without further purification.

The crude product (6.9 g, 20 mmols.) from the above reaction was under reflux for 10 hours with excess triethyl orthoformate (10 g) in 20 ml of pyridine solvent. The resulting dark brown solution was diluted with 8 ml of methanol and 15 ml of ether and set aside to crystallise. The product was collected by filtering and was recrystallised twice from acetone. 2.8 g (yield: 25%) pure product was obtained, its melting point is 221 to 222 °C.

The infrared spectrum of the product is showed in Figure 3-2. Microanalysis of the product for carbon, hydrogen and nitrogen elements indicated that it should be 3,3'-dihexyloxacarbocyanine iodide. The results are showed in Table 3-1. The analytical data are consistent with the desired structure.

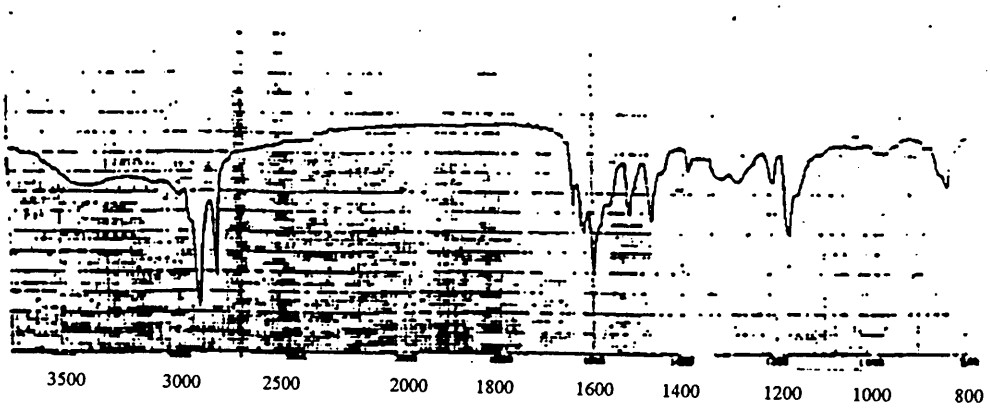

Fig. 3-2 Infrared spectrum of 3,3'-dihexyloxacarbocyanine iodide

Table 3-1
Microanalysis of 3,3'-dihexyloxacarbocyanine iodide

formula: $C_{29}H_{37}N_2O_2I$ (572.53)

	C	H	N
theory	60.84	6.51	4.89
found	60.79	6.43	4.86

3.3 Preparation of N-alkylquinolinium adduct of TCNQ

The structure of the N-alkylquinolinium Adduct of TCNQ and a simple preparation scheme are showed in Fig. 3-3.

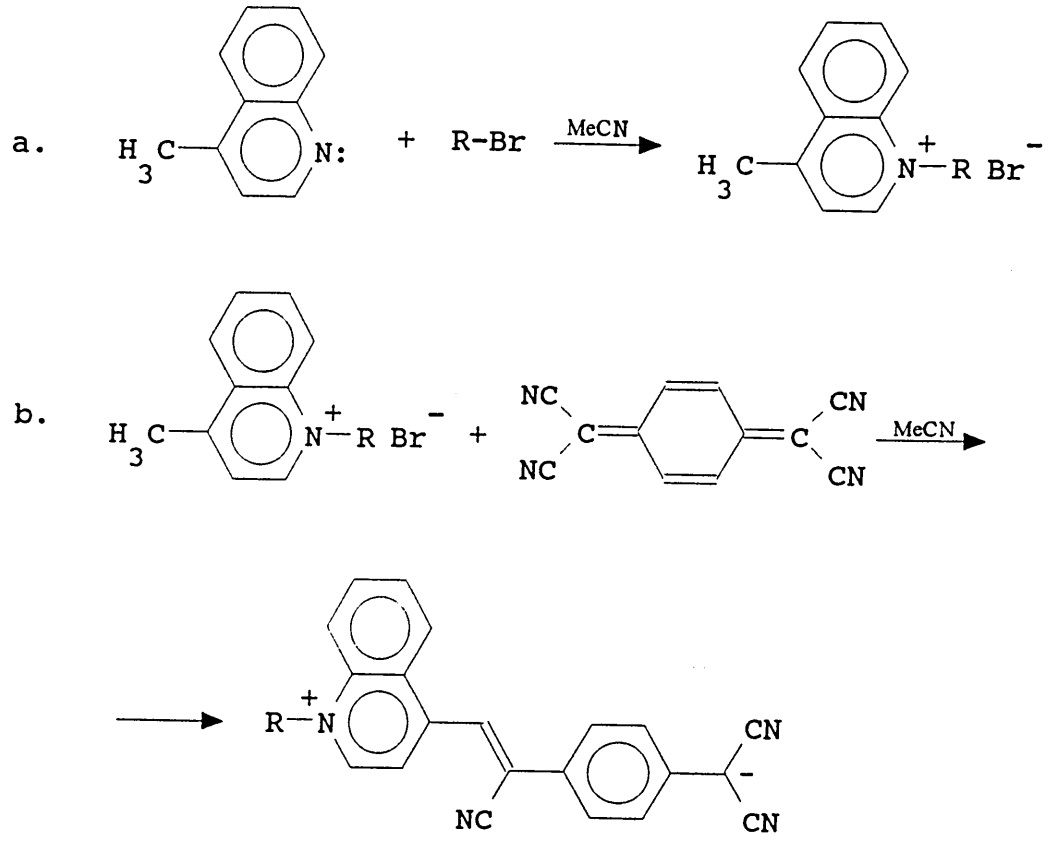

Fig. 3-3 Preparation scheme and structure for N-alkylquinolinium adduct of TCNQ

The preparation was carried out according to the procedures described by Broughton.[6] The alkyl chain of N-alkylquinolinium adduct of TCNQ prepared was $C_{16}H_{33}$.

(i) Equimolar amounts of lepidine (Aldrich, 2.88 g, 20 mmoles) and 1-bromohexadecane (Aldrich, 7.10 g, 20 mmoles) were dissolved in 50 ml of

MeCN. The mixture solution was heated under reflux for three days. The resulting solution was clear and mauve in colour. After adding about 1 litre of ether, precipitation occurred and 4.65 g pale pink solid, n-hexadecyl 4-methyl quinolinium bromide (yield: 53%), was obtained using vacuum filtering followed by further washing with ether.

(ii) 7,7,8,8-tetracyanoquinodimethane(TCNQ) (Aldrich, 0.80g, 3.42 mmoles) dissolved in MeCN was added dropwise to a refluxing solution of n-hexadecyl 4-methyl quinolinium bromide (1.26g, 2.8 mmoles) generated from step (i) in MeCN. The reaction mixture was allowed to reflux for three days and it became a turbid purple-blue solution. A precipitate of dark khaki-green crystals was generated after removing the bulk of the solvent by ice cooling and vacuum filtering. The product was recrystallised from MeCN. 0.61 g (yield: 40%) pure product was obtained, its melting point was found being 277-278 °C.

An infrared spectrum of the product recorded in a KBr disc showed its structure (Fig. 3-4). The bands found at 2900 cm^{-1} was assigned to aliphatic C-H stretch. The bands at 2177 and 2145 cm^{-1} were considered as nitrile C=N stretch. The bands at 1599 and 1548 cm^{-1} were thought of as aromatic C=C stretch.

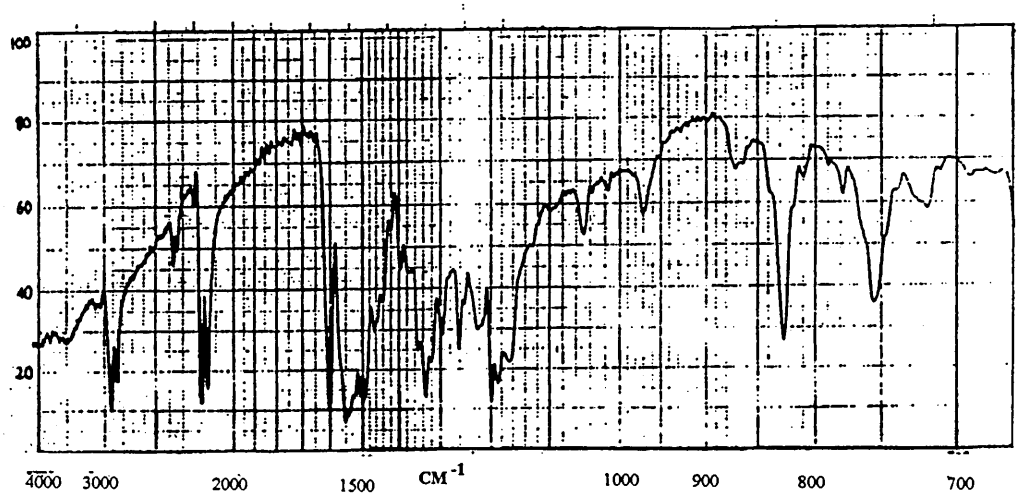

Fig. 3-4 Infrared spectrum of N-hexadecylquinolinium adduct of TCNQ

Table 3-2
Microanalysis of N-hexadecylquinolinium adduct of TCNQ

formula: $C_{37}H_{44}N_4$ (544.78)

	C	H	N
theory	81.58	8.14	10.28
found	80.54	8.01	10.08

A wide charge transfer band at 700 nm was found in its uv-vis spectrum, which was consistent with the literature.[4,5,6] Microanalysis of the product (Table 3-2) indicated that it should be N-hexadecylquinolinium adduct of TCNQ.

3.4 Preparation of 4-[1-methyl-4(1H)-pyridylidene]-3-phenyl-5(4H)-isoxazolone

This compound is a type of merocyanine dye, which has an extensive conjugated system. It was expected that this dye would show solvatochromism and might respond to some of the toxic gases. Preparation of the dye, 4-[1-methyl-4(1H)-pyridylidene]-3-phenyl-5(4H)-isoxazolone, was following the procedures described by Brooker et al.[2] A simple reaction scheme for preparation of the dye and two resonance structures of this dye are showed in Fig. 3-5 (A) and (B).

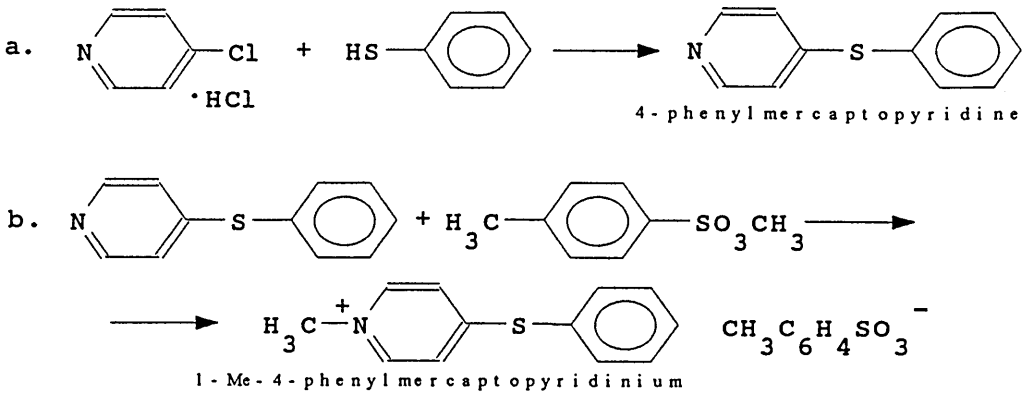

Fig. 3-5 (A)

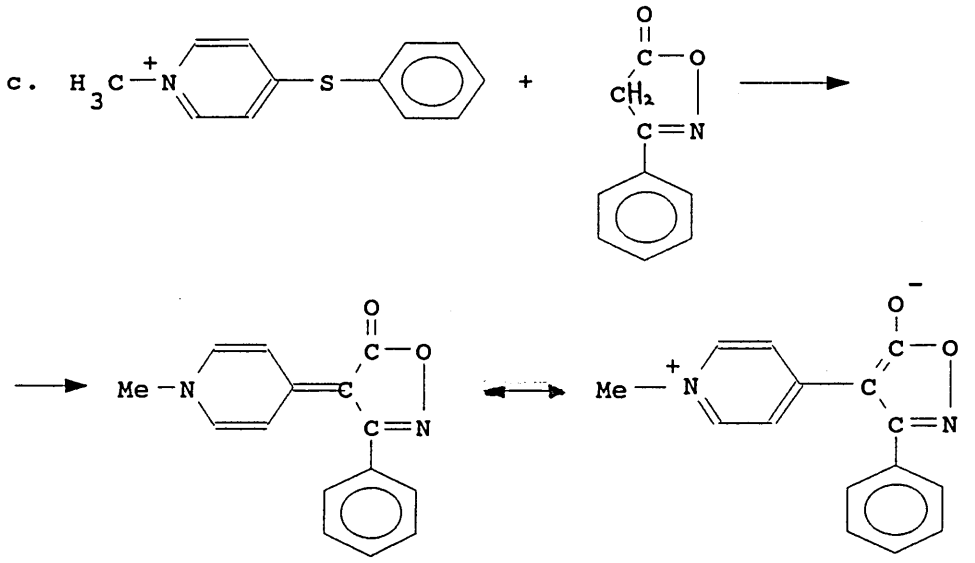

Fig. 3-5 (B) Reaction scheme for preparation of 4-[1-methyl-4(1H)-pyridylidene]-3-phenyl-5(4H)-isoxazolone and its resonance structures

(i) Triethylamine (Aldrich, 20 g, 0.2 moles) was added in small portions, with shaking, to a mixture of 4-chloropyridine hydrochloride (Aldrich, 15 g, 0.1 moles) and of thiophenol (Aldrich, 22 g, 0.2 moles). The reaction mixture became warm and was heated under nitrogen at 100 °C for two days. It was then made alkaline with NaOH solution and extracted four times with 500 ml of benzene. The combined extracts were washed with NaOH solution and solvent was taken off by a rotary evaporator. After distillation under 4 mmHg vacuum, a pale yellow oil, 4-phenylmercaptopyridine (18.2 g, yield:97%), was obtained.

(ii) Crude 4-phenylmercaptopyridine (9.4 g, 0.05 moles) was mixed with methyl p-toluenesulfonate (Aldrich, 9.3 g, 0.05 moles) and heated at 100 °C for 16 hours. The reaction mixture was left overnight and a viscous material product, 1-methyl-4-phenylmercaptopyridinium p-toluenesulfonate (13.2 g, yield: 71%), was obtained. The viscous mass was washed with ether and used without further purification.

(iii) 1-methyl-4-phenylmercaptopyridinium p-toluenesulfonate (3.8 g, 10 mmoles) and 3-phenyl-5-isoxazolone (Aldrich, 1.6 g, 10 mmoles) were dissolved in 30 ml ethanol. 5% excess triethylamine was added to the mixture. The reaction mixture was allowed to reflux for 30 mins.. After removing solvent, pale yellow crystals were generated as final product by cooling and vacuum filtering. 1.95 g pure product was obtained in 77% yield after recrystallising from ethanol and its melting point is 294 to 295 °C.

An infrared spectrum of final product was recorded in a KBr disc (Fig.3-6). Two bands at 2900 and 2840 cm^{-1} were assigned to C-H stretch from CH_3^-. The bands at 1650 and 1540 cm^{-1} were thought of as C=O and aromatic C=C stretch. The bands found at 1210 and 1105 cm^{-1} were considered to be C-H def. absorptions from the pyridine ring.

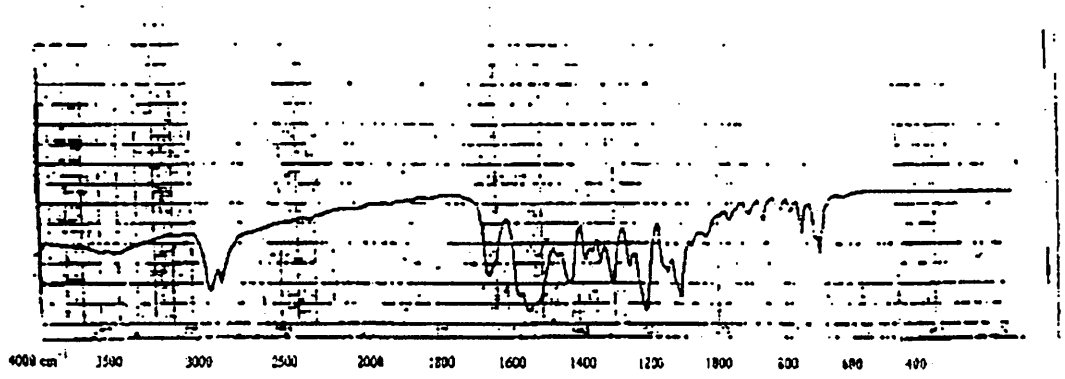

Fig. 3-6 Infrared spectrum of 4-[1-methyl-4(1H)-pyridylidene]-3-phenyl-5(4H)-isoxazolone

Microanalysis results of the product are shown in Table 3-3, which indicated that the resulting product was the compound expected.

Table 3-3

Microanalysis of 4-[1-methyl-4(1H)-pyridylidene]-3-phenyl-5(4H)-isoxazolone

formula: $C_{15}H_{12}N_2O_2$ (252.27)

	C	H	N
theory	71.42	4.79	11.10
found	71.46	4.87	11.15

3.5 Preparation of 3-ethyl-5-[1-ethyl-2(1H)-pyridylidene]-rhodanine

3-ethyl-5-[1-ethyl-2(1H)-pyridylidene]-rhodanine is also a merocyanine dye with a conjugated system, synthesised by Brooker et al.[2] Resonance structures of the dye are showed in Fig. 3-7.

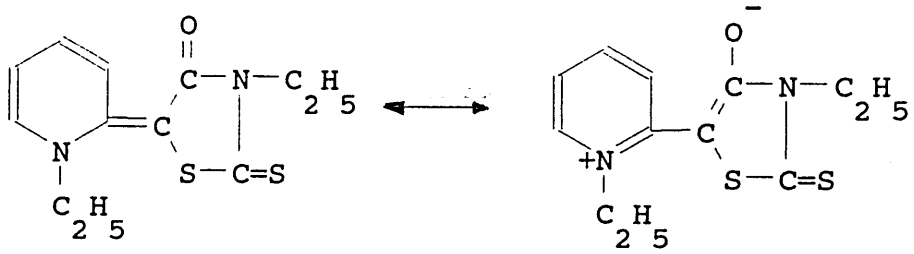

Fig. 3-7 Resonance structures of
3-ethyl-5-[1-ethyl-2(1H)-pyridylidene]-rhodanine

Preparation of the dye was carried out in the same way as that of 4-[1-methyl-4(1H)-pyridylidene]-3-phenyl-5(4H)-isoxazolone, only some starting materials were changed. 2-chloropyridine was used instead of 4-chloropyridine hydrochloride in step a), ethyl p-toluene sulfonate instead of methyl p-toluene sulfonate in step b), and 3-ethylrhodanine instead of 3-phenyl-5-isoxazolone in step c).[2] Same molar amounts of reagents were used as those used in preparation of 4-[1-methyl-4(1H)-pyridylidene]-3-phenyl-5(4H)-isoxazolone. The yields

were 18.7 g (97%) 2-phenylmercaptopyridine, 14.5 g (70%) 1-ethyl-2-phenylmercaptopyridinium p-toluenesulfonate, and 2.34 g (88%) 3-ethyl-5-[1-ethyl-2(1H)-pyridylidene]-rhodanine for the products in three different steps.

An infrared spectrum of the final product was recorded in a KBr disc (Fig.3-8). Bands consistent with the expected molecular structure were found. The strong bands below 3000 cm^{-1} in the spectrum were assigned to aliphatic C-H stretch. the bands from 1640 to 1670 cm^{-1} were thought of as C=O and C=C stretch. A C=S stretch band was found at 1220 cm^{-1} and a C-H bending band from pyridine ring was found at 1110 cm^{-1}.

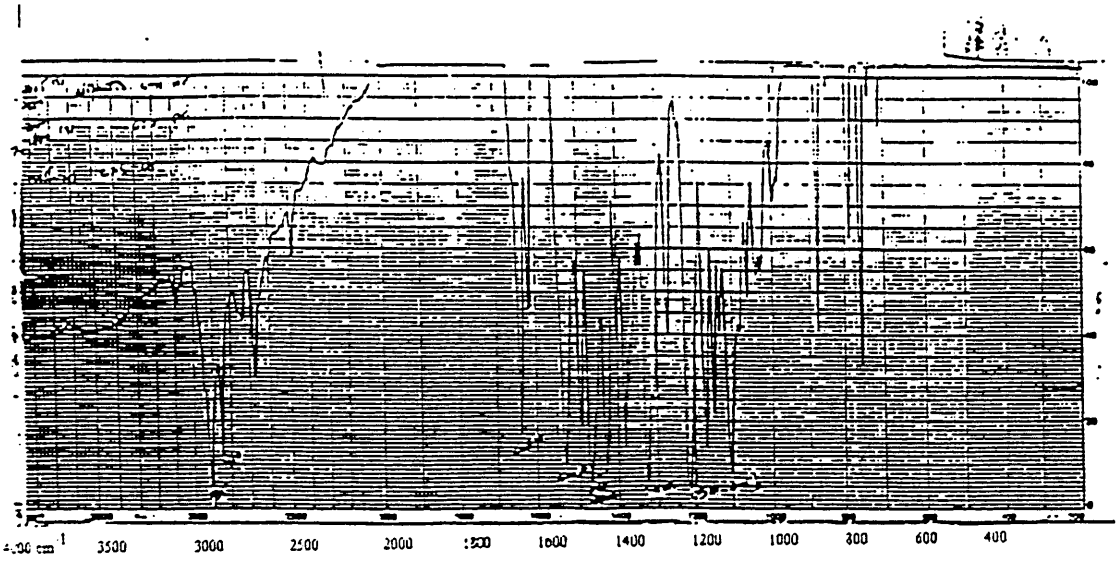

Fig. 3-8 Infrared spectrum of 3-ethyl-5-[1-ethyl-2(1H)-pyridylidene]-rhodanine

A mass spectrum of the product was recorded and the major peaks correlated to fragment structures as showed in Fig. 3-9.

Microanalysis of the product (Table 3-4) showed that it should be 3-ethyl-5-[1-ethyl-2(1H)-pyridylidene]-rhodanine, and its melting point is 145 - 146 °C.

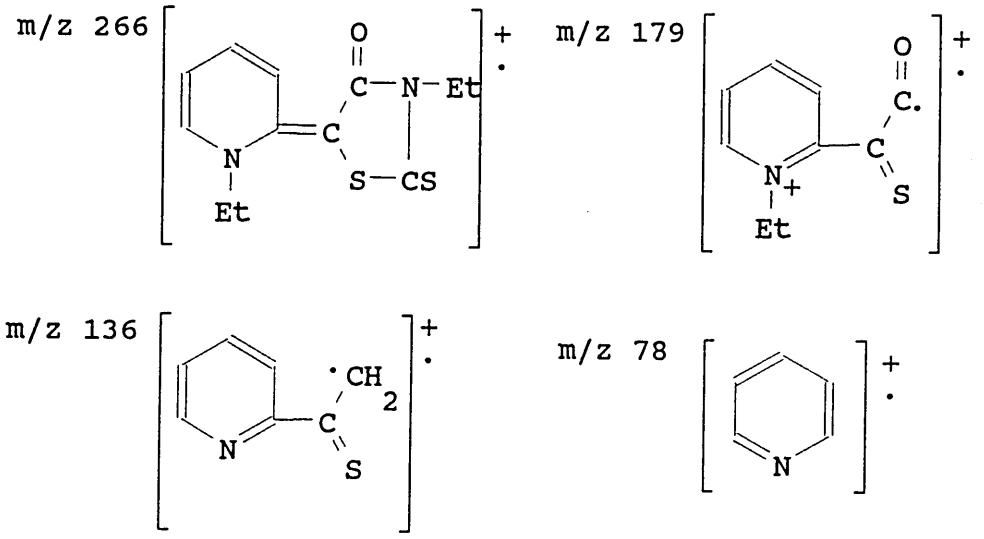

Fig. 3-9 Proposed fragments corresponding to the peaks found in mass spectrum of the product

Table 3-4

Microanalysis of 3-ethyl-5-[1-ethyl-2(1H)-pyridylidene]-rhodanine

formula: $C_{12}H_{14}N_2OS_2$ (266.38)

	C	H	N
theory	54.11	5.30	10.52
found	54.08	5.26	10.47

3.6 Synthesis of 3-ethyl-5-[1-dodecyl-2(1H)-pyridylidene]-rhodanine and 3-ethyl-5-[1-hexadecyl-2(1H)-pyridylidene]-rhodanine

These two dyes were synthesised by modification of the synthesis for 3-ethyl-5-[1-ethyl-2(1H)-pyridylidene]-rhodanine described in section 3.5. The purpose was to attach a long carbon chain to the dye so that a hydrophobic end would be produced. A simple reaction scheme is showed in Fig. 3-10.

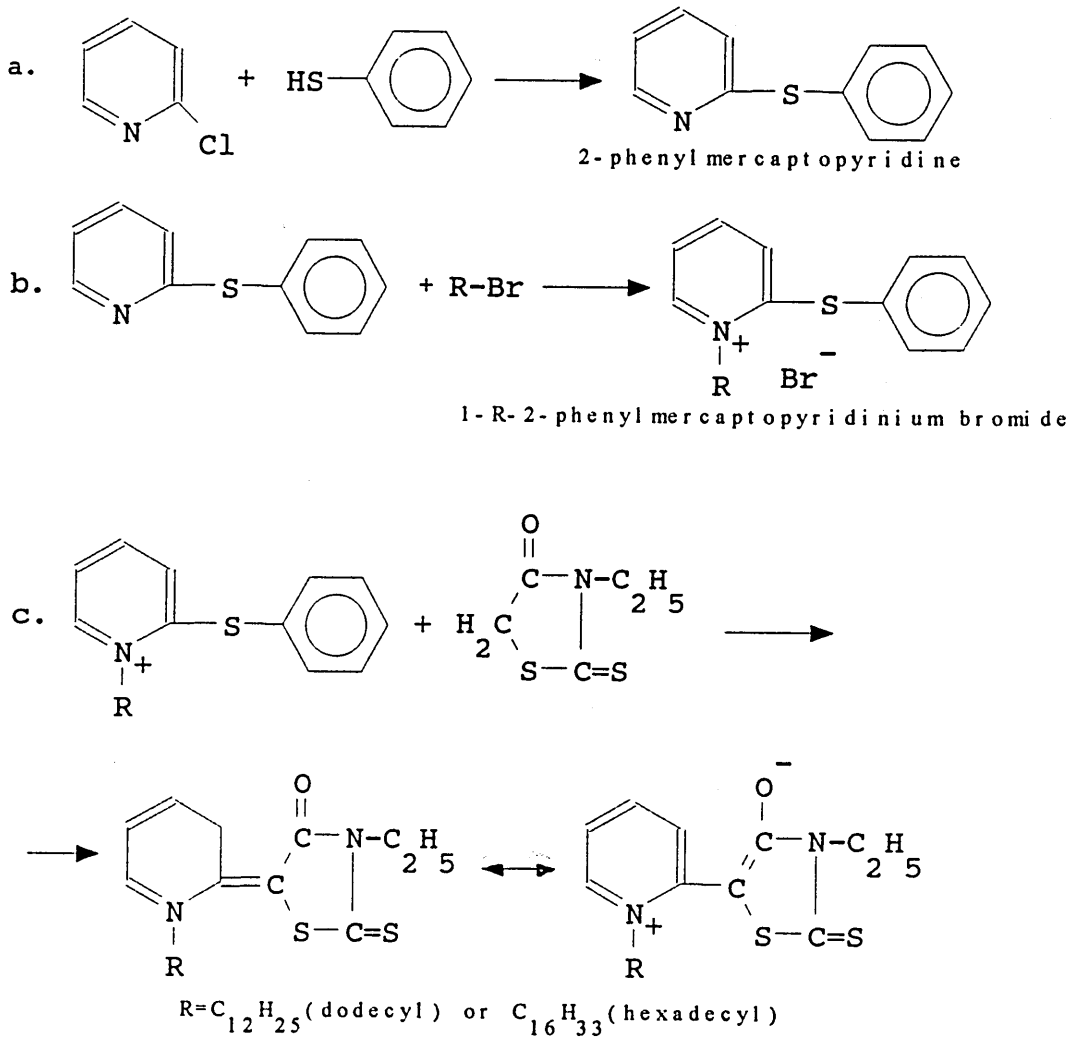

Fig. 3-10 Reaction scheme for preparation of 3-ethyl-5-[1-dodecyl-2(1H)-pyridylidene]-rhodanine and 3-ethyl-5-[1-hexadecyl-2(1H)-pyridylidene]-rhodanine, and their resonance structures

(i) 2-phenylmercaptopyridinium (1.9 g, 10 mmoles) produced in section 3.5 was mixed with 1-bromododecane (Aldrich, 2.5 g, 10 mmoles), or with 1-bromohexadecane (Aldrich, 3.1 g, 10 mmoles). The mixture was heated at 120-130 °C in an oil-bath for two days. The reaction mixture became brown and was left overnight. A brown viscous material, 1-dodecyl-2-phenylmercapto-pyridinium bromide (3.2 g, yield: 73%), or 1-hexadecyl-2-

phenylmercaptopyridinium bromide (3.9 g, yield: 79%) was generated. It was washed with ether and directly used for the next step without further purification.

(ii) Equimolar amounts (10 mmoles) of 1-dodecyl-2-phenylmercapto-pyridinium bromide (or 1-hexadecyl-2-phenylmercapto-pyridinium bromide) and 3-ethylrhodanine (Lancaster) were dissolved in 30 ml of ethanol, and 5% excess of triethylamine was added. The reaction mixture was refluxed for a half hour. After removing the bulk of the solvent, a red orange solid product was obtained by cooling and vacuum filtering. it was purified by recrystallising from methanol. The yields were 2.31 g (57%) for 3-ethyl-5-[1-dodecyl-2(1H)-pyridylidene]-rhodanine (m.p. 201 to 202 °C) and 2.45g (53%) for 3-ethyl-5-[1-hexadecyl-2(1H)-pyridylidene]-rhodanine (m.p. 213 to 214 °C).

Infrared spectra of both final products were recorded in KBr disc, showed in Fig. 3-11 and 3-12. Expected characteristic bands were found in both spectra. For example, aliphatic C-H stretch bands were found at below 3000 cm^{-1}, and C=O and C=C stretch bands were found at about 1600 and 1500 cm^{-1}.

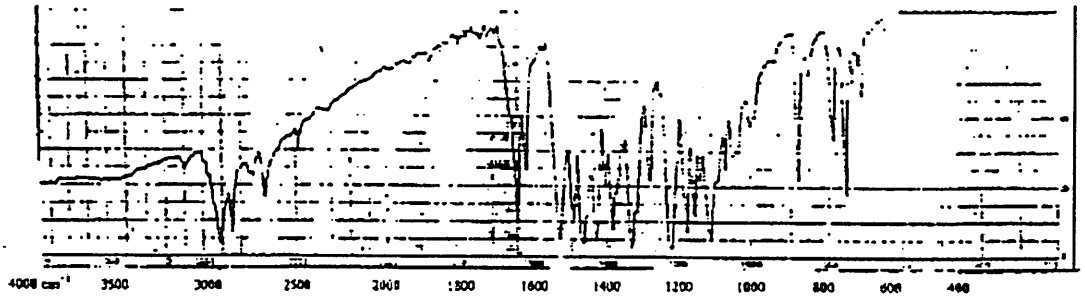

Fig. 3-11 Infrared spectrum of 3-ethyl-5-[1-dodecyl-2(1H)-pyridylidene]-rhodanine

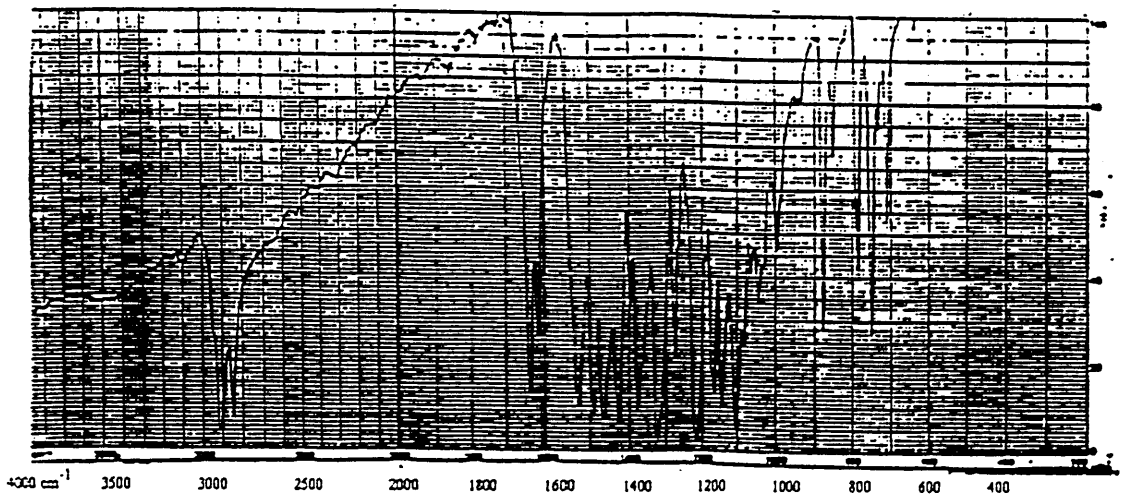

Fig. 3-12 Infrared spectrum of and 3-ethyl-
5-[1-hexadecyl-2(1H)-pyridylidene]-rhodanine

Mass spectra of two final products were taken as well. Some peaks corresponding to proposed fragments were found and assignments are given in Fig. 3-13 (A) and (B).

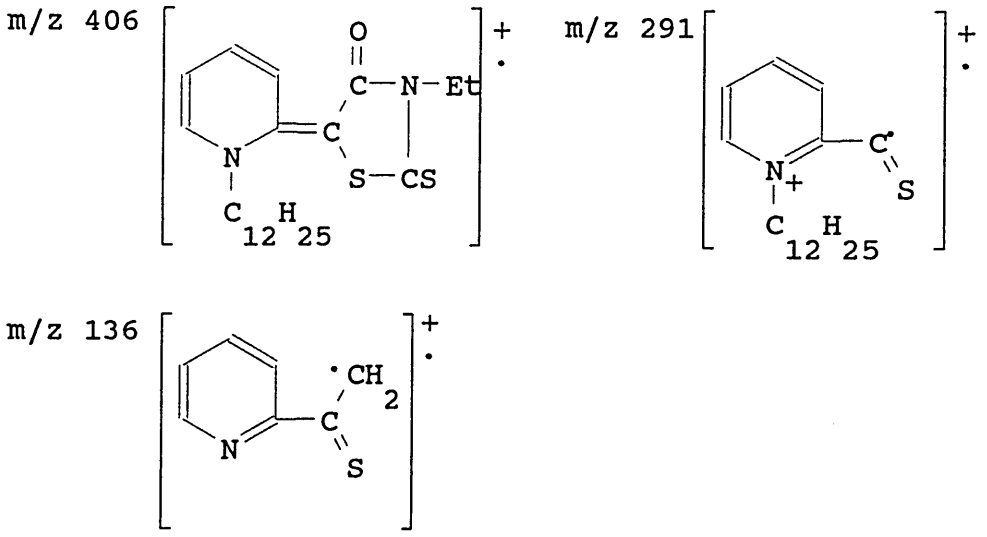

for dye 3-ethyl-5-[1-dodecyl-2(1H)-pyridylidene]-rhodanine

Fig.3-13 (A)

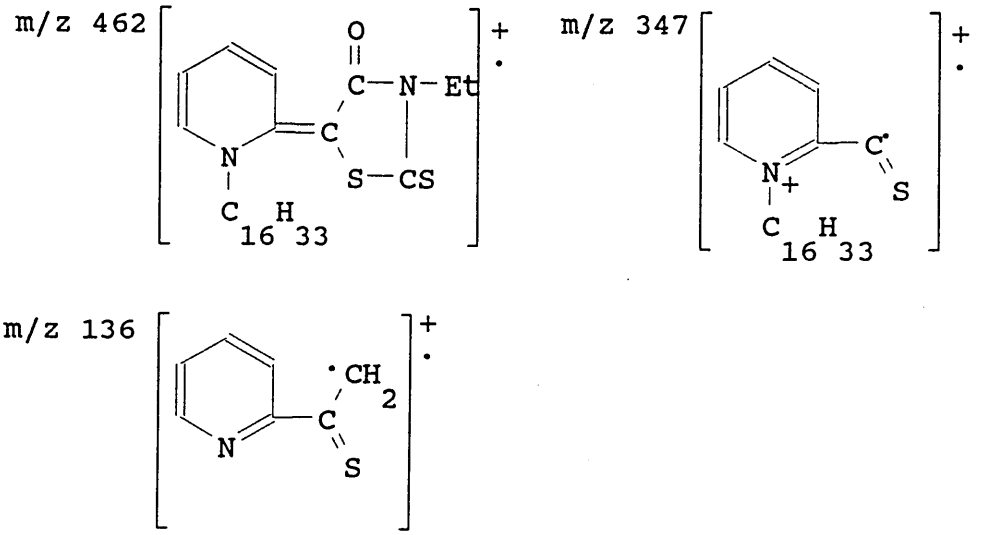

for dye 3-ethyl-5-[1-hexadecyl-2(1H)-pyridylidene]-rhodanine

Fig. 3-13 (B) Proposed fragments corresponding to the peaks found in the mass spectra of the two final products

Microanalysis of the two products (Table 3-5) indicated that they are the expected dye compounds, 3-ethyl-5-[1-dodecyl-2(1H)-pyridylidene]-rhodanine and 3-ethyl-5-[1-hexadecyl-2(1H)-pyridylidene]-rhodanine.

Table 3-5

Microanalysis of 3-ethyl-5-[1-dodecyl-2(1H)-pyridylidene]-rhodanine (A) and 3-ethyl-5-[1-hexadecyl-2(1H)-pyridylidene]-rhodanine (B)

(A) formula: $C_{22}H_{34}N_2OS_2$ (406.64)

	C	H	N
theory	54.11	5.30	10.52
found	54.08	5.26	10.47

(B) formula: $C_{26}H_{42}N_2OS_2$ (462.75)

	C	H	N
theory	67.48	9.15	6.05
found	67.75	9.53	5.92

3.7 Synthesis of 3-ethyl-5-{[1-dodecyl-2(1H)-pyridylidene]-ethylidene}-rhodanine and 3-ethyl-5-{[1-hexadecyl-2(1H)-pyridylidene]-ethylidene}-rhodanine

These two dyes were synthesised from a further modification of the process for 3-ethyl-5-[1-dodecyl-2(1H)-pyridylidene]-rhodanine and 3-ethyl-5-[1-hexadecyl-2(1H)-pyridylidene]-rhodanine. The conjugation system of the two compounds were lengthened by introducing an ethylidene group. The resonance structures of the dyes are showed in Fig. 3-14.

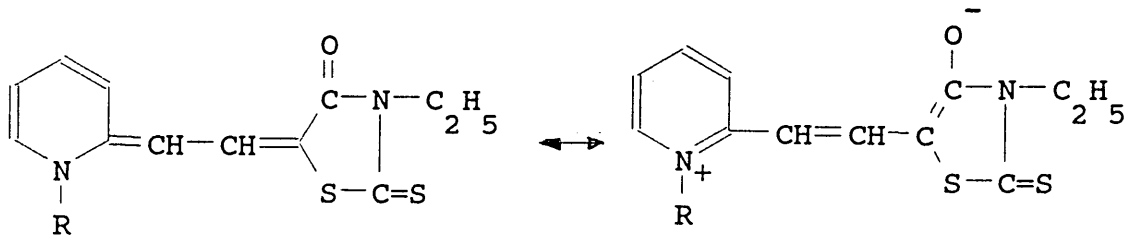

R=dodecyl($C_{12}H_{25}$) or hexadecyl ($C_{16}H_{33}$)

Fig. 3-14 Resonance structures of 3-ethyl-5-{[1-dodecyl-2(1H)-pyridylidene]-ethylidene}-rhodanine and 3-ethyl-5-{[1-hexadecyl-2(1H)-pyridylidene]-ethylidene}-rhodanine

A simple reaction scheme is presented in Fig. 3-15. Reagents 5-anilinomethylene-3-ethylrhodanine and 5-acetanilidomethylene-3-ethylrhodanine were prepared in the steps b) and c) according to the procedures described by Brooker.[2]

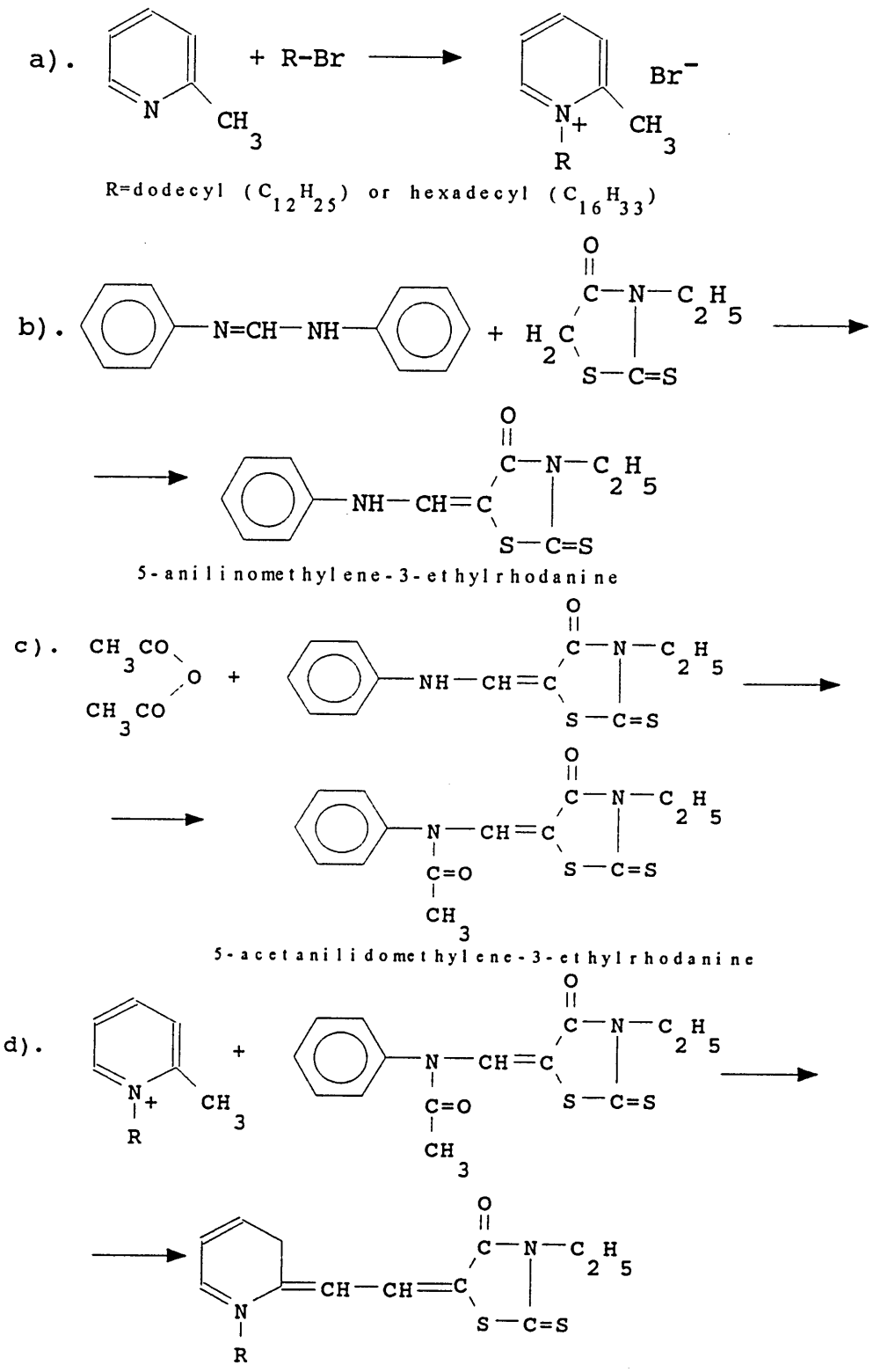

Fig. 3-15 Reaction scheme for preparation of 3-ethyl-5-{[1-R-2(1H)-pyridylidene]-ethylidene}-rhodanine

a) 2-picoline (20 mmoles) was mixed with 1-bromododecane or 1-bromohexadecane (20 mmoles) in a refluxing apparatus and heated gently on a hot plate for two days. The first product, 1-dodecyl-2-methylpyridinium bromide was obtained as a gelatinous solid (4.37 g, yield: 61%) and the second, 1-hexadecyl-2-methylpyridinium bromide, was obtained as a viscous material (4.81 g, yield: 58%) after the reaction mixtures had cooled to room temperature. They were washed with ether and dried by vacuum filtering.

Infrared spectra of the two products with different carbon chains from step a) were recorded and are showed in Figs. 3-16 and 3-17. Characteristic bands for aliphatic C-H stretch at about 2900 cm^{-1} were found in both spectra, which revealed that the long carbon chain had been attached to the 2-picoline. Their microanalysis (Table 3-6) showed that their compositions were consistent with the desired structures.

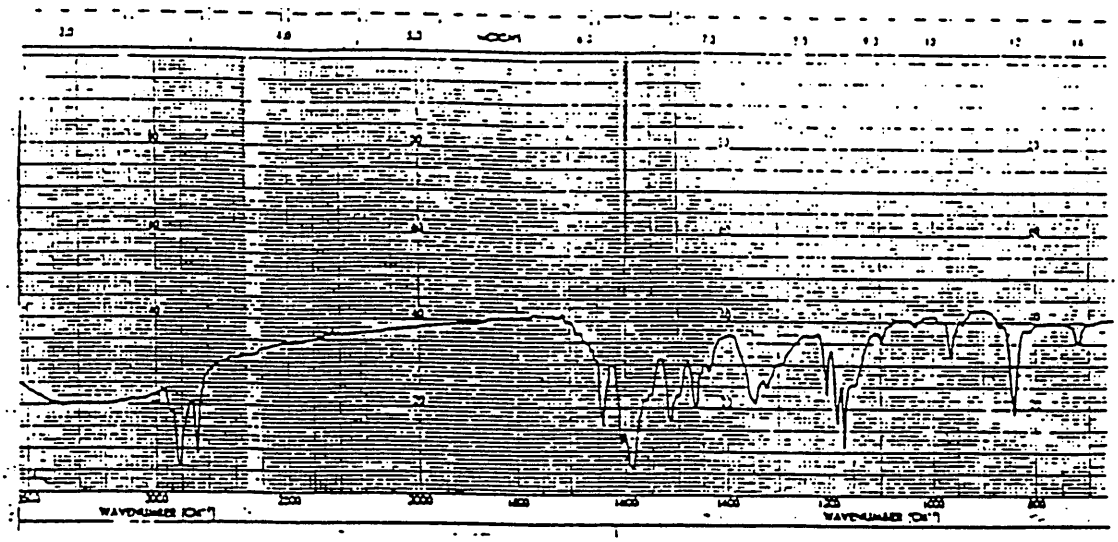

Fig. 3-16 Infrared spectrum of 1-dodecyl-2-methylpyridinium bromide

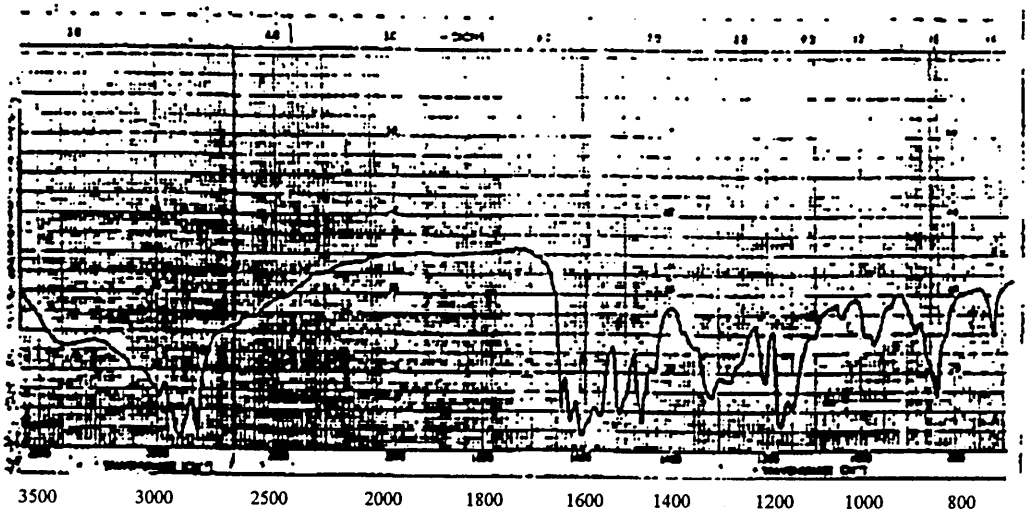

Fig. 3-17 Infrared spectrum of 1-hexadecyl-2-methylpyridinium bromide

Table 3-6

Microanalysis of 1-dodecyl-2-methylpyridinium bromide (A) and 1-hexadecyl-2-methylpyridinium bromide (B)

(A) formula: $C_{18}H_{32}NBr$ (342.36)

	C	H	N
theory	63.15	9.42	4.09
found	63.12	9.51	4.07

(B) formula: $C_{22}H_{40}NBr$ (398.47)

	C	H	N
theory	66.31	10.12	3.52
found	66.33	10.05	3.47

b) Diphenylformamidine (Aldrich, 3.9 g, 20 mmoles) and 3-ethylrhodanine (Lancaster, 3.2 g, 20 mmoles) were dissolved in 150 ml of kerosene and heated at 120 °C in an oil-bath for one day with stirring. Filtration and washing with methyl alcohol gave a yellow needle-like product (4.43 g), 5-

anilinomethylene-3-ethylrhodanine (yield: 84%). It was purified by recrystallising from 98% acetic acid.

c) The 5-anilinomethylene-3-ethylrhodanine (3.0 g, 11 mmoles) produced was heated for 10 mins. at 100 °C in 30 ml of acetic anhydride with triethylamine (3 g). A light yellow needle-like product, 5-acetanilidomethylene-3-ethyl-rhodanine (3.01 g, yield: 89%), was formed after cooling and filtering. It was recrystallised from methyl alcohol.

d) The 5-acetanilidomethylene-3-ethylrhodanine(1.53g, 5 mmoles) and 1-dodecyl-2-picolinium bromide (1.25 g, 5 mmoles) (A) or 1-hexadecyl-2-picolinium bromide (1.99 g, 5 mmoles) (B) were dissolved in 5 ml of pyridine, and 5% excess of triethylamine was added. The mixture was refluxed for 10 mins. A purple solid (1.54 g, 71% yield; m.p. 232-233 °C) for (A) and a purple solid product (1.61 g, 66% yield; m.p. 245 to 246 °C) with blue reflex for (B) were obtained after cooling and filtering. They were purified by recrystallising twice from methyl alcohol.

Two infrared spectra of the final products from step d), (one should be 3-ethyl-5-{[1-dodecyl-2(1H)-pyridylidene]-ethylidene}-rhodanine and the other should be 3-ethyl-5-{[1-hexadecyl-2(1H)-pyridylidene]-ethylidene}-rhodanine) were recorded in KBr discs. The spectra are showed Figs. 3-18 and 3-19. Two bands at about 2900 and 2840 cm^{-1} were assigned to aliphatic C-H stretch. The band at 1650 cm^{-1} was thought of as C=O stretch and band at 1540 cm^{-1} was thought of as C=C stretch. Characteristic C-N and C=S stretches were found at about 1310 and 1210 cm^{-1}

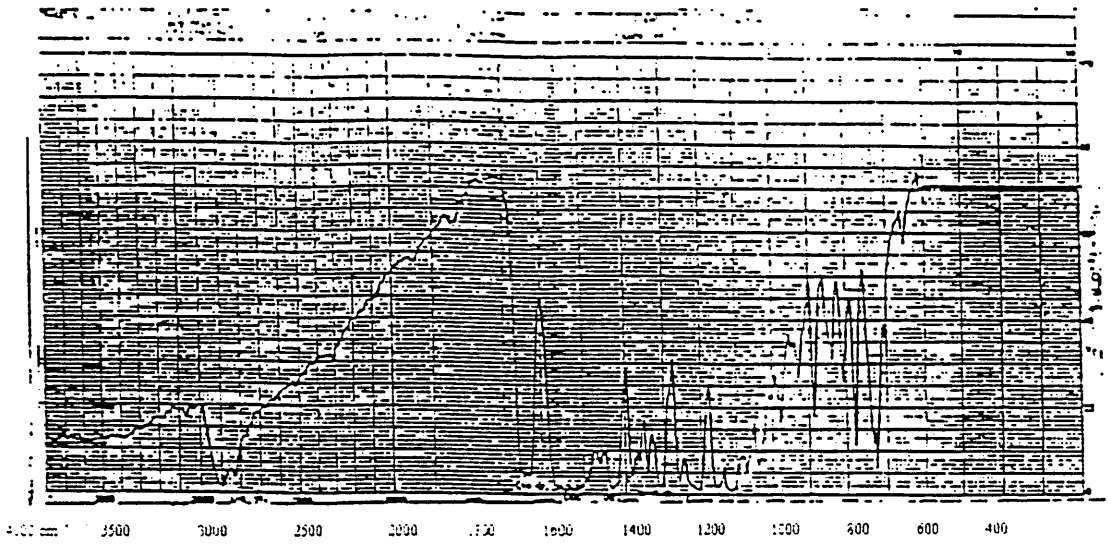

Fig. 3-18 Infrared spectrum of 3-ethyl-5-{[1-dodecyl-2(1H)-pyridylidene]-ethylidene}-rhodanine

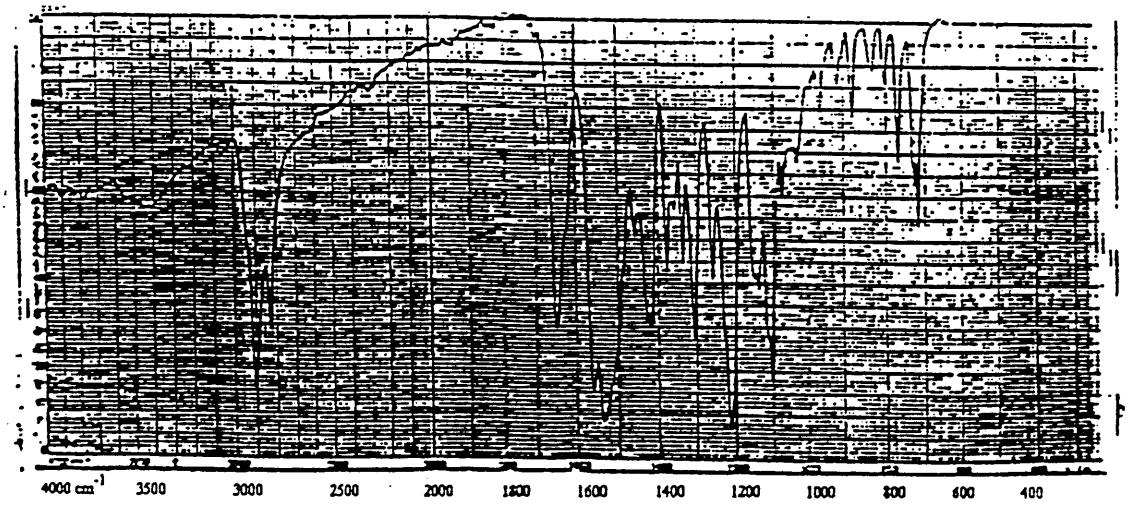

Fig. 3-19 Infrared spectrum of 3-ethyl-5-{[1-hexadecyl-2(1H)-pyridylidene]-ethylidene}-rhodanine

Mass spectra of the two products were recorded as well. Some peaks corresponding to fragment structures were found and are showed in Fig. 3-20.

for the compound R=dodecyl for the compound R=hexadecyl

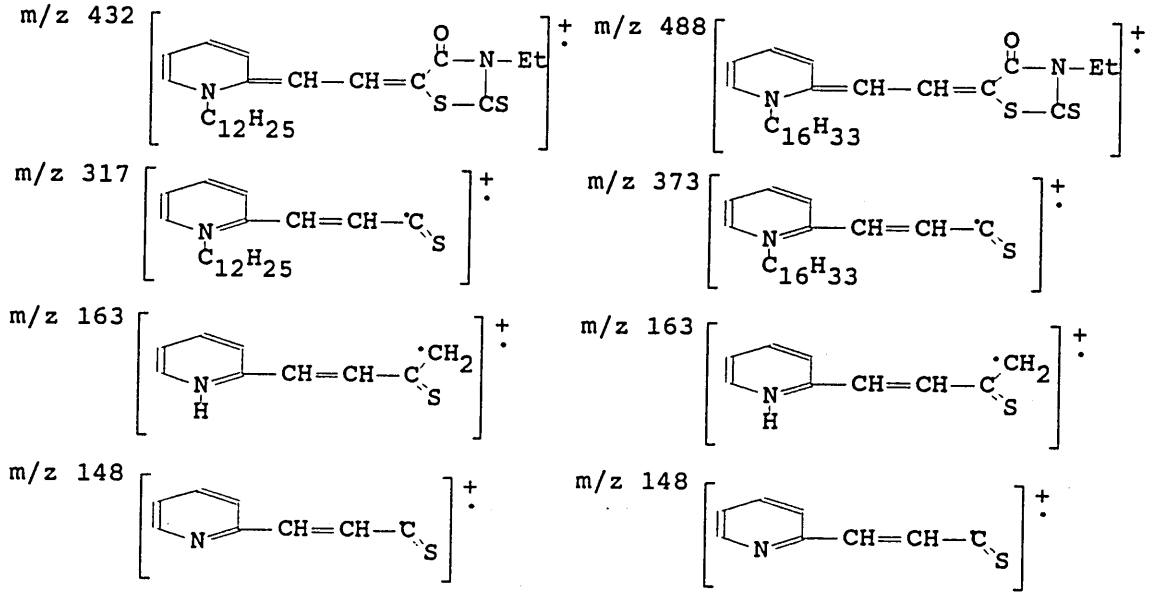

Fig. 3-20 Proposed fragments corresponding to the peaks found in the mass spectra of the two final products

Microanalysis results of the two final products are listed in Table 3-7, they are consistent with theoretical data and indicate that these two products are the compounds expected.

Table 3-7

Microanalysis of 3-ethyl-5-{[1-dodecyl-2(1H)-pyridylidene]-ethylidene}-rhodanine (A) and 3-ethyl-5-{[1-hexadecyl-2(1H)-pyridylidene]-ethylidene}-rhodanine (B)

(A) formula: $C_{24}H_{36}N_2OS_2$ (432.68)

	C	H	N
theory	66.62	8.39	6.47
found	66.60	8.44	6.35

(B) formula: $C_{28}H_{44}N_2OS_2$ (488.79)

	C	H	N
theory	68.80	9.07	5.73
found	68.82	9.17	5.79

3.8 Synthesis of 1-hexadecyl-4-[(4-oxocyclohexadienylidene)-ethylidene]-1,4-dihydropyridine[8,9]

This dye is also a type of merocyanine. It was modified from 1-methyl-4-[(4-oxocyclohexadienylidene)-ethylidene]-1,4-dihydropyridine (synthesised by Brooker et al.[8]) by introducing a long carbon chain. A simple reaction route is presented in Fig. 3-21, with two resonance structures of the dye.

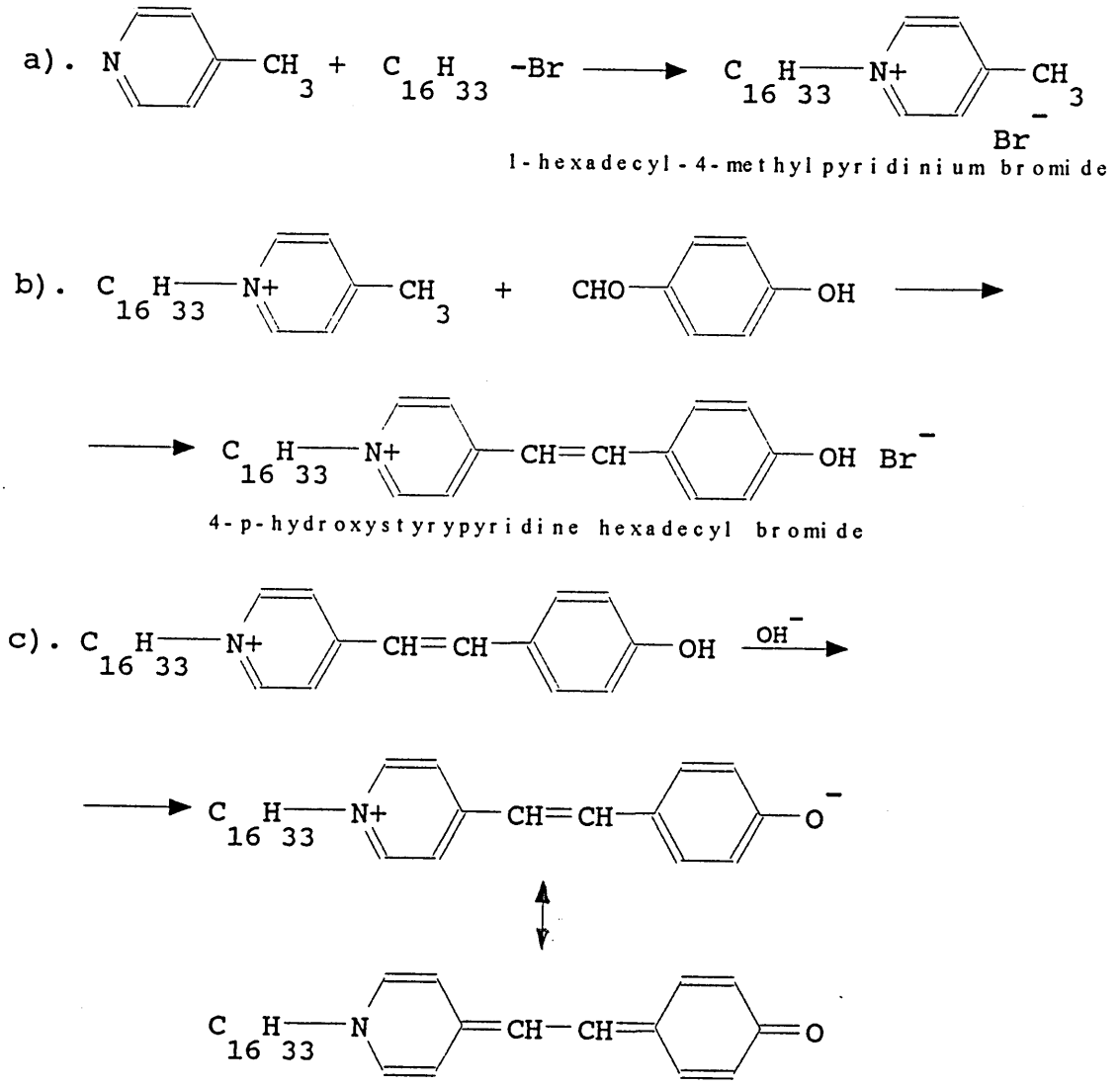

Fig. 3-21 Reaction scheme for preparation of 1-hexadecyl-4-[(4-oxocyclohexadienylidene)-ethylidene]-1,4-dihydropyridine and its resonance structures

a) 1-bromohexadecane (Aldrich, 6.12 g, 20 mmoles) was mixed with 4-picoline(Aldrich, 1.89 g, 20 mmoles). The mixture was heated gently on a hotplate for two days and left overnight. A light brown solid, 1-hexadecyl-4-methylpyridinium bromide (7.01 g, yield: 88%), was obtained after filtering and washing with ether.

An infrared spectrum of the product from the step a) was recorded in a KBr disc, and showed in Fig. 3-22. Typical aliphatic C-H stretch bands were found at about 2900 cm^{-1}, which revealed that the long carbon chain was attached to the 4-picoline.

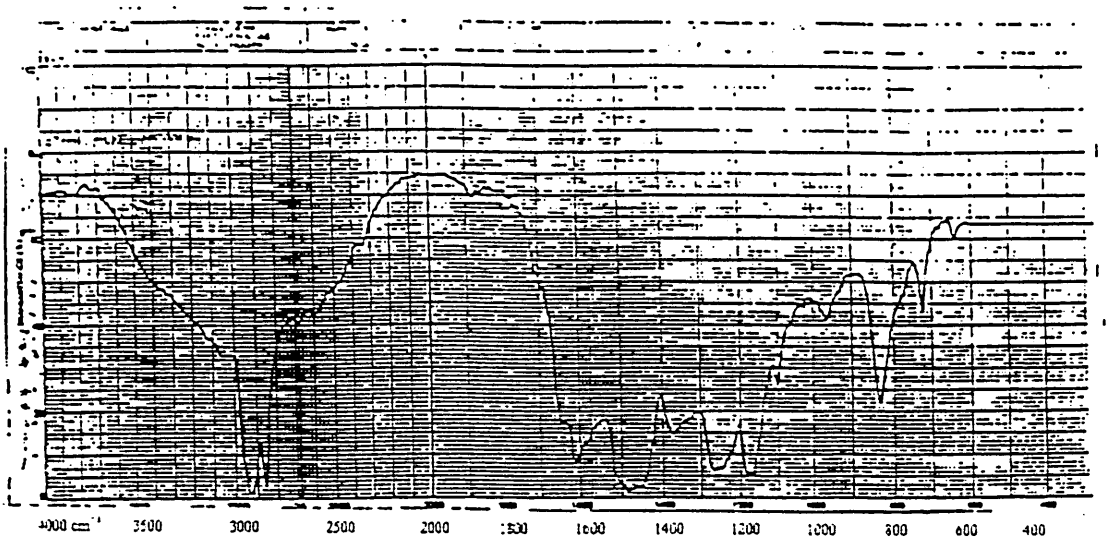

Fig. 3-22 Infrared spectrum of 1-hexadecyl-4-methylpyridinium bromide

b) 8.01 g (20 mmoles) of the 1-hexadecyl-4-methylpyridinium bromide generated and 4-hydroxybenzaldehyde (Aldrich, 3.6 g, 30 mmoles) were mixed and dissolved in 30 ml of methanol with 1 ml of piperidine as a catalyst. The reaction mixture was refluxed on a steam-bath for a period of seven hours. The colour of the mixture became red-brown. After cooling with ice, a red-brown solid product, 4-p-hydroxystyrylpyridine hexadecyl bromide (5.5 g, yield: 57%), was generated. It was recrystallised twice from methanol.

An infrared spectrum of the compound generated from step b) was also recorded in a KBr disc, some expected bands were found as well (Fig. 3-23). For example, a broad O-H stretch band was found at about 3400 cm^{-1} and aliphatic C-H stretch bands were found 2920 and 2850 cm^{-1}.

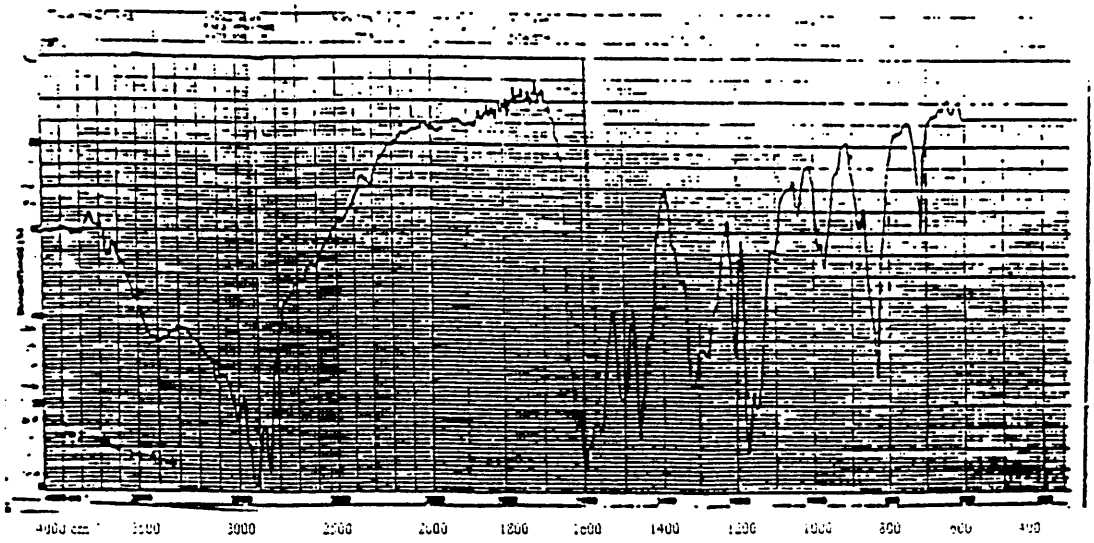

Fig. 3-23 Infrared spectrum of 4-p-hydroxystyrylpyridine hexadecyl bromide

Microanalysis of the compound produced (Table 3-8) indicated that results were consistent with theoretic data and it should be 4-p-hydroxystyrylpyridine hexadecyl bromide.

Table 3-8

Microanalysis of 4-p-hydroxystyrylpyridine hexadecyl bromide.

formula: $C_{29}H_{44}NOBr$ (502.58)

	C	H	N
theory	69.31	8.82	2.79
found	69.44	9.16	2.86

c) 1 g of the 4-p-hydroxystyryl-pyridine hexadecyl bromide produced was dissolved in 10 ml of acetone, and 25 ml of concentrated ammonia were added to the mixture. It was stirred for 3 hours. A bright red-brown solid appeared after acetone was evaporated. 0.74 g solid product (yield: 89%) was obtained by means of vacuum filtration. It was recrystallised from acetone, and its melting point was found being 258 to 259 °C.

The infrared spectrum (Fig. 3-24) of final product from step c) shows its characteristic structural groups. The constitution of the product was confirmed by microanalysis (Table 3-9).

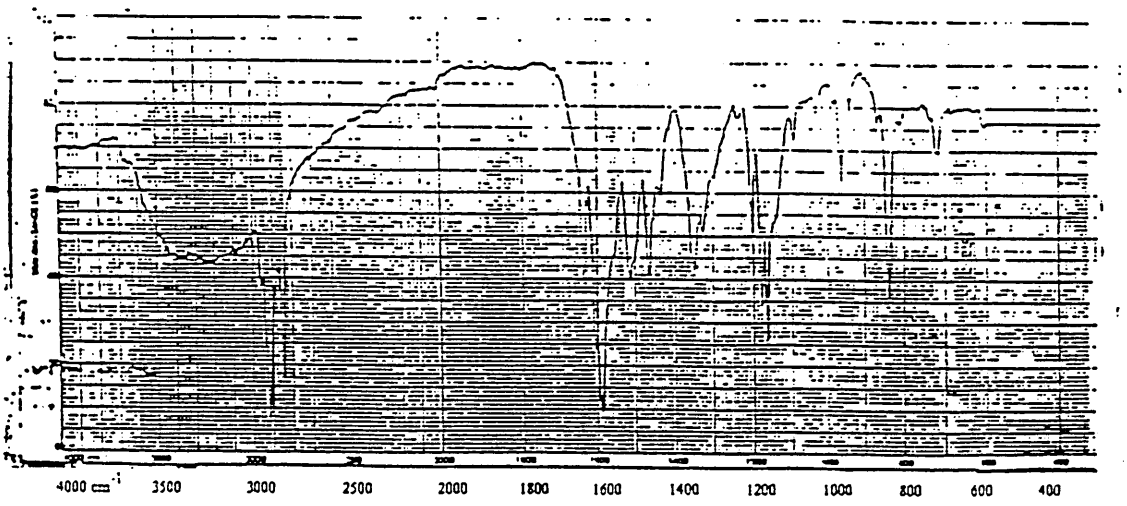

Fig. 3-24 Infrared spectrum of 1-hexadecyl-4-[(4-oxocyclohexadienylidene)-ethylidene]-1,4-dihydropyridine

Table 3-9

Microanalysis of 1-hexadecyl-4-[(4-oxocyclohexadienylidene)-ethylidene]-1,4-dihydropyridine

formula: $C_{29}H_{43}NO$ (421.67)

	C	H	N
theory	82.61	10.28	3.32
found	82.57	10.26	3.29

References:

1. L. G. S. Brooker, G. H. Keyes, R. H. Sprague, R. H. Vandyke, E. Vanlare, G. Vanzandt, and F. L. White, J. Am. Chem. Soc. 73, 5326 (1951).

2. L. G. S. Brooker, G. H. Keyes, R. H. Sprague, R. H. Vandyke, E. Vanlare, G. Vanzandt, F. L. White, H. W. J. Cressman, and S. G. Dent, J. Am. Chem. Soc. 73, 5332 (1951).

3. L. G. S. Brooker, G. H. Keyes, and W. W. Williams, J. Am. Chem. Soc. 64, 199 (1942).

4. G. J. Ashwell, E. J. C. Dawnay, A. P. Kuczynski, M. Szablewski, I. M. Sandy, M. R. Bryce, A. M. Grainger, and M. Hasan, J. Chem. Soc. Faraday Trans., 1990, 86(7), 1117-1121.

5. N. A. Bell, R.A. Broughton, J. S. Brooks, T. A. Jones, S. C. Thorpe, and G. J. Ashwell, J. Chem. Soc., Chem. Commun., 1990, p325.

6. R. A. Broughton, July, 1987, Transfer Report, sheffield City Polytechnic.

7. L. B. Cohen, B.M. Salzberg, H. V. Davila, W. N. Ross, D. Landowne, A. S. Waggoner, and C. H. Wang, J. Membrane Biol. 19, 1-36 (1974).

8. L. G. S. Brooker, G. H. Keyes and D. W. Heseltine, J. Am. Chem. Soc. 73, 5350 (1951).

9. A. P. Phillips, J. Org. Chem., 14, 302(1949).

Chapter 4

Synthesis of the solvatochromic compounds with a functional group

4.1 Introduction

A series of pyridinium N-phenoxide betaine dyes are known that possess solvatochromic properties, undergoing large solvent-induced absorbance shifts on transition from water to less polar solvents. They were well studied by Reichardt and Dimroth in the 1960s, and have been widely used as probes of solvent polarity.[1,2,3] These betaine dyes are of a special structural character, that is, their electronic ground state exists as a dipolar ion in which the nitrogen atom carries a positive charge and the oxygen atom carries a negative charge (Fig. 4-1).

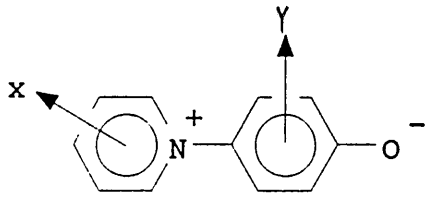

Fig. 4-1 Dipolar structure of the betaine dyes

They possess, therefore, very large ground-state dipole moments, which decrease significantly upon excitation due to intramolecular charge transfer. This is the basic reason for them having such high solvatochromism, which result in their uv-visible absorption spectra being highly solvent dependent. A very good example of these betaine dyes is 2,6-diphenyl-4-(2,4,6-triphenyl-N-pyridinio)-phenolate (popularly called ET-30). Its absorption maxima of longwave absorption are 453 nm in water and 764 nm in tetrahydrofuran (THF).[1] The longwave absorption band is due to intramolecular charge transfer excitation and shows the solvatochromism.

The reason for synthesis of solvatochromic compounds with a functional group is to link the compounds to a solid support by covalent binding. Although attachment of a compound to the solid matrix support can be made by physical adsorption, linkage by a covalent coupling that links the compound to the solid matrix support by a chemical reaction is more efficient and often desirable. Covalent linkage is generally more stable than physical attachment, so that it can last longer than the latter. This linking method has been widely used in biological systems for coupling an antibody with a solid matrix.[4,5,6,7,8,9] Some studies based on the use of immobilised dye on solid support as pH indicators by an adsorption technique have been reported.[10,11] Only a few examples of covalent coupling were found being used in chemical field; for example, an acid-base indicator has been successfully immobilised on quartz powder and on controlled pore glass by means of a silylation process.[12]

In the present work, the pyridinium N-phenoxide betaine dyes are chosen to be modified in order to synthesise some new compounds which not only have the solvatochromic properties, but also can be linked with a solid support by covalent binding via a chemical reaction. It is desirable that their solvatochromic properties should not be diminished after covalent linkage.

An amino group was introduced into the pyridinium N-phenoxide betaine dyes. The reasons for choice of the amino group are because it is reactive, reacts readily with many other functional groups such as -CHO and -NCS, which can be easily introduced into a solid support, and because it is easy to introduce a nitro group into the betaine dyes by nitration and then to reduce the nitro group into amino group.

For the most of the pyridinium N-phenoxide betaine dyes studied by Reichardt and Dimroth,[1,2,3] they possess a basic structure shown in Fig. 4-2.

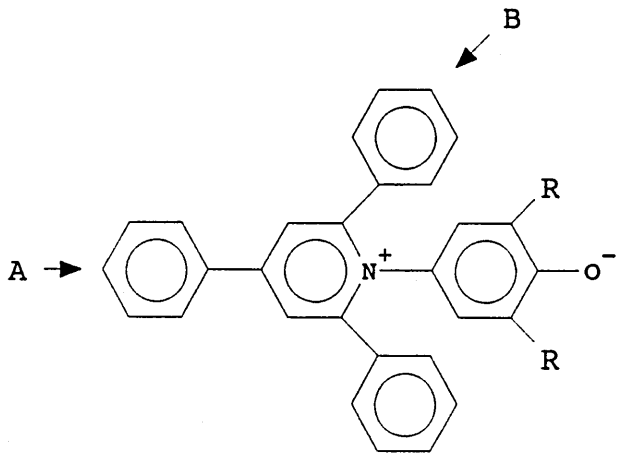

Fig. 4-2 Basic structure of the pyridinium N-phenoxide betaine dyes

It was attempted to introduce the amino group into A or B position of the betaine dyes. It is ideal to have the amino group on the one end of the dyes, i.e. A position, because it is on the p-position of the straight axial phenyl group of the dyes, would be easy to link to a solid support without space block affection. Introducing the amino group into B position was just for comparison with the A position.

In these dyes, the oxygen with a negative charge would be protonated at low or neutral pH. The protonated dyes are colourless and display no solvatochromism. Therefore, two R groups in the the pyridinium N-phenoxide betaine dyes are very important, because they can control the pKa values of the dyes. Based on this consideration, fluorine and chlorine, which have a high affinity, were used to replace the R groups, in order to reduce the pKa values of the dyes.

In the present work, syntheses of the pyridinium N-phenoxide betaine dyes were achieved in four main steps which are described as below:

4.1.1 Synthesis of pyrylium salt

The pyrylium salt was synthesised by two methods which are based on virtually the same mechanism.

a) by dehydrogenating condensation of unsaturated ketones with methyl ketones[13]

Using the following synthetic route (Fig. 4-3), a series of different pyrylium salts were produced.

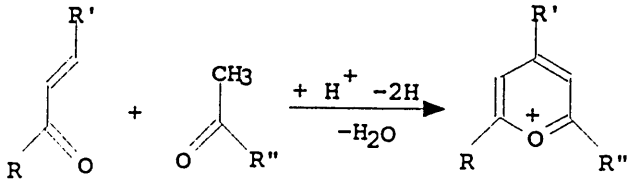

(A) (B) (C)

where R, R' R" are all aromatic groups

Fig. 4-3 Synthetic route of the pyrylium salts

Dilthey[14] discovered that chalcone reacted with acetophenone in acetic anhydride with ferric chloride to produce 2,4,6-triphenylpyrylium salt, and afterward this method was widely used to synthesise various 2,4,6-trisubstituted pyrylium salts. With aromatic groups R, R', and R", many pyrylium salts were generated and the results shown that the synthesis was generally successful.[15,16,17,18] For example, Dilthey synthesised 2-aryl-4,6-diphenyl-pyrylium either from (A, R=R'=Ph) and p-substituted acetophenones (B, R"=aryl) or from (A, R=aryl, R'=Ph) and acetophenone (B, R"=Ph), where the aryl was p-anisyl,[19] p-tolyl,[20] or p-bromophenyl.[20]

B) by dehydrogenative condensation of aromatic aldehyde with methyl ketone[13]

The following reaction route, Fig. 4-4, can also be used to prepare the pyrylium salt.

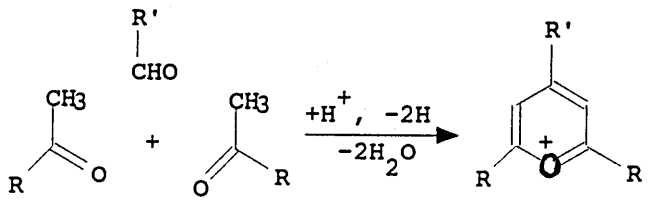

where R, R' are aromatic groups

Fig. 4-4 The synthetic route of the pyrylium salt from aromatic aldehyde and methyl ketone

The pyrylium salt can be formed when one mole of 4-nitrobenzaldehyde reacts with 2 moles of acetophenone in acid medium of BF_4H through the route of Fig. 4-4, where the R=Ph and R'=4-nitrophenyl. The reaction takes place firstly between one mole of 4-nitrobenzaldehyde and one mole of acetophenone to form the compound 4-nitrochalcone under the action of BF_4H.[21,22] The 4-nitrochalcone generated then reacts with acetophenone to produce the pyrylium salt, which follows the same reaction route showed in Fig. 4-3. Dilthey[20] thought the reaction type shown in Fig. 4-4 to be the most convenient method for preparation of the pyrylium salt. This reaction route has been used as standard method for preparing 2,4,6-triarylpyrylium salts with identical 2- and 6-substituents, in particular 2,4,6-triphenylpyrylium salts.[23,24,25,26]

4.1.2 Coupling of the pyrylium salts with aminophenol

The betaine salts can be obtained by a simple coupling reaction betwen pyrylium salts and aminophenol. The basic reaction route is showed in Fig. 4-5.

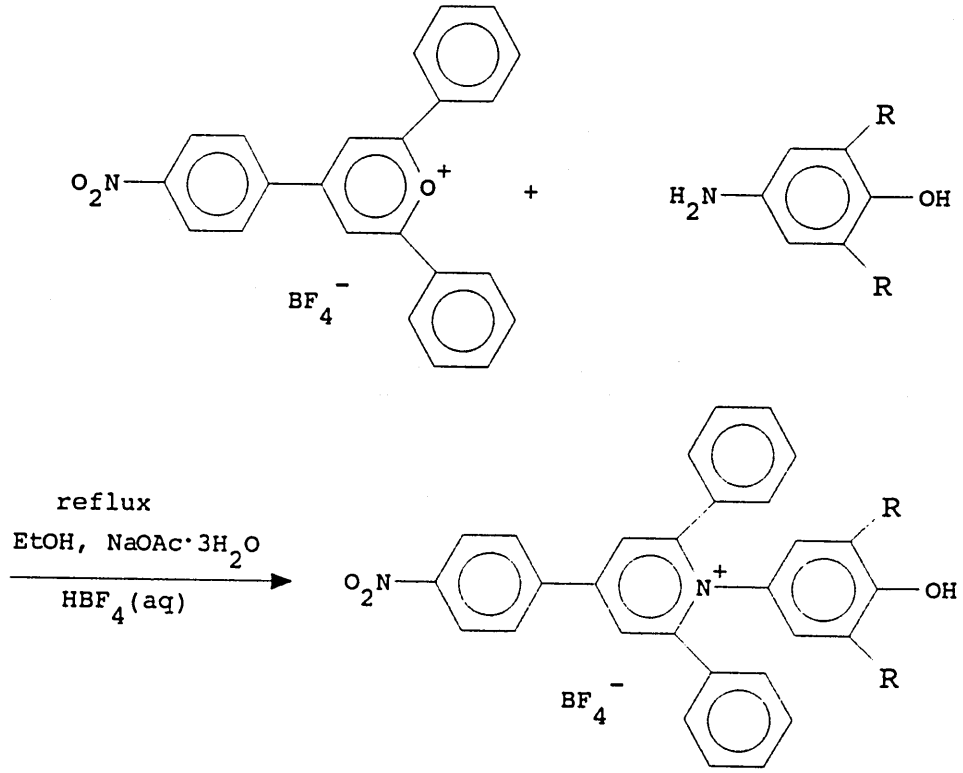

Fig. 4-5 Reaction route for coupling of the pyrylium salt with aminophenol

Using this synthetic route, similar betaine salts were synthesised by Johnson[27] and Paley.[28]

4.1.3 Reduction of the nitro betaine salt into amino betaine salt

The nitro betaine salts were reduced in formic acid under the action of a catalyst, palladium-charcoal (Fig. 4-6).

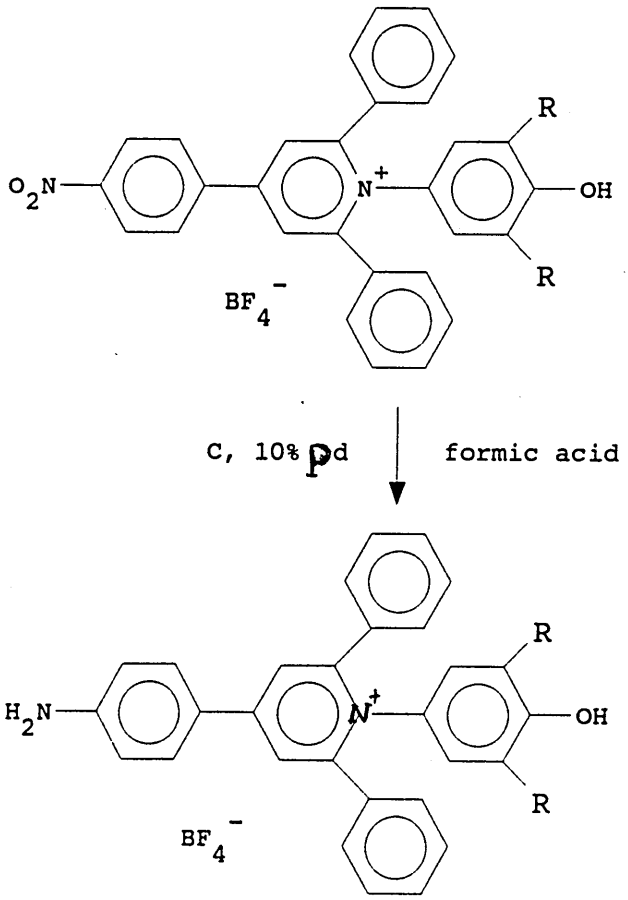

Fig. 4-6 Reduction of nitro betaine salt into amino betaine salt

Using this method, a large number of nitro-compounds have been reduced to amines with formic acid and palladium-charcoal catalyst included: p-nitrobenzyl alcohol, m-nitroaniline, o-nitroanisole, p-fluoronitrobenzene, and 5-nitro-2-trifluoromethylbenzimidazole etc..[29]

4.1.4 Coversion of the betaine salts into the betaine dyes

The betaine dyes were obtained by conversion of their betaine salts under the action of NaOMe and NaOH (Fig. 4-7). This method has been widely used to convert similar betaine salts into betaine dyes. [27, 28, 30]

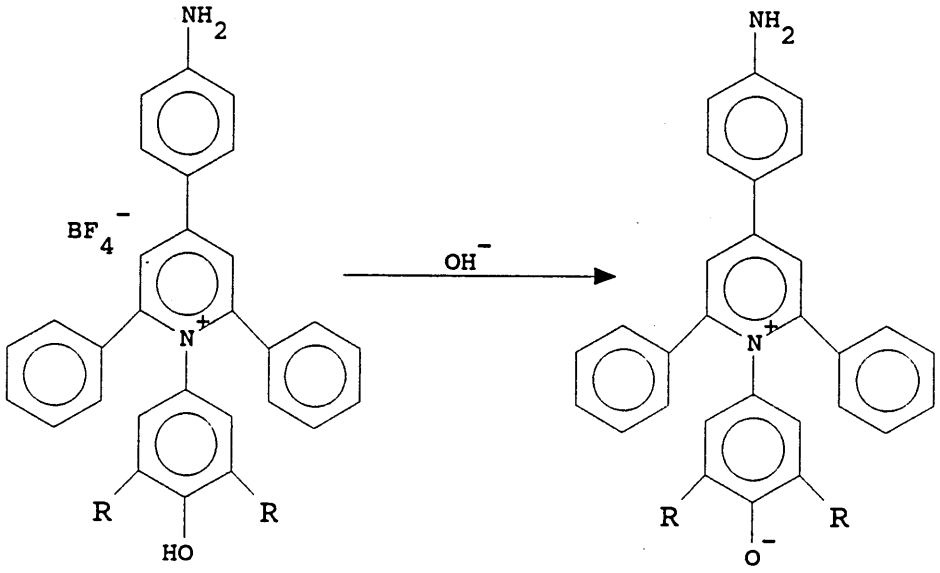

Fig. 4-7 Coversion of betaine salt into betaine dye

4.2 Synthesis of 2,6-dimethyl-4-[(2,6-diphenyl)-4-(p-aminophenyl)-N-pyridinio]-phenolate

The structure of the compound expected is showed in Fig. 4-8.

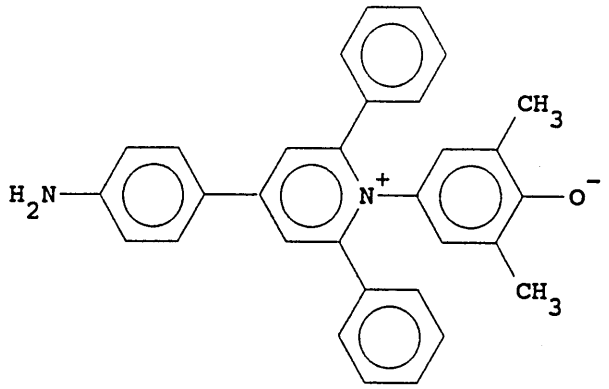

Fig. 4-8 The structure of 2,6-dimethyl-4-(2,6-diphenyl-4-aminophenyl-N-pyridinio)-phenolate

4.2.1 Synthesis of 4-(4-nitrophenyl)-2,6-diphenylpyrylium tetrafluoroborate

The pyrylium salt was synthesised by two methods which described in section 4.1.1.

Experimental method (a):

Acetophenone (Aldrich, 4.8 g, 0.04 moles) and 4-nitrochalcone (Aldrich,5.1 g, 0.02 moles) were dissolved in 20 ml of 1,2-dichloroethane and the mixture was placed into a three necks flask. It was heated to 80-85 ^{0}C, and 25 ml of 54% ethereal fluoroboric acid was added dropwise from the addition funnel over about 30 mins. As soon as the ethereal fluoroboric acid was added, the mixture became blood-red from original yellow colour. it was left for refluxing overnight and became to purple-brown colour. The mixture then was cooled overnight in a refrigerator to precipitate the crude yellow pyrylium salt. The crude salt was filtered, and about 100 ml of diethyl ether was added to the filtrate, and it was again refrigerated overnight to precipitate the rest of salt, which was then filteredand combined wtih the first portion. The crude solid product was dissolved in 20 ml of hot acetonitrile for purification and the solution was added dropwise to 200 ml of diethyl ether and left overnight to reprecipitate pyrylium salt. A yellow solid product (2.5 g, yield: 28%) was obtained after filtering.

The reaction scheme is showed in Fig. 4-9, and a reaction mechanism is proposed as follows in Fig. 4-10. An important step is that the acetophenone can change to its resonant enol form, which reacts with the nitrochalcone by dehydrogenation condensation in acidic and hot conditions. This kind of reaction mechanism has been systematically reviewed by Balaban et al[13] through plenty of pyrylium salt preparations.

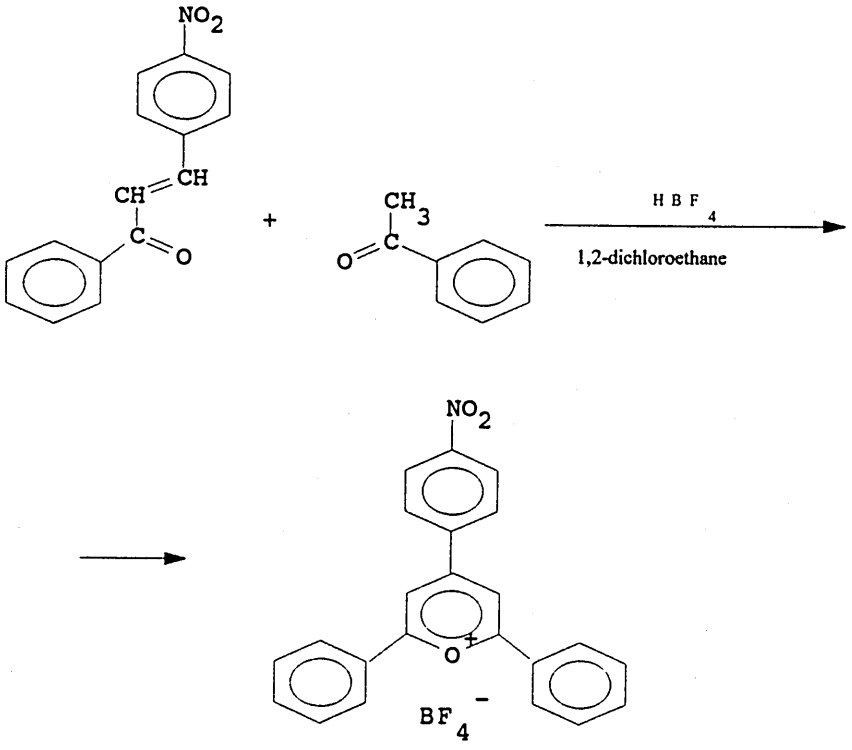

Fig. 4-9 The synthetic scheme of 4-(4-nitrophenyl)-2,6-diphenylpyrylium tetrafluoroborate

Experimental method (b):

4-nitrobenzaldehyde (Aldrich, 6.08 g, 40 mmoles) and Acetophenone (Aldrich, 11g, 80 mmoles) were dissolved in 15 ml of 1,2-dichloroethane and placed in a three-neck flask. The mixture was refluxed for overnight at around 80 ^{0}C. The colour of the mixture solution became clear brown from original light yellow. About 10 ml of 54% ethereal fluoroboric acid was added dropwise by a addition funnel to the mixture over about half hour. The mixture was kept refluxing for another 2 hours and it became to red brown colour, it was then cooled in a refrigerator overnight to precipitate crude solid pyrylium salt. The solid salt was filtered, and about 50 ml of diethyl ether was added to the filtrate. The filtrate was cooled in the refrigerator overnight again to precipitate the rest of

salt, which was filtered and combined with the first portion. The yellow solid salt generated was purified by dissolved in 10 ml of hot acetonitrile and precipitated with 400 ml of diethyl ether under stirring. About 3.23 g (yield: 30%) yellow solid crystal was obtained as final pure product after filtering.

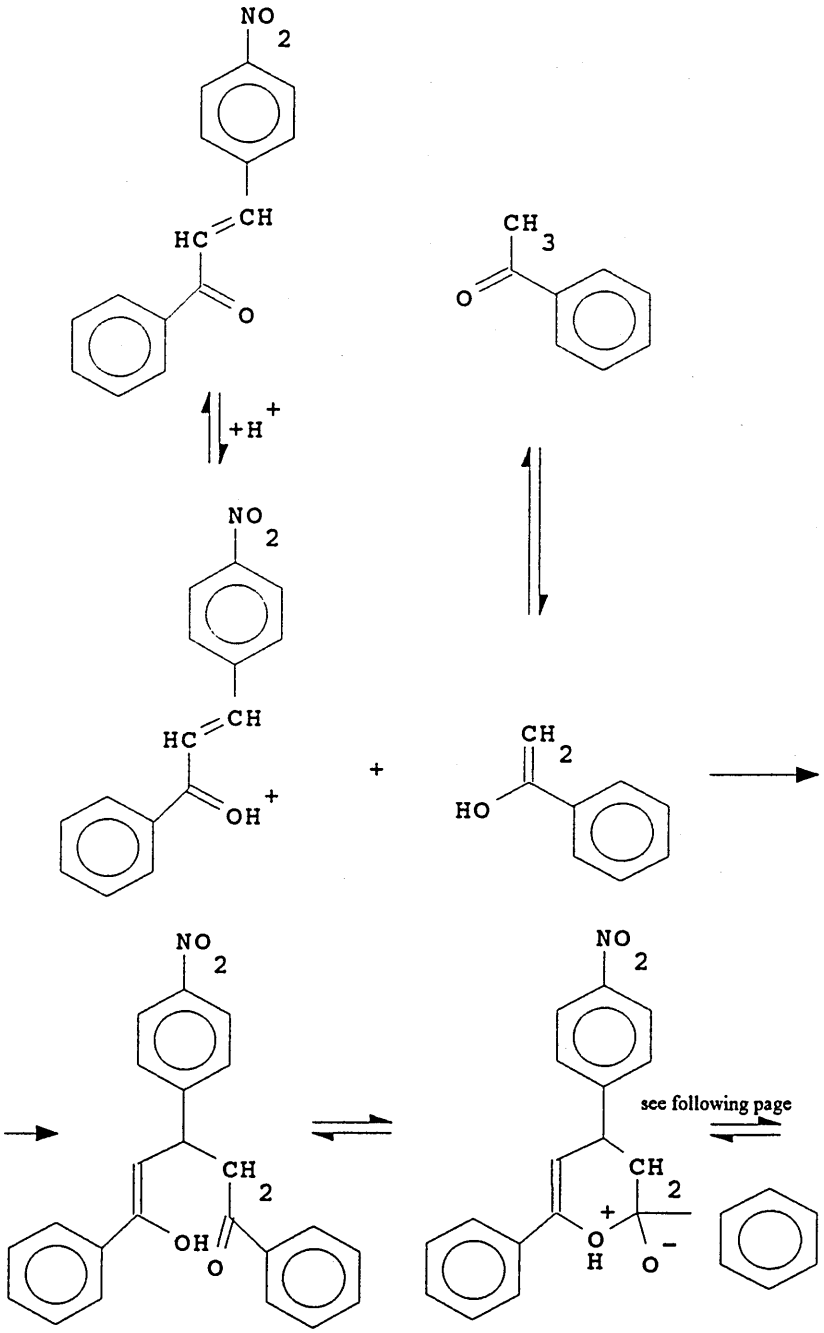

Fig. 4-10 Reaction mechanism for synthesis of
4-(4-nitrophenyl)-2,6-diphenylpyrylium salt

following the page above

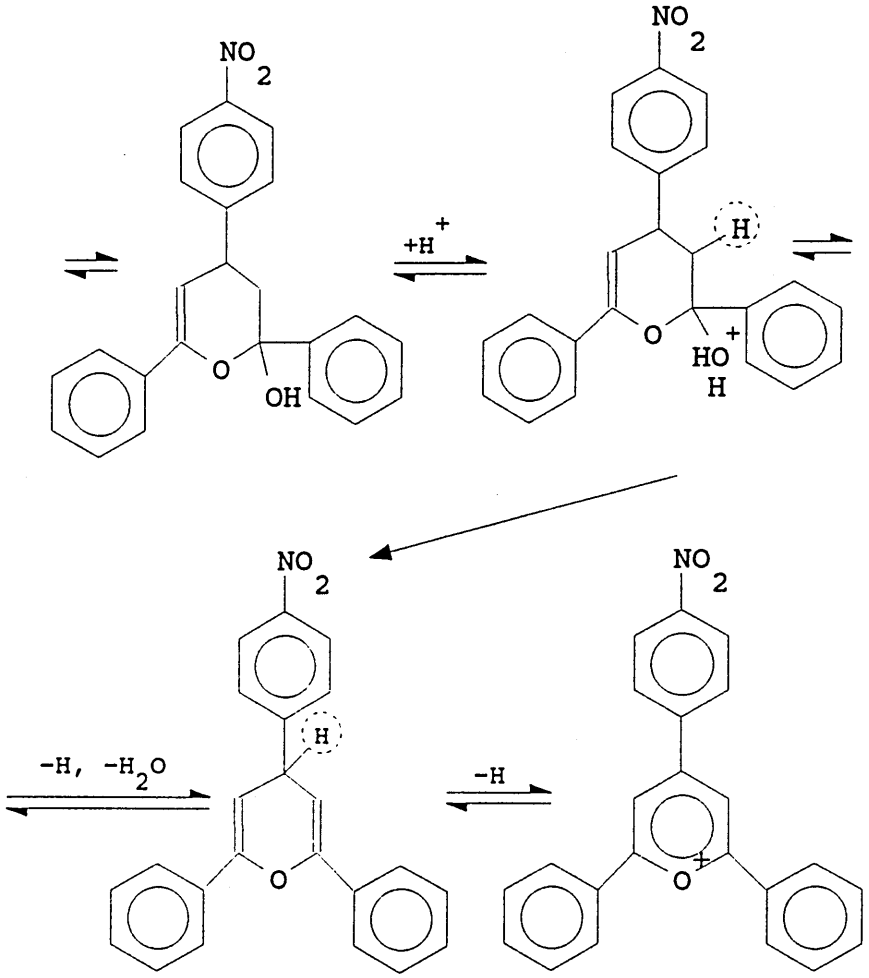

Fig.4-10 The following part

The pure products, 4-(4-nitrophenyl)-2,6-diphenylpyrylium tetrafluoroborate, from two methods (a) and (b) have the same appearance, both are yellow solid. When the products were not purified enough, they had some brown colour.

The structure and constitution of the products from the two methods were consistent with the compound, 4-(4-nitrophenyl)-2,6-diphenylpyrylium tetrafluoroborate, which was confirmed by their infrared spectra (Table 4-1), ^{1}H n. m. r. spectrum (Table 4-2) and elemental analysis(Table 4-3).

Table 4-1

Infrared spectral data of 4-(4-nitrophenyl)-2,6-diphenylpyrylium tetrafluoroborate in KBr

A: the compound from method (a)

band position (cm^{-1})	arrangement
3070 m	C-H str., aromatic
1633 s	C=C str., aromatic
1514 s	N=O str.
1346 s	
1275 s	C-O str.
1215 s	
1066 s and broad	$BF_4^-(\nu_3)$
858 s	
779 s	

B: the compound from method (b)

band position (cm^{-1})	arrangement
3075 m	C-H str., aromatic
1640 s	C=C str., aromatic
1520 s	N=O str.
1350 s	
1280 s	C-O str.
1225 s	
1070 sand broad	$BF_4^-(\nu_3)$
860 s	C-H b
775 s	

Table 4-2

^{1}H n.m.r. spectral data of 4-(4-nitrophenyl)-2,6-diphenylpyrylium tetrafluoroborate in d_6-DMSO

A: the compound from method (a)

chemical shift (δ, p.p.m)	type	arrangement
9.27	s	2H, 3,5-H of pyrylium ring
8.52-8.87	m	8H, aromatic
7.75	m	6H, aromatic

B: the compound from method (b)

chemical shift (δ, p.p.m)	type	arrangement
9.30	s	2H, 3,5-H of pyrylium ring
8.52-8.85	m	8H, aromatic
7.51-8.09	m	6H, aromatic

s: singlet; m: multiplet.

Table 4-3

Microanalysis of 4-(4-nitrophenyl)-2,6-diphenylpyrylium tetrafluoroborate

formula: $C_{23}H_{16}N_2O_2BF_4$

A: the compound from method (a)

	C	H	N
theory	62.62	3.66	3.17
found	62.36	3.55	3.11

B: the compound from method (b)

	C	H	N
theory	62.62	3.66	3.17
found	62.17	3.68	3.19

4.2.2 Synthesis of 2,6-dimethyl-4-aminophenol hydrochloride[29]

The expected compound, 2,6-dimethyl-4-aminophenol, was synthesised by reduction of 2,6-dimethyl-4-nitrophenol in formic acid under the action of a catalyst, palladium-charcoal. The reaction scheme is showed in Fig. 4-11.

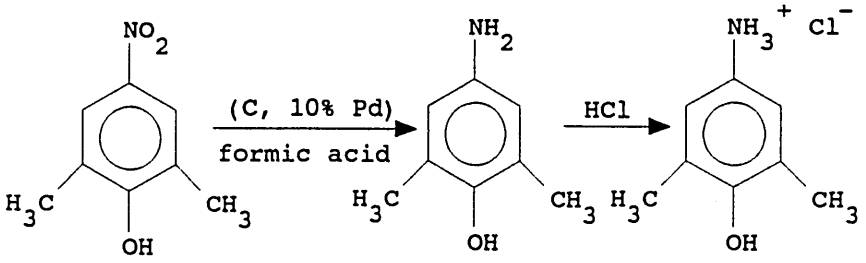

Fig. 4-11 The reaction sheme for reduction of nitrophenol into aminophenol

Experimental method:

Compound, 2,6-dimethyl-4-nitrophenol (Aldrich, 1.0 g, 6 mmoles) and 2.0 g of 10% palladium on activated carbon (Aldrich) were placed in a 50 ml two necked flask equipped with a magnetic stirring bar. The flask was flushed thoroughly with nitrogen gas and during whole reaction course the apparatus was kept under nitrogen atmosphere. About 15 ml of 97% formic acid was very slowly added dropwise to the stirring mixture so as to avoid an explosion. The stirred mixture was heated on a water bath at 90-100 ^{0}C for about 2 hours to carry out the reduction of the nitro group to an amino group.

The mixture was then removed from the water bath and 10 ml of concentrated hydrochloric acid was added. The palladium/carbon catalyst was filtered off and washed with 20-25 ml of hot water which was combined with the filtrate. The light yellow solution was rotoevaporated to a volume of about 5-10 ml and 10 ml of concentrated hydrochloric acid was added again. The solution was placed in a fridge overnight to precipitate a white solid. The solid was filtered and washed with 5 ml of concentrated hydrochloric acid, and dried under vacuum for 3 days. About 0.6 g (yield: 58%) white fine solid was obtained as product, 2,6-dimethyl-4-aminophenol hydrochloride.

An ^1H n. m. r. spectrum of the compound generated was recorded using d_6-DMSO as solvent. The spectral results are listed in Table 4-4. The constitution of the compound 2,6-dimethyl-4-aminophenol hydrochloride was confirmed by the microanalysis results showed in Table 4-5.

Table 4-4

^1H n.m.r. spectral data of 2,6-dimethyl-4-aminophenol hydrochloride in d_6-DMSO

chemical shift (δ, p.p.m)	type	arrangement
10.10	s	3H, NH_3^+
6.93	s	2H, aromatic
2.20	s	6H, CH_3

s: singlet.

Table 4-5

Microanalysis of 2,6-dimethyl-4-aminophenol hydrochloride

formula: $C_8H_{11}NO \cdot HCl$

	C	H	N
theory	55.34	6.97	8.07
found	55.39	6.89	8.04

4.2.3 Synthesis of 2,6-dimethyl-4-[(2,6-diphenyl)-4-(p-nitrophenyl)-N-pyridinio]-phenol tetrafluoroborate

The structure of the compound expected is showed in Fig. 4-12. It was synthesised by coupling of 2,6,-dimethyl-4-aminophenol hydrochloride with 4-(4-nitrophenyl)-2,6,-diphenylpyrylium tetrafluoroborate in a solvent of 95% aqueous ethanol. The basic synthetic route has already been showed in Fig. 4-5 of the section 4.1.2.

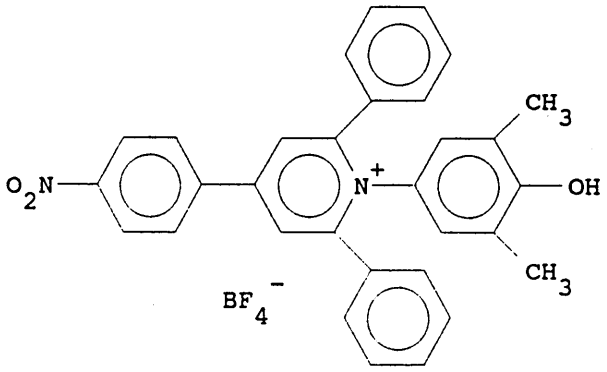

Fig. 4-12 The structure of 2,6-dimethyl-4-[(2,6-diphenyl)-4-(p-nitrophenyl)-N-pyridinio]-phenol tetrafluoroborate

Experimental method:

2,6-dimethyl-4-aminophenol hydrochloride produced from section 4.2.2 (0.69 g, 4.0 mmoles) was dissolved in 10 ml of 95% aqueous ethanol and it was then mixed with 14 ml of 0.333 M ethanolic KOH (about 4.0 mmol of KOH). This strongly coloured mixture was then placed in a 100 ml one necked flask equipped with a magnetic stirring bar and a reflux condenser. 1.78 g (4.0 mmoles) of 4-(4-nitrophenyl)-2,6-diphenylpyrylium tetrafluoroborate synthesised from the previous section 4.2.1 and 0.8 g of sodium acetate trihydrate (Aldrich)

were added to the mixture. The mixture was refluxed for 9 hours and it was then filtered to remove KCl generated during the reaction, and 10 ml of 50% aqueous fluoroboric acid (BDH) was added to the filtrate. The filtrate was poured into 500 ml of distilled water and refrigerated overnight to 'knock' the crude salt out of solution. The crude salt was filtered and dissolved in 20 ml of warmed glacial acetic acid. The solution was then added dropwise very slowly into 1000 ml of stirring anhydrous diethyl ether (this large quantity of ether is important, otherwise the betaine salt will coagulate into a lump) to precipitate the betaine salt as a yellow solid. The salt was filtered and washed with 50 ml of diethyl ether and then dissolved into 20 ml of warmed methanol for a further purification. The procedure for this time was the same as the first one using glacial acetic acid. Finally, the salt was filtered, washed with ether and dried under vacuum for 2 days to yield about 0.6 g (yield: 27%) yellow 2,6-dimethyl-4-[(2,6-diphenyl)-4-(p-nitrophenyl)-N--pyridinio]-phenol tetrafluoroborate.

An infrared spectrum of the product was recorded in a KBr disc and the bands found are listed in Table 4-6, which shown that the product contained -NO_2, -OH BF_4^- and aromatic ring. It was revealed by microanalysis of the product that it contained two crystallised water molecules. The microanalysis results are showed in Table 4-7.

4.2.4 Reduction of 2,6-dimethyl-4-[(2,6-diphenyl)-4-(p-nitrophenyl)-N-pyridinio]-phenol tetrafluoroborate into 2,6-dimethyl-4-[(2,6-diphenyl)-4-(p-aminophenyl)-N-pyridinio]-phenol tetrafluoroborate

The structure of 2,6-dimethyl-4-[(2,6-diphenyl)-4-(p-aminophenyl)-N-pyridinio]-phenol tetrafluoroborate, is showed in Fig. 4-13. It was produced by the route in Fig. 4-6.

Table 4-6

Infrared spectral data of 2,6-dimethyl-4-[(2,6-diphenyl)-4-(p-nitrophenyl)-N-pyridinio]-phenol tetrafluoroborate in KBr

band position (cm^{-1})	arrangement
3600-3200 s and broad	O-H str. and H_2O of crystallisation
3050 w	C-H str., aromatic
2900 w	C-H str., aliphatic
1605 s	C=C str., aromatic
1525 s	N=O str.
1490 s	
1410 m	C-H b., aliphatic
1370 m	
1335 s	C-O str.
1190 m	C-H def. pyridine ring
1100-960 s and broad	$BF_4^-(\nu_3)$
850 s	C-H b. aromatic
750 s	
680 s	N=O b.

Table 4-7

Microanalysis of 2,6-dimethyl-4-[(2,6-diphenyl)-4-(p-nitrophenyl)-N-pyridinio]-phenol tetrafluoroborate

formula: $C_{31}H_{25}N_2O_3BF_4 \cdot 2H_2O$

	C	H	N
theory	62.43	4.90	4.70
found	62.48	5.01	4.72

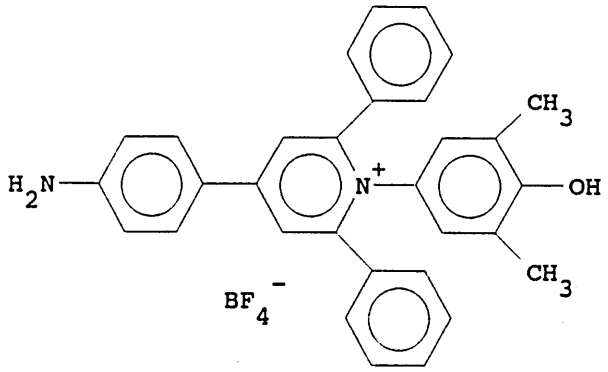

Fig. 4-13 The structure of 2,6-dimethyl-4-[(2,6-diphenyl)-4-(p-aminophenyl)-N-pyridinio]-phenol tetrafluoroborate

Experimental method:

Following the procedure used in the section 4.2.2, 1.0 g 2,6-dimethyl-4-[(2,6-diphenyl)-4-(p-nitrophenyl)-N-pydinio]-phenol tetrafluoroborate was reduced to its amino betaine salt by using formic acid and palladium/carbon catalyst and under nitrogen atmosphere. A different procedure was that the filtrate was rotoevaporated to near dryness, about 5 ml, after the pd/C catalyst was filtered off and washed with ether. 30 ml of 95% aqueous ethanol was added to this solution and it was rotoevaporated to near dryness again to remove the hydrochloric acid used. This step was repeated a second time, only this time the solution was rotoevaporated to complete dryness. A orange solid was obtained at a yield of about 53% (0.5 g) as pure product, 2,6-dimethyl-4-[(2,6-diphenyl)-4-(p-aminophenyl)-N-pydinio]-phenol tetrafluoroborate. Its elemental analysis of C, H and N (Table 4-8) revealed that it contained two crystallised water molecules.

Table 4-8

Microanalysis of 2,6-dimethyl-4-[(2,6-diphenyl)-4-(p-aminophenyl)-N-pyridinio]-phenol tetrafluoroborate

formula: $C_{31}H_{27}N_2OBF_4 \cdot 2H_2O$

	C	H	N
theory	65.74	5.52	4.95
found	65.66	5.59	4.89

4.2.5 Conversion of 2,6-dimethyl-4-[(2,6-diphenyl)-4-(p-aminophenyl)-N-pyridinio]-phenol tetrafluoroborate into 2,6-dimethyl-4-[(2,6-diphenyl)-4-(p-aminophenyl)-N-pyridinio]-phenolate[27,28]

The structure of the compound expected is showed in Fig. 4-8. The reaction route has showed in the section 4.1.4 (Fig. 4-7) before.

Experimental method:

1.0 g of 2,6-dimethyl-4-[(2,6-diphenyl)-4-(p-aminophenyl)-N-pydinio]-phenol tetrafluoroborate generated from the section 4.2.4 was dissolved in 75 ml of methanol, and 10 ml of 15% sodium methoxide in methanol was added to the solution. The resulting red-brown mixture solution was heated for 10 mins. The solution was poured into 200 ml of 10 % aqueous NaOH solution, and the mixture was refrigerated overnight to bring the dye out of solution. The dye was then extracted into 500 ml of chloroform in 100 ml portions forming a dark blue solution. The chloroform layers were combined and washed with 2 or 3 50 ml portions of distilled water until the wash water was neutral to litmus paper. The

solution was dried over anhydrous sodium sulphate. 0.55 g dark blue solid (about 66% yield) was obtained as product, 2,6-dimethyl-4-[(2,6-diphenyl)-4-(p-aminophenyl)-N-pydinio]-phenolate, after evaporation of the chloroform and drying in vacuum. Its melting point was found between 221-223 °C.

Microanalysis results of the betaine dye generated are given in Table 4-9, which show that the dye contained two crystallised water molecules.

Table 4-9

Microanalysis of 2,6-dimethyl-4-[(2,6-diphenyl)-4-(p-aminophenyl)-N-pyridinio]-phenolate

formula: $C_{31}H_{26}N_2O \cdot 2H_2O$

	C	H	N
theory	77.80	6.32	5.85
found	77.86	6.34	5.86

4.3 Synthesis of 2,6-diphenyl-4-[(2,6-diphenyl)-4-(p-aminophenyl)-N-pyridinio]-phenolate

The structures of both compound ET-30[1] and modified compound, 2,6-diphenyl-4-[(2,6-diphenyl)-4-(p-aminophenyl)-N-pyridinio]-phenolate are showed in Fig 4-14.

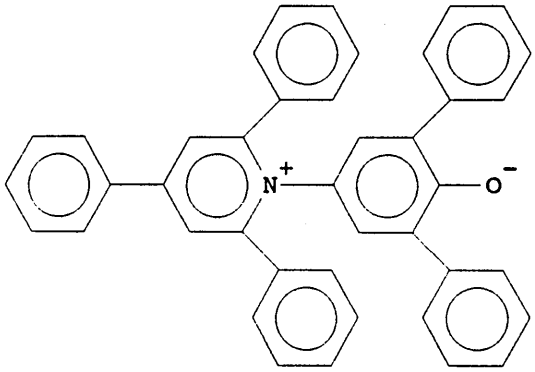

A: ET-30

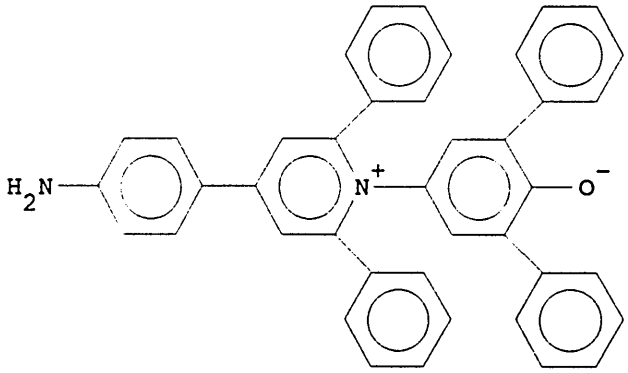

B: Modified dye

Fig. 4-14 The structure of ET-30 and modified dye

A sole difference between these two dyes in structure is that the latter has a amino group on the p-position of its straight axial phenyl group.

4.3.1 Synthesis of 2,6-diphenyl-4-[(2,6-diphenyl)-4-(p-nitrophenyl)-N-pyridinio]-phenol tetrafluoroborate

Following the reaction route in Fig. 4-5 of the section 4.1.2, 2,6-diphenyl-4-[(2,6-diphenyl)-4-(p-nitrophenyl)-N-pyridinio]-phenol tetrafluoroborate (Fig. 4-15) was synthesised by a direct coupling of 4-(4-nitrophenyl)-2,6-diphenylpyrylium tetrafluoroborate generated from previous section 4.2.1 and 4-amino-2,6-diphenylphenol (Aldrich) in 95% aqueous ethanol with $NaOAc.3H_2O$ and HBF_4. The pure product was a yellow solid.

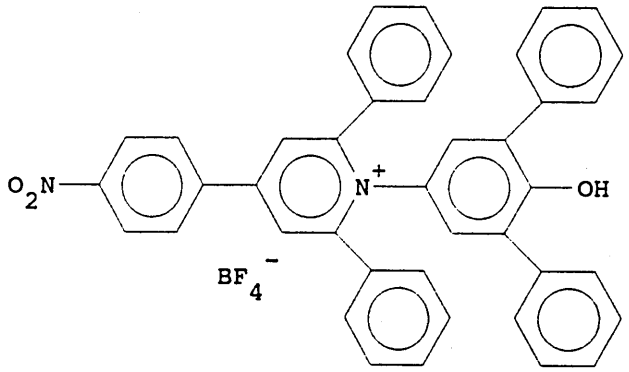

Fig. 4-15 The structure of 2,6-diphenyl-4-[(2,6-diphenyl)-4-(p-nitrophenyl)-N-pyridinio]-phenol tetrafluoroborate

Experimental method:

Synthetic reaction was carried out in the almost same way as for the 2,6-dimethyl-4-[(2,6-diphenyl)-4-(p-nitrophenyl)-N-pyridinio]-phenol tetrafluoroborate in the section 4.2.3, but without using 0.333 M ethanolic KOH solution.

Reagents used are listed as below:

a: 0.51 g 4-amino-2,6-diphenylphenol (Aldrich, 1.91 mmoles);

b: 0.85 g (1.91 mmoles) 4-(4-nitrophenyl)-2,6-diphenylpyrylium tetrafluoroborate synthesised from the previous section 4.2.1;

c: 0.55 g $NaOAc.3H_2O$ (Aldrich);

d: 15 ml of 95% aqueous ethanol;

e: 8 ml of 50% aqueous fluoroboric acid (BDH).

The mixture of reagents a, b, c, and d was refluxed overnight, and then reagent e was added to the mixture solution. The solution was poured into 500 ml of distilled water and refrigerated overnight to 'knock' the crude salt out of solution. Purification procedure was following exactly the same way in the section 4.2.3. Finally, 0.76 g (55% yield) yellow solid was obtained as product.

An ^1H n. m. r. spectrum of the compound formed was recorded in a solvent of d_6-DMSO, and the results and arrangement are showed in Table 4-10. Microanalysis results of the compound for C. H. N elements are given in Table 4-11. Analytical data showed that the yellow solid produced should be 2,6-diphenyl-4-[(2,6-diphenyl)-4-(p-nitrophenyl)-N-pyridinio]-phenol tetrafluoroborate with two crystallised water molecules.

Table 4-10

^{1}H n.m.r. spectral data of 2,6-diphenyl-4-[(2,6-diphenyl)-4-(p-nitrophenyl)-N-pyridinio]-phenol tetrafluoroborate in d_6-DMSO

formula: $C_{41}H_{29}N_2O_3BF_4 \cdot 2H_2O$

chemical shift (δ, p.p.m)	type	arrangement
8.85	s	2H, 3,5-H of pyridine ring
8.6-8.7	m	2H, aromatic
8.4-8.5	m	2H, aromatic
7.25-7.65	m	18H, aromatic
7.08-7.19	m	4H, aromatic
3.35	s, broad	OH and H_2O of crystallisation

s: singlet; m: multiplet.

Table 4-11

Microanalysis of 2,6-diphenyl-4-[(2,6-diphenyl)-4-(p-nitrophenyl)-N-pyridinio]-phenol tetrafluoroborate

formula: $C_{41}H_{29}N_2O_3BF_4 \cdot 2H_2O$

	C	H	N
theory	68.34	4.62	3.89
found	68.41	4.65	3.93

4.3.2 Reduction of 2,6-diphenyl-4-[(2,6-diphenyl)-4-(p-nitrophenyl)-N-pyridinio]-phenol tetrafluoroborate into 2,6-diphenyl-4-[(2,6-diphenyl)-4-(p-aminophenyl)-N-pyridinio]-phenol tetrafluoroborate

The structure of 2,6-diphenyl-4-[(2,6-diphenyl)-4-(p-aminophenyl)-N-pyridinio]-phenol tetrafluoroborate is showed in Fig. 4-16.

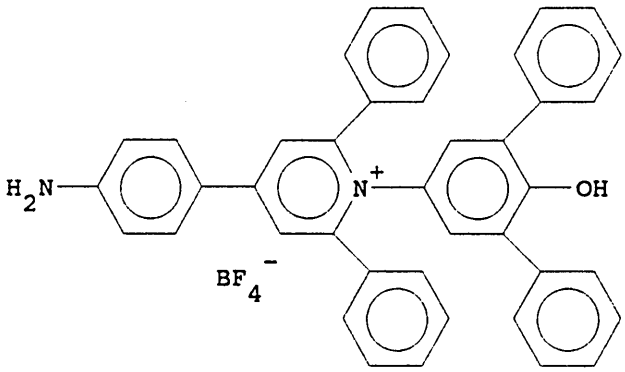

Fig. 4-16 The structure of 2,6-diphenyl-4-[(2,6-diphenyl)-4-(p-aminophenyl)-N-pyridinio]-phenol tetrafluoroborate

The reduction reaction was carried out in the same manner as for reduction of 2,6-dimethyl-4-[(2,6-diphenyl)-4-(p-nitrophenyl)-N-pydinio]-phenol tetrafluo-roborate in the section 4.2.4. 1.0 g of 2,6-diphenyl-4-[(2,6-diphenyl)-4-(p-nitrophenyl)-N-pyridinio]-phenol tetrafluoroborate was reduced by 2.0 g of 10% palladium on activated carbon in 15 ml of 97% formic acid under nitrogen atmosphere. About 0.7 g (73% yield) brown solid was produced as final pure product, 2,6-diphenyl-4-[(2,6-diphenyl)-4-(p-aminophenyl)-N-pyridinio]-phenol tetrafluorobo-rate. Its ^1H n. m. r. spectrum in $CDCl_3$ revealed that it has 26 aromatic hydrogen atoms, 2 pyridine ring hydrogen atoms and some hydrogen atoms in $-NH_2$, -OH and H_2O of crystallisation, which is listed in Table 4-12.

The compound formed by this way contained two crystallised water molecules, which was revealed by its microanalysis results for C. H. N elements in Table 4-13.

Table 4-12

^{1}H n.m.r. spectral data of 2,6-diphenyl-4-[(2,6-diphenyl)-4-(p-aminophenyl)-N-pyridinio]-phenol tetrafluoroborate in $CDCl_3$

formula: $C_{41}H_{31}N_2OBF_4 \cdot 2H_2O$

chemical shift (δ, p.p.m)	type	arrangement
8.36	s	2H, 3,5-H of pyridine ring
8.15	m	2H, aromatic
7.10-7.48	m	22H, aromatic
6.70-6.78	m	2H, aromatic
3.68±0.4	m	NH_2, OH and H_2O of crystallisation

s: singlet; m: multiplet.

Table 4-13

Microanalysis of 2,6-diphenyl-4-[(2,6-diphenyl)-4-(p-aminophenyl)-N-pyridinio]-phenol tetrafluoroborate in $CDCl_3$

formula: $C_{41}H_{31}N_2OBF_4 \cdot 2H_2O$

	C	H	N
theory	71.31	5.11	4.06
found	71.47	5.26	4.07

4.3.3 Conversion of 2,6-diphenyl-4-[(2,6-diphenyl)-4-(p-aminophenyl)-N-pyridinio]-phenol tetrafluoroborate into 2,6-diphenyl-4-[(2,6-diphenyl)-4-(p-aminophenyl)-N-pyridinio]-phenolate

2,6-diphenyl-4-[(2,6-diphenyl)-4-(p-aminophenyl)-N-pyridinio]-phenolate was produced by a direct converting reaction of 2,6-diphenyl-4-[(2,6-diphenyl)-4-(p-aminophenyl)-N-pyridinio]-phenol tetrafluoroborate under basic conditions, which was similar to the conversion of 2,6-dimethyl-4-[(2,6-diphenyl)-4-(p-aminophenyl)-N-pyridinio]-phenol tetrafluoroborate in the previous section 4.2.5, but the dye was, finally, isolated by different way.

Experimental method:

2,6-diphenyl-4-[(2,6-diphenyl)-4-(p-aminophenyl)-N-pyridinio]-phenol tetrafluoroborate (0.60 g, 0.87 mmoles) was dissolved in 40 ml of methanol and 6 ml of 15% sodium methoxide in methanol was added to the solution. The solution was heated for 20 mins. Then, 40 ml of 5% aqueous solution of sodium hydroxide was added to the hot solution. When the methanol was removed from the mixture solution by rotoevaporator, dark blue fine crystals were appeared. The solid crystals were filtered off and washed first with 1% sodium hydroxide solution until the washing liquid became pale yellow. They were washed well with distilled water and dried over P_4O_{10} at 100 ^{o}C under vacuum overnight. 0.33 g (62% yield) dark blue product (m.p. 208-209 ^{o}C) was obtained finally.

The structure and composition of the dye generated were confirmed by its ^{1}H n. m. r. spectrum and C. H. N element analysis. Analytical results are showed in Table 4-14 and Table 4-15, separately. It was known that the dye, 2,6-diphenyl-4-[(2,6-diphenyl)-4-(p-aminophenyl)-N-pyridinio]-phenolate, formed from present work contained 2.5 crystallised water molecules.

Table 4-14

^1H n.m.r. spectral data of 2,6-diphenyl-4-[(2,6-diphenyl)-4-(p-aminophenyl)-N-pyridinio]-phenolate in $CDCl_3$

formula: $C_{41}H_{30}N_2O \cdot 2.5H_2O$

chemical shift (δ, p.p.m)	type	arrangement
8.0	m	2H, 3,5-H of pyridine ring
7.66-7.75	m	2H, aromatic
7.35-7.60	m	10H, aromatic
7.27	m	12H, aromatic
6.66-7.06	m	2H, aromatic
3.50	s	NH_2, and H_2O of crystallisation

s: singlet; m: multiplet.

Table 4-15

Microanalysis of 2,6-diphenyl-4-[(2,6-diphenyl)-4-(p-aminophenyl)-N-pyridinio]-phenolate

formula: $C_{41}H_{30}N_2O \cdot 2.5H_2O$

	C	H	N
theory	80.49	5.76	4.58
found	80.39	5.47	4.47

4.4 Synthesis of 2,6-dichloro-4-[(2,6-diphenyl)-4-(p-aminophenyl)-N-pyridinio]-phenolate

The structure of the compound mentioned in the title is shown in the Fig. 4-17 B as below. A similar compound, 2,6-dichloro-4-(2,4,6-triphenyl-N-pyridinio)-phenolate (called ET-33) shown in Fig. 4-16 A, has been synthesised by M. A. Kessler and Otto S. Wolfbeis.[31]

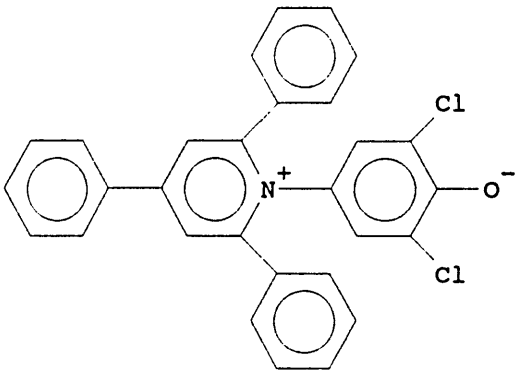

A: The structure of ET-33

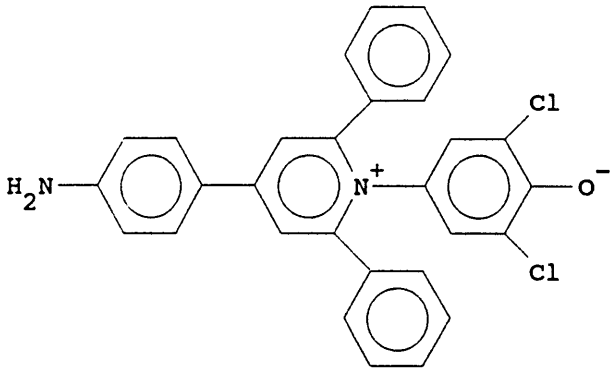

B: modified dye

Fig. 4-17 The structure of the ET-33 and modified dye

The purpose of making ET(33) was to obtain a new probe which can be used for polarity studies at neutral pH, because a series of pyridinium-N-phenoxide betaine polarity probe materials including ET-30, have a major drawback, i.e. they all have a high pKa value. This limits their applications so that experiments can only be performed in alkaline solutions for polarity measurements. The dye ET(33) has a sufficient low pKa value (4.78) to make it suitable for investigations at near neutral pH values, but without any serious change of spectral properties when compared to other pyridinium-N-phenoxide betaine dyes.[31] 2,6-dichloro-4-[(2,6-diphenyl)-4-(p-aminophenyl)-N-pyridinio]-phenolate is a similar betaine dye containing a functional group to link it with a solid support.

The synthetic route is the same as other modified betaine dyes described in the previous sections. Only a starting material was changed.

4.4.1 Synthesis of 2,6-dichloro-4-[(2,6-diphenyl)-4-(p-nitrophenyl)-N-pyridinio]-phenol tetrafluoroborate

The structure of 2,6-dichloro-4-[(2,6-diphenyl)-4-(p-nitrophenyl)-N-pyridinio]-phenol tetrafluoroborate is showed in Fig. 4-18.

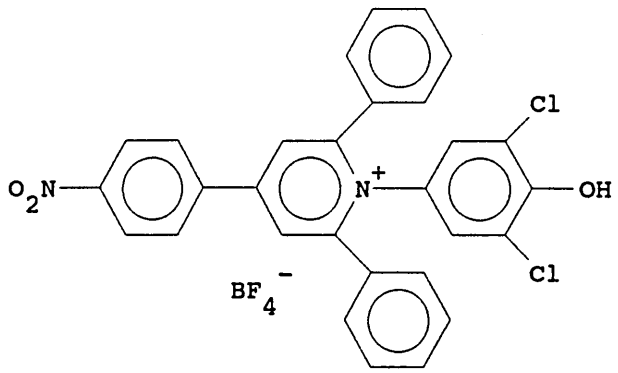

Fig. 4-18 The structure of 2,6-dichloro-4-[(2,6-diphenyl)-4-(p-nitrophenyl)-N-pyridinio]-phenol tetrafluoroborate

Experimental method:

Synthetic work was carried out in the same manner as for 2,6-diphenyl-4-[(2,6-diphenyl)-4-(p-nitrophenyl)-N-pyridinio]-phenol tetrafluoroborate in the section 4.3.1, using 1.1 g (2.5 mmoles) of 4-(4-nitrophenyl)-2,6-diphenylpyrylium tetrafluoroborate synthesised from the previous section 4.2.1, 0.5 g (> 2.5 mmoles) of 2,6-dichloro-4-aminophenol (Aldrich), 0.5 g of $NaOAc.3H_2O$, 12 ml of 95% aqueous ethanol and 10 ml of 50% aqueous fluoroboric acid (BDH). After purification, 1.16 g (73% yield) light brown solid was obtained as 2,6-dichloro-4-[(2,6-diphenyl)-4-(p-nitrophenyl)-N-pyridinio]-phenol tetrafluoroborate.

An infrared spectrum of the compound generated was recorded in KBr disc. Some typical bands were found. A broad band between 3650-3150 cm^{-1} was assigned to O-H stretch of phenol and a medium band at 3040 cm^{-1} was assigned to aromatic C-H stretch. A broad band between 1100-1020 cm^{-1} was thought as υ_3 vibration of BF_4^-. Three bands found at 1620, 1490 and 1340 cm^{-1} were considered as C=C stretch of aromatic ring and N=O stretch of aromatic nitro group. The infrared spectral bands found and arrangements are given in Table 4-16. Microanalysis (Table 4-17) of the compound for C. H. and N was consistent with 2,6-dichloro-4-[(2,6-diphenyl)-4-(p-nitrophenyl)-N-pyridinio]-phenol tetrafluoro-borate containing two crystallised water molecules.

Table 4-16

Infrared spectral data of 2,6-dichloro-4-[(2,6-diphenyl)-4-(p-nitrophenyl)-N-pyridinio]-phenol tetrafluoroborate in KBr

band position (cm^{-1})	arrangement
3650-3150 s and broad	O-H str. and H_2O of crystallisation
3040 m	C-H str., aromatic
1620 s	C=C str., aromatic
1490 s	N=O str., aromatic nitro group
1340 s	
1100-1020 s and broad	$BF_4^-(\upsilon_3)$
850 s	C-H b. aromatic
750 s	
680 s	N=O b., aromatic nitro group

s: strong; m: medium.

Table 4-17

Microanalysis of 2,6-dichloro-4-[(2,6-diphenyl)-4-(p-nitrophenyl)-N-pyridinio]-phenol tetrafluoroborate

formula: $C_{29}H_{19}N_2O_3Cl_2BF_4 \cdot 2H_2O$

	C	H	N
theory	54.36	3.64	4.40
found	54.69	3.60	4.43

4.4.2 Reduction of 2,6-dichloro-4-[(2,6-diphenyl)-4-(p-nitrophenyl)-N-pyridinio]-phenol tetrafluoroborate into 2,6-dichloro-4-(2,6-diphenyl-4-aminophenyl-N-pyridinio)-phenol tetrafluoroborate

Following the procedures used in the section 4.3.2, 1.0 g of 2,6-dichloro-4-[(2,6-diphenyl)-4-(p-nitrophenyl)-N-pyridinio]-phenol tetrafluoroborate was reduced by 2.0 g of 10% palladium on activated carbon in 15 ml of 97% formic acid and under nitrogen atmosphere. Finally 0.66 g of yellow solid (69% yield) was generated as 2,6-dichloro-4-[(2,6-diphenyl)-4-(p-aminophenyl)-N-pyridinio]-phenol tetrafluoroborate.

Its infrared spectrum (KBr) revealed that it contained -OH, $-NH_2$, BF_4^- and aromatic group. The infrared spectral results and arrangements are given in Table 4-18. Microanalysis (Table 4-19) of the compound formed confirms its constitution.

Table 4-19

Microanalysis of 2,6-dichloro-4-[(2,6-diphenyl)-4-(p-aminophenyl)-N-pyridinio]-phenol tetrafluoroborate

formula: $C_{29}H_{21}N_2OCl_2BF_4 \cdot 2H_2O$

	C	H	N
theory	57.36	4.15	4.61
found	57.41	4.22	4.64

Table 4-18

Infrared spectral data of 2,6-dichloro-4-[(2,6-diphenyl)-4-(p-aminophenyl)-N-pyridinio]-phenol tetrafluoroborate in KBr

band position (cm^{-1})	arrangement
3650-3200 s and broad	O-H str., N-H str., and H_2O of crystallisation
3020 m	C-H str., aromatic
1620 s	C=C str., aromatic
1570 s and broad	N-H b.
1100-1020 s and broad	$BF_4^-(\upsilon_3)$
800 s	C-H b. aromatic
760 s	
690 s	

s: strong; m: medium.

4.4.3 Synthesis of 2,6-dichloro-4-[(2,6-diphenyl)-4-(p-aminophenyl)-N-pyridinio]-phenolate

As showed in Fig. 4-7, 2,6-dichloro-4-(2,6-diphenyl-4-aminophenyl-N-pyridinio)-phenolate was produced by conversion of 2,6-dichloro-4-[(2,6-diphenyl)-4-(p-aminophenyl)-N-pyridinio]-phenol tetrafluoroborate under basic conditions. Reaction was carried out following the procedure used in the section 4.3.3. 0.65 g of 2,6-dichloro-4-[(2,6-diphenyl)-4-(p-aminophenyl)-N-pyridinio]-phenol tetrafluoroborate was used to produce its dye compound. 0.36 g (65% yield) dark purple solid was finally obtained as 2,6-dichloro-4-[(2,6-diphenyl)-4-(p-aminophenyl)-N-pyridinio]-phenolate (m.p. 213-215 °C). An infrared spectrum of the compound generated was recorded in KBr disc. It showed that

the compound contained -OH, $-NH_2$ and aromatic ring groups. Infrared spectral bands found and arrangements are listed in Table 4-20. Microanalysis results of the compound for C, H, and N are given in Table 4-21, which indicate that 2,6-dichloro-4-[(2,6-diphenyl)-4-(p-aminophenyl)-N-pyridinio]-phenolate synthesised contained 1.5 crystallised water molecules per molecule of dye.

Table 4-20

Infrared spectral data of 2,6-dichloro-4-(2,6-diphenyl-4-aminophenyl-N-pyridinio)-phenolate in KBr

band position (cm^{-1})	arrangement
3600-3150 s and broad	O-H str., N-H str., and H_2O of crystallisation
3055 m	C-H str., aromatic
1600 s	N-H b. str.
1500 s	C=C str., aromatic
842 s	C-H b. aromatic
767 s	
700 s	

s: strong; m: medium.

Table 4-21

Microanalysis of 2,6-dichloro-4-(2,6-diphenyl-4-aminophenyl-N-pyridinio)-phenolate

formula: $C_{29}H_{20}N_2OCl_2 \cdot 1.5H_2O$

	C	H	N
theory	68.23	4.54	5.49
found	68.28	4.48	5.23

4.5 Synthesis of 2,6-dichloro-4-[(4,6-diphenyl)-2-(p-aminophenyl)-N-pyridinio]-phenolate

The compound mentioned above is almost the same as the compound, 2,6-dichloro-4-[(2,6-diphenyl)-4-(p-aminophenyl)-N-pyridinio]-phenolate described in the section 4.4. The only difference between these two dyes is the position of the amino group on different phenyl ring. One is in the p-position of straight axial phenyl ring and another is in the p-position of side phenyl ring. The structures of these two dyes are showed together in Fig. 4-19.

The purpose of making 2,6-dichloro-4-[(4,6-diphenyl)-2-(p-aminophenyl)-N-pyridinio]-phenolate was to investigate the effect on absorption maxima when the amino group is in a different phenyl ring. Synthesis of 2,6-dichloro-4-[(4,6-diphenyl)-2-(p-aminophenyl)-N-pyridinio]-phenolate was performed in four steps.

4.5.1 Synthesis of 2-(p-nitrophenyl)-4,6-diphenylpyrylium tetrafluoroborate

The reaction route and mechanism for preparation of 2-(p-nitrophenyl)-4,6-diphenylpyrylium tetrafluoroborate is the same as that for 4-(4-nitrophenyl)-2,6-diphenylpyrylium tetrafluoroborate described in Fig. 4-3 and Fig. 4-10. Only the starting materials were changed.

Experimental method:

3.3 g (20 mmoles) of 4-nitroacetophenone (Aldrich) and 4.2 g (20 mmoles) of benzalacetophenone (shortly called chalcone, Aldrich) were

dissolved in 20 ml of 1,2-dichloroethane and placed in a three-necked flask equipped with a

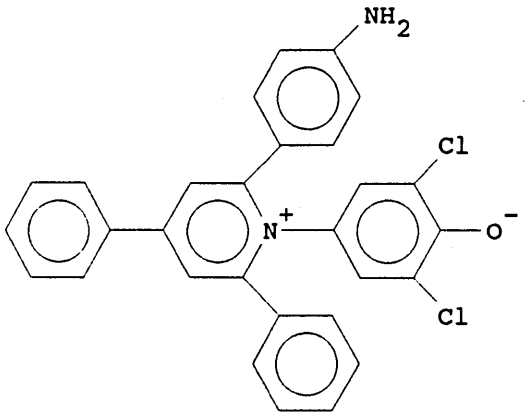

A: The structure of 2,6-dichloro-4-[(4,6-diphenyl)-2-(p-aminophenyl)-N-pyridinio]-phenolate

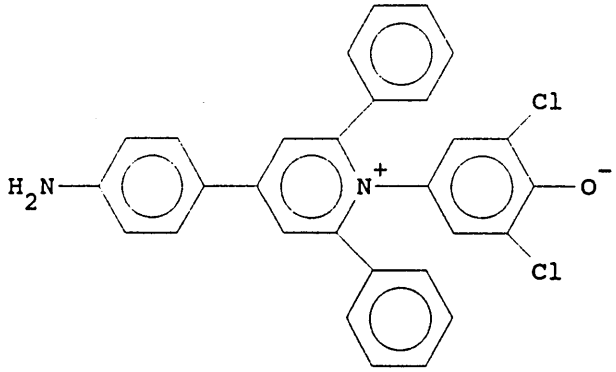

B: The structure of 2,6-dichloro-4-[(2,6-diphenyl)-4-(p-aminophenyl)-N-pyridinio]-phenolate

Fig. 4-19 The structure of two similar dyes

magnetic stirring bar. The stirring mixture was heated to about 75 ^{0}C and 10 ml of 54% ethereal fluoroboric acid (BDH) was added dropwise to the mixture from a addition funnel over about half a hour. The mixture solution became red-brown colour from original light yellow. It was refluxed for 4 hours and cooled in ice to precipitate some of the crude pyrylium salt. A yellow green solid was obtained

after filtering. 20 ml of diethyl ether was added to the filtrate and the filtrate was cooled in ice again to precipitate the rest of the pyrylium salt, which was then filtered and combined with the first portion. The crude pyrylium salt was purified by dissolved in 50 ml of hot acetonitrile and followed by precipitation with 250 ml of diethyl ether. The mixture was left in a refrigerator overnight to allow the precipitation complete. A yellow-green solid (3.65 g, yield: 41%) was obtained after filtering, which was thought of as 2-(p-nitrophenyl)-4,6-diphenylpyrylium tetrafluoro-borate.

An infrared spectrum of the compound was recorded in KBr disc, which showed that it contained $-NO_2$, aromatic ring and BF_4^- group. The bands found in its infrared spectrum and arrangements are listed in Table 4-22. Elemental analysis (Table 4-23) of the compound generated for C, H and N showed that its composition was consistent with 2-(p-nitrophenyl)-4,6-diphenylpyrylium tetrafluoroborate.

Table 4-22

Infrared spectral data of 2-(p-nitrophenyl)-4,6-diphenylpyrylium tetrafluoroborate in KBr

band position (cm^{-1})	arrangement
3070 m	O-H str., aromatic
1625 s	C=C str., aromatic
1514 s	N=O str.
1346 s	
1246 s	C-O str.
1066 s and broad	$BF_4^-(\upsilon_3)$
869 s	C-H b. aromatic
773 s	N=O b., aromatic nitro group

s: strong; m: medium.

Table 4-23

Microanalysis of 2-(p-nitrophenyl)-4,6-diphenylpyrylium tetrafluoroborate

formula: $C_{23}H_{16}NO_3BF_4$

	C	H	N
theory	62.62	3.66	3.17
found	62.98	3.59	3.15

4.5.2 Synthesis of 2,6-dichloro-4-[(4,6-diphenyl)-2-(p-nitrophenyl)-N-pyridinio]-phenol tetrafluoroborate

Experimental method:

1.1 g (2.5 mmoles) of 2-(p-nitrophenyl)-4,6-diphenylpyrylium tetrafluoroborate produced from the section 4.5.1, 0.53 g (3.0 mmoles) of 2,6-dichloro-4-aminophenol (Aldrich) and 0.8 g of sodium acetate trihydrate (Aldrich) were dissolved in 20 ml of 95% aqueous ethanol and placed in a 100 ml one necked flask with a magnetic stirring bar. It was refluxed overnight and then 10 ml of 50% aqueous fluoroboric acid (BDH) was added to the hot mixture solution. The solution was poured into 300 ml of distilled water and refrigerated overnight to precipitate crude salt as lump in yellow colour. The crude salt was dissolved in 20 ml of hot methanol and the solution was added dropwise to 300 ml of diethyl ether in stirring to precipitate the betaine salt again. This step was repeated a second time. A purified light brown solid product (1.22 g, yield: 77%) was obtained as 2,6-dichloro-4-[(4,6-diphenyl)-2-(p-nitrophenyl)-N-pyridinio]-phenol tetrafluoroborate.

An infrared spectrum of the solid product was recorded in a KBr disc and revealed that it contained -OH, $-NO_2$, BF_4^- and aromatic ring structures. The infrared spectral band positions and arrangements are given in the Table 4-24. An ^1H n. m. r. spectrum of the compound was also recorded in solvent of d_6-DMSO, which further confirmed the structure of the product having the groups, -OH and aromatic ring, the results are given in Table 4-25. Microanalysis results (Table 4-26) of the product for elements C, H and N revealed that it should be 2,6-dichloro-4-[(4,6-diphenyl)-2-(p-nitrophenyl)-N-pyridinio]-phenol tetrafluoroborate with two crystallised water molecules.

Table 4-24

Infrared spectral data of 2,6-dichloro-4-[(4,6-diphenyl)-2-(p-nitrophenyl)-N-pyridinio]-phenol tetrafluoroborate in KBr

band position (cm^{-1})	arrangement
3650-3150 s and broad	O-H str. and H_2O of crystallisation
3050 w	C-H str., aromatic
1610 s	C=C str., aromatic
1530 s	N=O str., aromatic nitro group
1505 s	
1110-980 s and broad	$BF_4^-(\upsilon_3)$
840 s	C-H b. aromatic
750 s	
690 s	N=O b., nitro group

s: strong; w: weak.

Table 4-25

^1H n.m.r. spectral data of 2,6-dichloro-4-[(4,6-diphenyl)-2-(p-nitrophenyl)-N-pyridinio]-phenol tetrafluoroborate in d_6-DMSO

formula: $C_{29}H_{19}N_2O_3Cl_2BF_4 \cdot 2H_2O$

chemical shift (δ, p.p.m)	type	arrangement
8.8	m	2H, 3,5-H of pyridine ring
8.35	m	4H, aromatic
7.55-7.85	m	7H, aromatic
7.40-7.52	m	5H, aromatic
3.40	s and broad	OH and H_2O of crystallisation

s: singlet; m: multiplet.

Table 4-26

Microanalysis of 2,6-dichloro-4-[(4,6-diphenyl)-2-(p-nitrophenyl)-N-pyridinio]-phenol tetrafluoroborate

formula: $C_{29}H_{19}N_2O_3Cl_2BF_4 \cdot 2H_2O$

	C	H	N
theory	54.36	3.64	4.40
found	54.51	3.52	4.37

4.5.3 Reduction of 2,6-dichloro-4-[(4,6-diphenyl)-2-(p-nitrophenyl)-N-pyridinio]-phenol tetrafluoroborate into 2,6-dichloro-4-[(4,6-diphenyl)-2-(p-aminophenyl)-N-pyridinio]-phenol tetrafluoroborate

Reduction reaction was carried out following the procedures used in the section 4.2.4 for reduction of 2,6-diphenyl-4-[(4,6-diphenyl)-2-(p-nitrophenyl)-N-pyridinio]-phenol tetrafluoroborate. The main materials used are:

1. 1.0 g (1.6 mmoles) of 2,6-dichloro-4-[(4,6-diphenyl)-2-(p-nitrophenyl)-N-pyridinio]-phenol tetrafluoroborate synthesised from previous step 4.5.2;
2. 2 g of 10% palladium on activated carbon (Aldrich);

Finally a yellow solid (0.68 g, yield: 71%) was produced and considered as 2,6-dichloro-4-[(4,6-diphenyl)-2-(p-aminophenyl)-N-pyridinio]-phenol tetrafluorobo-rate. Its infrared spectrum recorded in a KBr disc, and the bands found and arrangements are listed in Table 4-27. Microanalysis results (Table 4-28) of the product for elements, C, H and N indicate that its composition is consistent with 2,6-dichloro-4-[(4,6-diphenyl)-2-(p-aminophenyl)-N-pyridinio]-phenol tetrafluo-roborate containing two crystallised water molecules.

Table 4-28

Microanalysis of 2,6-dichloro-4-[(4,6-diphenyl)-2-(p-aminophenyl)-N-pyridinio]-phenol tetrafluoroborate

formula: $C_{29}H_{21}N_2OCl_2BF_4 \cdot 2H_2O$

	C	H	N
theory	57.36	4.15	4.61
found	57.32	4.09	4.58

Table 4-27

Infrared spectral data of 2,6-dichloro-4-[(4,6-diphenyl)-2-(p-aminophenyl)-N-pyridinio]-phenol tetrafluoroborate in KBr

band position (cm^{-1})	arrangement
3600-3100 s and broad	O-H str., N-H str., and H_2O of crystallisation
3040 m	C-H str., aromatic
1595 s	N-H b.
1530 s	C=C str., aromatic
1470 s	
1325 s	C-N str.
1130-950 s and broad	$BF_4^-(\upsilon_3)$
835 s	C-H b. aromatic
750 s	
685 s	

s: strong; m: medium.

4.5.4 Conversion of 2,6-dichloro-4-[(4,6-diphenyl)-2-(p-aminophenyl)-N-pyridinio]-phenol tetrafluoroborate into 2,6-dichloro-4-[(4,6-diphenyl)-2-(p-aminophenyl)-N-pyridinio]-phenolate

The same method for conversion of 2,6-diphenyl-4-[(4,6-diphenyl)-2-(p-nitrophenyl)-N-pyridinio]-phenol tetrafluoroborate in the section 4.3.3 was used for conversion of 2,6-dichloro-4-[(4,6-diphenyl)-2-(p-aminophenyl)-N-pyridinio]-phenol tetrafluoroborate into its dye form. The main materials used are:

1. 0.60 g of 2,6-dichloro-4-[(4,6-diphenyl)-2-(p-aminophenyl)-N-pyridinio]-phenol tetrafluoroborate;

2. 40 ml of methanol;

3. 6 ml of 15% sodium methoxide in methanol.

A dark purple crystal (0.32 g, yield: 63%) was obtained as dye, 2,6-dichloro-4-[(4,6-diphenyl)-2-(p-aminophenyl)-N-pyridinio]-phenolate (m.p. 214-216 °C). An infrared spectrum of the compound generated was recorded in a KBr disc, which shows that the produced dye had desirable structures such as amino group and aromatic ring. The infrared spectral data and arrangements are given in Table 4-29. A ^1H n. m. r. spectrum of the dye was also recorded in a solvent of $CDCl_3$, which further confirms the aromatic structure and amino group of the dye formed, spectral data are given in Table 4-30. Elemental analysis (Table 4-31) of the dye indicate that it should be 2,6-dichloro-4-[(4,6-diphenyl)-2-(p-aminophenyl)-N-pyridinio]-phenolate containing two crystallised water molecules per molecule of dye.

Table 4-31

Microanalysis of 2,6-dichloro-4-[(4,6-diphenyl)-2-(p-aminophenyl)-N-pyridinio]-phenolate

formula: $C_{29}H_{21}N_2OCl_2 \cdot 2H_2O$

	C	H	N
theory	67.06	4.66	5.39
found	67.11	4.59	5.32

Table 4-29

Infrared spectral data of 2,6-dichloro-4-[(4,6-diphenyl)-2-(p-aminophenyl)-N-pyridinio]-phenolate in KBr

band position (cm^{-1})	arrangement
3450 s and broad	H_2O of crystallisation
3202 m and broad	N-H str.
3055 m and broad	
1595 s	N-H b.
1590 s	
1460 s	C=C str., aromatic
1361 s	C-N str.
842 s	C-H b. aromatic
795 s	
705 s	

s: strong; m: medium.

Table 4-30

^1H n.m.r. spectral data of 2,6-dichloro-4-[(4,6-diphenyl)-2-(p-aminophenyl)-N-pyridinio]-phenolate in $CDCl_3$

formula: $C_{29}H_{21}N_2OCl_2 \cdot 2H_2O$

chemical shift (δ, p.p.m)	type	arrangement
8.4	m	2H, 3,5-H of pyridine ring
8.25-7.7	m	5H, aromatic
7.5	s	5H, aromatic
7.15	m	2H, aromatic
6.85-6.5	m	4H, aromatic
3.40	s and broad	NH_2 and H_2O of crystallisation

s: singlet; m: multiplet.

4.6 Synthesis of 2,6-difluoro-4-[(2,6-diphenyl)-4-(p-aminophenyl)-N-pyridinio]-phenolate

The structure of 2,6-difluoro-4-[(2,6-diphenyl)-4-(p-aminophenyl)-N-pyridinio]-phenolate, is showed in Fig. 4-20.

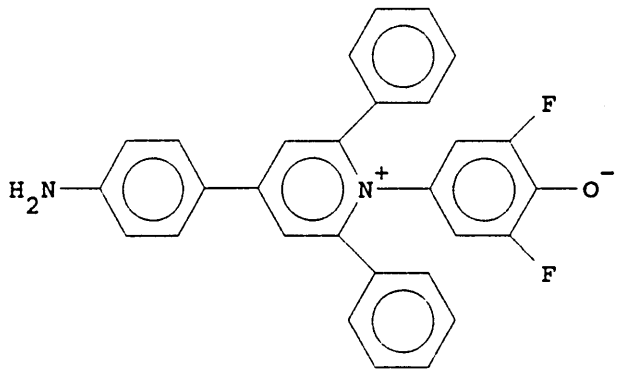

Fig. 4-20 The structure of structure of 2,6-difluoro-4-[(2,6-diphenyl)-4-(p-aminophenyl)-N-pyridinio]-phenolate

It was thought that if 2,6-dichloro-4-[(2,6-diphenyl)-4-(p-aminophenyl)-N-pyridinio]-phenolate, can reduce its pKa value to increase its applications in a wider pH range, 2,6-difluoro-4-[(2,6-diphenyl)-4-(p-aminophenyl)-N-pyridinio]-phenolate, then would have this effect as well, even more efficiently. Because the fluorine atom has a higher electronegativity than chlorine, this allows it to delocalize the negative charge on the oxygen atom more efficiently so that the oxygen atom would not easily be protonated.

4.6.1 Synthesis of 2,6-difluoro-4-nitrophenol by nitration of 2,6-difluorophenol

The compound expected, 2,6-difluoro-4-nitrophenol, was easily obtained by a nitration reaction showed in Fig. 4-21 as below.

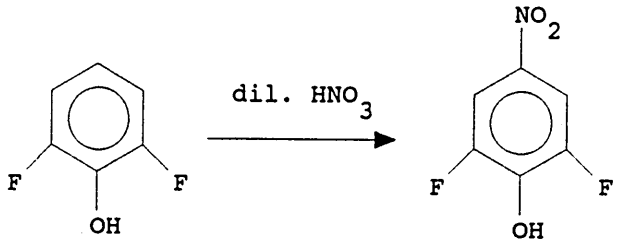

Fig. 4-21 The reaction scheme for 2,6-difluoro-4-nitrophenol

Similar reaction was carried out by Kessler and Wolfbeis.[32] They nitrated 2,6-diphenylphenol by diluted nitric acid and obtained 4-nitro-2,6-diphenylphenol.

Experimental method:

4 g (31 mmoles) of 2,6-difluorophenol (Fluorochem Limited) and a magnetic stirring bar were placed in a 100 ml beaker, 25 ml of 1:5 (V/V) aqueous nitric acid (HNO_3) was added dropwise to the 2,6-difluorophenol under stirring at room temperature. The mixture became red-brown from the colourless of the 2,6-difluorophenol crystal. The reaction mixture was left overnight to complete the nitration reaction. The resulting red-brown oil compound at the bottom of the solution was extracted by 20 ml of diethyl ether (in two times). About 4 g (74% yield) red-brown solid was obtained as 2,6-difluoro-4-nitrophenol after removal of diethyl ether and dried completely by rotoevaporator.

An infrared spectrum of the solid product was recorded in a KBr disc, which shows it contains the structural groups like -NO_2, -OH, and aromatic ring. The infrared data and arrangements are given in Table 4-32. Microanalysis results of the solid generated for C, H and N are given in Table 4-33, which reveal that its composition are consistent with the compound, 2,6-difluoro-4-nitrophenol.

Table 4-32

Infrared spectral data of 2,6-difluoro-4-nitrophenol in KBr

band position (cm^{-1})	arrangement
3236 s and broad	O-H str.
3095 m	C-H str., aromatic
1614 s	C=C str., aromatic
1520 s	N=O str.
1346 s	
1232 s	O-H def.
881 s	C-H b. aromatic
755 s	N=O b.

s: strong; m: medium.

Table 4-33

Microanalysis of 2,6-difluoro-4-nitrophenol

formula: $C_6H_3NO_3F_2$

	C	H	N
theory	41.16	1.73	8.00
found	41.77	1.95	7.99

4.6.2 Reduction of 2,6-difluoro-4-nitrophenol into 2,6-difluoro-4-aminophenol[29]

2,6-difluoro-4-aminophenol was obtained by using the same method in the section 4.2.2 for reduction of 2,6-dimethyl-4-nitrophenol. The main materials used are:

1. 4.0 g (27.6 mmoles) of 2,6-difluoro-4-nitrophenol produced from previous step 4.6.1;
2. 10% palladium on activated carbon (Aldrich, 8g);
3. 50 ml of 97% formic acid.

Finally, a light brown solid, about 3.5 g (70% yield), was obtained as final pure product .

Its infrared spectrum recorded in KBr disc revealed that it contained the groups -OH, $-NH_2$ and aromatic ring, spectral data and arrangements are listed in Table 4-34. A ^1H n. m. r. spectrum of the solid formed was recorded in a solvent of d_6-DMSO, which showed it has $-NH_3^+$ group and 2 aromatic hydrogen atoms. The spectral data are given in Table 4-35. Elemental analysis (Table 4-36) of the product for C, H and N further confirmed that the product's composition were consistent with 2,6-difluoro-4-aminophenol hydrochloride showed in Fig. 4-21.

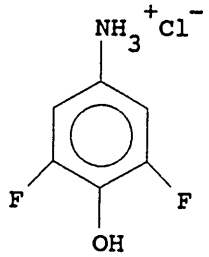

Fig. 4-21 The structure of 2,6-difluoro-4-aminophenol hydrochloride

Table 4-34

Infrared spectral data of 2,6-difluoro-4-aminophenol hydrochloride in KBr

band position (cm^{-1})	arrangement
3600-2600 s and broad	O-H str., N-H str., and C-H str.
1650 s	N-H b.
1630 s	
1541 s	C=C str., aromatic
1520 s	
1348 s	C-N str.
862 s	C-H b. aromatic
805 s	
644 s	

s: strong; m: medium.

Table 4-35

^1H n.m.r. spectral data of 2,6-difluoro-4-aminophenol hydrochloride in d_6-DMSO

formula: $C_6H_5NOF_2 \cdot HCl$

chemical shift (δ, p.p.m)	type	arrangement
10.40	s and broad	3H, from NH^+_3
7.05	m	2H, aromatic

s: singlet; m: multiplet.

Table 4-36

Microanalysis of 2,6-difluoro-4-aminophenol hydrochloride

formula: formula: $C_6H_5NOF_2 \cdot HCl$

	C	H	N
theory	39.69	3.33	7.71
found	39.65	3.44	7.81

4.6.3 Synthesis of 2,6-difluoro-4-[(2,6-diphenyl)-4-(p-nitrophenyl)-N-pyridinio]-phenol tetrafluoroborate

The structure of 2,6-difluoro-4-[(2,6-diphenyl)-4-(p-nitrophenyl)-N-pyridinio]-phenol tetrafluoroborate is showed in Fig. 4-22.

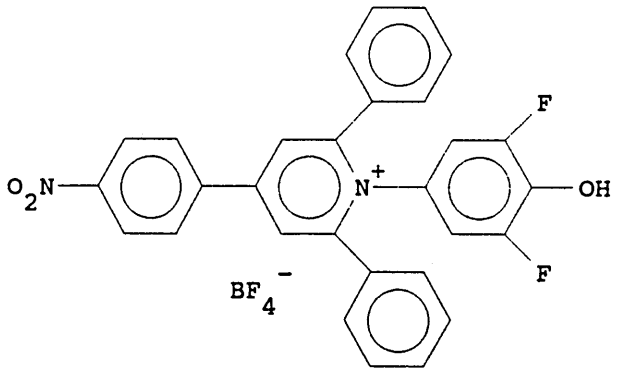

Fig. 4-22 The structure of 2,6-difluoro-4-[(2,6-diphenyl)-4-(p-nitrophenyl)-N-pyridinio]-phenol tetrafluoroborate

Synthetic method was the same as that used in the section 4.2.3. The main materials used are:

1. 0.73 g (5 mmoles) of 2,6-difluoro-4-aminophenol hydrochloride produced from the previous section 4.6.2;
2. 10 ml of 95% aqueous ethanol and 18 ml of 0.333 M ethanolic KOH solution;
3. 2.21 g (5 mmoles) of 4-(4-nitrophenyl)-2,6-diphenylpyrylium tetrafluoroborate generated from the previous section 4.2.1;
4. 0.72 g (5 mmoles) of sodium acetate trihydrate.

Finally, 1.81 g (60% yield) yellow solid was obtained as 2,6-difluoro-4-[(2,6-diphenyl)-4-(p-nitrophenyl)-N-pyridinio]-phenol tetrafluoroborate. An infrared spectrum of the solid generated was recorded in a KBr disc, the bands found in its infrared spectrum and arrangements are listed in Table 4-37. A strong and broad band between 3700 and 3100 cm^{-1} was assigned to O-H stretch, which might be from both -OH on the compound and H_2O of crystallisation, and a band at 3040 cm^{-1} was thought as C-H stretch from planar aromatic ring. A band found at 1610 cm^{-1} was considered as C=C stretch of aromatic ring. Bands at 1500 and 1430 cm^{-1} were assigned to N=O stretch. A broad band around 1100 cm^{-1} was thought as υ_3 vibration of BF_4^-. The infrared spectrum of the product showed that it contained a number of structural groups that should have in the compound expected. An ^1H n. m. r. spectrum recorded from a solvent of d_6-DMSO further confirmed that the product contained 18 aromatic hydrogen atoms, spectral data are given in Table 4-38. Microanalysis results(Table 4-39) of the solid formed in this section reveal that its composition is consistent with 2,6-difluoro-4-[(2,6-diphenyl)-4-(p-nitrophenyl)-N-pyridinio]-phenol tetrafluoroborate with two crystallised water molecules.

Table 4-37

Infrared spectral data of 2,6-difluoro-4-[(2,6-diphenyl)-4-(p-nitrophenyl)-N-pyridinio]-phenol tetrafluoroborate in KBr

band position (cm^{-1})	arrangement
3700-3100 s and broad	O-H str. and H_2O of crystallisation
3040 m	C-H str., aromatic
1610 s	C=C str., aromatic
1500 s	N=O str., aromatic nitro group
1430 m	
1330 s	C-N str.
1120-950 s and broad	BF_4^- (υ_3)
845 s	C-H b. aromatic
740 s	
680 s	N=O b., aromatic nitro group

s: strong; m: medium.

Table 4-38

^1H n.m.r. spectral data of 2,6-difluoro-4-[(2,6-diphenyl)-4-(p-nitrophenyl)-N-pyridinio]-phenol tetrafluoroborate in d_6-DMSO

formula: $C_{29}H_{19}N_2O_3BF_6 \cdot 2H_2O$

chemical shift (δ, p.p.m)	type	arrangement
8.8	m	2H, 3,5-H of pyridine ring
8.6	m	2H, aromatic
8.45	m	2H, aromatic
7.45	m	12H, aromatic
3.5	s and broad	OH and H_2O of crystallisation

s: singlet; m: multiplet.

Table 4-39

Microanalysis of 2,6-difluoro-4-[(2,6-diphenyl)-4-(p-nitrophenyl)-N-pyridinio]-phenol tetrafluoroborate

formula: $C_{29}H_{19}N_2O_3BF_6 \cdot 2H_2O$

	C	H	N
theory	57.64	3.84	4.64
found	57.59	3.96	4.68

4.6.4 Reduction of 2,6-difluoro-4-[(2,6-diphenyl)-4-(p-nitrophenyl)-N-pyridinio]-phenol tetrafluoroborate into 2,6-difluoro-4-[(2,6-diphenyl)-4-(p-aminophenyl)-N-pyridinio]-phenol tetrafluoroborate

2,6-difluoro-4-[(2,6-diphenyl)-4-(p-nitrophenyl)-N-pyridinio]-phenol tetra-fluoroborate was obtained by following the procedures used in the section 4.2.4 for reduction of 2,6-dimethyl-4-[(2,6-diphenyl)-4-(p-nitrophenyl)-N-pyridinio]-phenol tetrafluoroborate. The reagents used are listed below:

1. 1.37 g of 2,6-difluoro-4-[(2,6-diphenyl)-4-(p-nitrophenyl)-N-pyridinio]-phenol tetrafluoroborate;
2. 2.74 g of 10% palladium on activated carbon;
3. 20 ml of 97% formic acid.

Finally, 0.92 g (71% yield) yellow solid was obtained as product, 2,6-difluoro-4-[(2,6-diphenyl)-4-(p-aminophenyl)-N-pyridinio]-phenol tetrafluoroborate. An infrared spectrum of the solid product was recorded in a KBr disc and the infrared spectral data and arrangements are given in Table 4-40.

Microanalysis results of the product (Table 4-41) revealed it should be 2,6-difluoro-4-[(2,6-diphenyl)-4-(p-aminophenyl)-N-pyridinio]-phenol tetrafluoroborate with two crystallised water molecules.

Table 4-40

Infrared spectral data of 2,6-difluoro-4-[(2,6-diphenyl)-4-(p-aminophenyl)-N-pyridinio]-phenol tetrafluoroborate in KBr

band position (cm^{-1})	arrangement
3600-3100 s and broad	O-H str., N-H str. and H_2O of crystallisation
1620 s	N-H b.
1610 s	
1510 s	C=C str., aromatic
1480 s	
1330 s	C-N str.
1110-1000 s and broad	BF_4^- (υ_3)
835 s	C-H b. aromatic
770 s	
675 s	

s: strong.

Table 4-41

Microanalysis of 2,6-difluoro-4-[(2,6-diphenyl)-4-(p-aminophenyl)-N-pyridinio]-phenol tetrafluoroborate

formula: $C_{29}H_{21}N_2OBF_6 \cdot 2H_2O$

	C	H	N
theory	60.65	4.39	4.88
found	60.77	4.43	4.79

4.6.5 Conversion of 2,6-difluoro-4-[(2,6-diphenyl)-4-(p-aminophenyl)-N-pyridinio]-phenol tetrafluoroborate into 2,6-difluoro-4-[(2,6-diphenyl)-4-(p-aminophenyl)-N-pyridinio]-phenolate

Conversion reaction was carried out following the procedure used in the previous section 4.3.3. 0.90 g of 2,6-difluoro-4-[(2,6-diphenyl)-4-(p-aminophenyl)-N-pyridinio]-phenol tetrafluoroborate was used to produce its dye. Finally 0.6 g (79% yield) dark purple fine crystals were obtained as dye, 2,6-difluoro-4-[(2,6-diphenyl)-4-(p-aminophenyl)-N-pyridinio]-phenolate (m.p. 207-208 °C). Its infrared spectrum recorded in KBr disc revealed that it had -NH_2, aromatic ring and crystallised water, spectral data are given in Table 4-42. Typical N-H stretch and O-H stretch bands were found at 3445 and 3202 cm^{-1}, they were strong and broad. The C-H stretch and C=C stretch bands of aromatic ring were found at 3059 and 1496 cm^{-1}. Two N-H bending bands at 1635 and 1505 cm^{-1} further showed existence of NH_2 group. An ^1H n. m. r. spectrum of the product confirmed that it contained 18 aromatic hydrogen atoms, and spectral data and arrangements are listed in Table 4-43. Elemental analysis (Table 4-44) of the dark purple solid generated showed that its composition was consistent with 2,6-difluoro-4-[(2,6-diphenyl)-4-(p-aminophenyl)-N-pyridinio]-phenolate and had two crystallised water molecules.

Table 4-44

Microanalysis of 2,6-difluoro-4-[(2,6-diphenyl)-4-(p-aminophenyl)-N-pyridinio]-phenolate

formula: $C_{29}H_{20}N_2OF_2 \cdot 2H_2O$

	C	H	N
theory	71.59	4.97	5.76
found	71.61	5.01	5.76

Table 4-42

Infrared spectral data of 2,6-difluoro-4-[(2,6-diphenyl)-4-(p-aminophenyl)-N-pyridinio]-phenolate in KBr

band position (cm^{-1})	arrangement
3445 s and broad	N-H str. and H_2O of crystallisation
3202 s and broad	
3059 m	C-H str., aromatic
1635 s	N-H b.
1505 s	
1496 s	C=C str., aromatic
1354 s	C-N str.
842 s	C-H b. aromatic
761 s	
700 s	

s: strong; m: medium.

Table 4-43

^1H n.m.r. spectral data of 2,6-difluoro-4-[(2,6-diphenyl)-4-(p-aminophenyl)-N-pyridinio]-phenolate in d_6-DMSO

formula: $C_{29}H_{20}N_2OF_2 \cdot 2H_2O$

chemical shift (δ, p.p.m)	type	arrangement
8.20	s	2H, 3,5-H of pyridine ring
8.05	m	2H, aromatic
7.40	m	10H, aromatic
6.70-6.35	m	4H, aromatic
3.5	s	NH_2 and H_2O of crystallisation

s: singlet; m: multiplet.

4.7 Synthesis of 2,6-difluoro-4-[(4,6-diphenyl)-2-(p-aminophenyl)-N-pyridinio]-phenolate

2,6-difluoro-4-[(4,6-diphenyl)-2-(p-aminophenyl)-N-pyridinio]-phenolate is almost the same as the compound, 2,6-difluoro-4-[(2,6-diphenyl)-4-(p-aminophenyl)-N-pyridinio]-phenolate described in section 4.6. A sole difference between these two dyes is the position of the amino group on different phenyl ring.

4.7.1 Synthesis of 2,6-difluoro-4-[(4,6-diphenyl)-2-(p-nitrophenyl)-N-pyridinio]-phenol tetrafluoroborate

Experimental method:

1.2 g (2.5 mmoles) of 2-(p-nitrophenyl)-4,6-diphenylpyrylium tetrafluoroborate synthesised in the section 4.5.1 and 0.5 g (>2.5 mmoles) of 2,6-difluoro-4-aminophenol hydrochloride generated from the section 4.6.2 were dissolved in 10 ml of 95% aqueous ethanol. 0.8 g of sodium acetate trihydrate and 14 ml of 0.333 M ethanolic KOH solution were added to the mixture. It was refluxed overnight. The KCl generated from the reaction was removed by filtering. 10 ml of 50% aqueous fluroboric acid (BDH) was added to the filtrate and then the filtrate was poured into 300 ml of distilled water. It was refrigerated overnight to precipitate the crude salt. A light yellow solid was obtained after filtering. It was purified by dissolving in 20 ml of hot methanol, precipitating with 300 ml of diethyl ether and finally filtering. This step was repeated a second time. About 1.0 g (66% yield) of light yellow solid was obtained as 2,6-difluoro-4-[(4,6-diphenyl)-2-(p-nitrophenyl)-N-pyridinio]-phenol tetrafluoroborate.

The infrared spectral data of the product and arrangements are listed in Table 4-45. An ^1H n. m. r. spectrum of the product recorded in a solvent of d_6-DMSO confirmed that the solid product had 18 aromatic hydrogen atoms, spectral data are listed in Table 4-46. Microanalysis results of the compound formed are listed in Table 4-47, which indicated that its compositions were 2,6-difluoro-4-[(4,6-diphenyl)-2-(p-nitrophenyl)-N-pyridinio]-phenol tetrafluoroborate with two crystallised water molecules.

Table 4-45

Infrared spectral data of 2,6-difluoro-4-[(4,6-diphenyl)-2-(p-nitrophenyl)-N-pyridinio]-phenol tetrafluoroborate in KBr

band position (cm^{-1})	arrangement
3600-3150 s and broad	O-H str. and H_2O of crystallisation
3010 s and broad	C-H str., aromatic
1600 s	C=C str., aromatic
1530 s	N=O str., aromatic nitro group
1500 s	
1325 s	C-N str.
1100-980 s and broad	BF_4^- (υ_3)
835 s	C-H b. aromatic
740 s	
680 s	N=O b., aromatic nitro group

s: strong; m: medium.

Table 4-46

^1H n.m.r. spectral data of 2,6-difluoro-4-[(4,6-diphenyl)-2-(p-nitrophenyl)-N-pyridinio]-phenol tetrafluoroborate in d_6-DMSO

formula: $C_{29}H_{19}N_2O_3BF_6 \cdot 2H_2O$

chemical shift (δ, p.p.m)	type	arrangement
8.80	m	2H, 3,5-H of pyridine ring
8.40	m	4H, aromatic
7.85-7.55	m	6H, aromatic
7.50-7.30	m	6H, aromatic
3.50	s and broad	OH and H_2O of crystallisation

s: singlet; m: multiplet.

Table 4-47

Microanalysis of 2,6-difluoro-4-[(4,6-diphenyl)-2-(p-nitrophenyl)-N-pyridinio]-phenol tetrafluoroborate

formula: $C_{29}H_{19}N_2O_3BF_6 \cdot 2H_2O$

	C	H	N
theory	57.64	3.84	4.64
found	57.67	3.72	4.61

4.7.2 Reduction 2,6-difluoro-4-[(4,6-diphenyl)-2-(p-nitrophenyl)-N-pyridinio]-phenol tetrafluoroborate into 2,6-difluoro-4-[(4,6-diphenyl)-2-(p-aminophenyl)-N-pyridinio]-phenol tetrafluoroborate

Method used for reduction of 2,6-difluoro-4-[(4,6-diphenyl)-2-(p-nitrophenyl)-N-pyridinio]-phenol tetrafluoroborate was the same as that used for reduction of 2,6-dichloro-4-[(4,6-diphenyl)-2-(p-nitrophenyl)-N-pyridinio]-phenol tetrafluoroborate in the previous section 4.5.3. 1.0 g (1.7 mmoles) of 2,6-difluoro-4-[(4,6-diphenyl)-2-(p-nitrophenyl)-N-pyridinio]-phenol tetrafluoroborate was used, and 0.65 g (68% yield) yellow solid was obtained as 2,6-difluoro-4-[(4,6-diphenyl)-2-(p-aminophenyl)-N-pyridinio]-phenol tetrafluoroborate. Its infrared spectrum recorded in KBr disc revealed that it contained -OH, $-NH_2$, BF_4^- groups and aromatic ring. The infrared spectral data and arrangements are given in Table 4-48. Elemental analysis (Table 4-49) of the solid product for C, H and N showed that the product should be 2,6-difluoro-4-[(4,6-diphenyl)-2-(p-aminophenyl)-N-pyridinio]-phenol tetrafluoroborate with two crystallised water molecules.

Table 4-49

Microanalysis of 2,6-difluoro-4-[(4,6-diphenyl)-2-(p-aminophenyl)-N-pyridinio]-phenol tetrafluoroborate

formula: $C_{29}H_{21}N_2OBF_6 \cdot 2H_2O$

	C	H	N
theory	60.65	4.39	4.88
found	60.62	4.51	4.92

Table 4-48

Infrared spectral data of 2,6-difluoro-4-[(4,6-diphenyl)-2-(p-aminophenyl)-N-pyridinio]-phenol tetrafluoroborate in KBr

band position (cm^{-1})	arrangement
3600-3100 s and broad	O-H str., N-H str., and H_2O of crystallisation
3010 m	C-H str., aromatic
1635 s	N-H b.
1600 s	
1550 s	C=C str., aromatic
1470 s	
1350 s	C-N str.
1100-1020 s and broad	BF_4^- (υ_3)
790 s	C-H b., aromatic
745 s	
685 s	

s: strong; m: medium.

4.7.3 Synthesis of 2,6-difluoro-4-[(4,6-diphenyl)-2-(p-aminophenyl)-N-pyridinio]-phenolate

0.6 g (1.1 mmoles) of 2,6-difluoro-4-[(4,6-diphenyl)-2-(p-aminophenyl)-N-pyridinio]-phenol tetrafluoroborate was dissolved in 50 ml of methanol, and 10 ml of 15% sodium methoxide in methanol was added to the solution. The solution was heated for 10 mins. and then poured into 100 ml of 10% aqueous NaOH solution. The mixture solution was left in a refrigerator overnight to

precipitate the dye. The dye was extracted into 300 ml of chloroform in 50 ml portions to form a dark purple solution. the solution was dried over anhydrous sodium sulphate. 0.37 g (73% yield) dark purple solid (m.p. 211-212 °C) was obtained as dye 2,6-difluoro-4-[(4,6-diphenyl)-2-(p-amino-phenyl)-N-pyridinio]-phenolate after removing chloroform and drying under vacuum. An ^1H n. m. r. spectrum of the solid generated was recorded in solvent of d_6-DMSO and showed that it had desirable 18 aromatic hydrogen atoms, spectral data are given in Table 4-50. Microanalysis results (Table 4-51) of the product revealed that its compositions were consistent with 2,6-difluoro-4-[(4,6-diphenyl)-2-(p-aminophenyl)-N-pyridinio]-phenolate with two crystallised water molecules per molecule of dye.

Table 4-50

^1H n.m.r. spectral data of 2,6-difluoro-4-[(4,6-diphenyl)-2-(p-amino-phenyl)-N-pyridinio]-phenolate in d_6-DMSO

formula: $C_{29}H_{20}N_2OF_2 \cdot 2H_2O$

chemical shift (δ, p.p.m)	type	arrangement
8.30	m	2H, 3,5-H of pyridine ring
7.65	m	4H, aromatic
7.40	m	7H, aromatic
7.10	m	2H, aromatic
6.60	m	3H, aromatic
3.40	s	NH_2 and H_2O of crystallisation

s: singlet; m: multiplet.

Table 4-51

Microanalysis of 2,6-difluoro-4-[(4,6-diphenyl)-2-(p-amino-phenyl)-N-pyridinio]-phenolate

formula: $C_{29}H_{20}N_2OF_2 \cdot 2H_2O$

	C	H	N
theory	71.59	4.97	5.76
found	71.52	4.78	5.74

4.8 Solvatochromic properties of the dyes synthesised in this work

As mentioned before, the purpose of synthesis of the dyes described above is to find some dyes which have not only excellent solvatochromic property, but also have a functional group in order to link it with a solid support. Therefore, having a good solvatochromic property is very important for our dyes. This type of property was investigated by their uv-vis spectra in a number of different solvents in the range 300-800 nm. The longest wavelength absorption band of each dye was considered as its highly solvatochromic charge transfer band.[29] The maximum of this band for all dyes synthesised in this work was determined in each solvent and listed in Table 4-52 together with the literature data of dyes ET(30), ET(33) and 2,6-dimethyl-4-(2,4,6-triphenyl-N-pyridinio)-phenolate for comparison. The transition energy of the charge transfer band in the maximum wavelength was expressed by a ET value which was calculated by equation[31] (A) as follow.

$$ET(kJ/mol) = 1.1959 \times 10^{-2}\ \upsilon\ (cm^{-1}) \qquad (A)$$

where υ is wavenumber

ET value is a parameter used widely for polarity of solvent, so the ET values of the dyes synthesised in this work were calculated and listed in Table 4-52 as well.

Table 4-52

Absorption maxima and ET values of the dyes

solvent	ET (30) (ref. 3)		ET (33) (ref. 29)		dye* (ref. 29)		dye 1		dye 2		dye 3		dye 4		dye 5		dye 6	
	λ_{max} (nm)	ET (kJ/mol)	λ_{max} (nm)	ET (kJ/mol)	λ_{max} (nm)	ET (kJ/mol)	λ_{max} (nm)	ET (kJ/mol)	λ_{max} (nm)	ET (kJ/mol)	λ_{max} (nm)	ET (kJ/mol)	λ_{max} (nm)	ET (kJ/mol)	λ_{max} (nm)	ET (kJ/mol)	λ_{max} (nm)	ET (kJ/mol)
H_2O	453.0	264.0	409.0	292.4	436.0	274.1	insoluble	insoluble	400.0	298.8	394.0	303.3	399.0	299.5	**	**	**	**
MeOH	515.0	232.2	442.0	270.6	478.0	250.0	428.0	279.2	428.1	279.2	426.0	280.5	428.4	279.0	393.0	304.1	398.0	300.3
EtOH	551.0	217.0	470.0	254.4	519.0	230.3	432.0	276.6	433.6	275.6	433.0	276.0	435.2	274.6	406.0	294.4	409.0	292.4
MeCN	622.0	192.3	516.0	231.8	635.0	188.2	588.0	203.2	480.0	249.0	557.0	214.6	500.0	239.0	495.0	241.4	490.0	243.9
DMF	653.0	183.1	536.0	223.1	.....	.....	612.8	195.0	500.0	239.0	629.0	190.0	517.0	231.2	550.0	217.3	536.0	223.0
acetone	677.0	176.6	551.0	217.0	660.0	181.1	636.0	187.9	516.0	231.6	630.0	189.7	523.0	228.5	553.0	216.1	545.0	219.3
CH_2Cl_2	696.0	171.8	575.0	208.0	685.0	174.5	658.9	181.4	536.8	222.6	634.0	188.6	526.0	227.2	**	**	561.0	213.0
$CHCl_3$	731.0	163.5	.....	.....	725.0	164.8	661.6	180.6	544.2	219.6	643.0	185.9	538.0	222.1	561.0	213.0	569.0	210.0
THF	764.0	156.5	646.0	185.1	.....	.....	715.2	167.1	602.0	198.5	664.0	180.0	588.0	203.2	610.0	195.9	625.0	191.2

dye*: 2,6-dimethyl-4-(2,4,6-triphenyl-N-pyridinio)-phenolate;

dye 1: 2,6-diphenyl-4-[(2,6-diphenyl)-4-(p-aminophenyl)-N-pyridinio]-phenolate;

dye 2: 2,6-dichloro-4-[(2,6-diphenyl)-4-(p-aminophenyl)-N-pyridinio]-phenolate;

dye 3: 2,6-dimethyl-4-[(2,6-diphenyl)-4-(p-aminophenyl)-N-pyridinio]-phenolate;

dye 4: 2,6-difluoro-4-[(2,6-diphenyl)-4-(p-aminophenyl)-N-pyridinio]-phenolate;

dye 5: 2,6-difluoro-4-[(4,6-diphenyl)-2-(p-aminophenyl)-N-pyridinio]-phenolate;

dye 6: 2,6-dichloro-4-[(4,6-diphenyl)-2-(p-aminophenyl)-N-pyridinio]-phenolate.

From the Table 4-52, it can be seen that for the most highly solvatochromic dye ET(30), it has a maximum at 453 nm (ET=264 kJ/mol) in water and in THF it has a maximum at 764 nm (ET=156.5 kJ/mol), a shift of 311 nm (ΔET=107.5 kJ/mol). And for modified dye ET(33), it has a maximum at 409 nm (ET=292.4 kJ/mol) in water and in THF it has a maximum at 646 nm (ET=185.1 kJ/mol), a shift of 237 nm (ΔET=107.3 kJ/mol). Comparison with the dyes generated in the present work, they also have similar values for band shift and change in ET values, for example, dye, 2,6-dichloro-4-[(2,6-diphenyl)-4-(p-aminophenyl)-N-pyridinio]-phenolate (dye 2 in Table 4-52) has a maximum at 400 nm (ET=298.8 kJ/mol) and in THF it has a maximum at 602 nm (ET=198.5 kJ/mol), a shift of 202 nm (ΔET=100.3). This shows that modification of the betaine dyes in the present work is successful. Modified dyes have both solvatochromic property and a functional group which can be linked with a solid support.

4.9 The pKa values of the dyes 2,6-dichloro-4-[2,6-diphenyl-4-(p-aminophenyl)-N-pyridinio]-phenolate and 2,6-difluoro-4-[2,6-diphenyl-4-(p-aminophenyl)-N-pyridinio]-phenolate

Apart from the purpose of synthesis of dyes having both solvatochromic property and a functional group, another purpose of synthesis of these two dyes mentioned in the title is to reduce the pKa value of the dye in order to apply them in a wider pH range.

The pKa values of the two dyes were obtained by the spectrophotometric method at room temperature according to the equation [E][33].

pKa=pH-log[base]/[acid] [E]

The betaine dye can be considered as a Lewis base and its protonated form can be considered as Lewis acid. There is an equilibrium between these two forms as below.

$$A \rightleftharpoons H^+ + B^-$$

Therefore,

$$pKa=pH-\log[base]/[acid]=pH-\log[B]/[A] \qquad [F]$$

If a solution of a betaine dye with a certain concentration [C] is prepared at a given pH value, its pH value can be measured by pH meter and the [B] can known by absorption data from Beer's law $A=\varepsilon[B]l$, (ε is molar extinction coefficient and l is cell length). The value of [A] will then be known from equation: [A]=[C]-[B]. Finally the pKa of the betaine dye can be obtained from the equation [F].

4.9.1 Determination of pKa value of 2,6-difluoro-4-[(2,6-diphenyl-4-p-aminophenyl)-N-pyridinio]-phenolate

Two values of pKa were obtained separately from distilled water and 1% aqueous methanol solution. The average of the two values was considered as pKa value of the dye.

(a). Determination of pKa value of 2,6-difluoro-4-[(2,6-diphenyl-4-p-aminophenyl)-N-pyridinio]-phenolate in distilled water

Two solutions of the betaine dye were prepared with precise concentration $1.332*10^{-4}$ M in distilled water, but the pH value of one solution was adjusted to 1.5 measured by pH meter by a couple of drops concentrated hydrochloric acid.

From the solution without concentrated hydrochloric acid, the maxium absorption wavelength and molar extinction coefficient of the dye in distilled water were determined as below:

λ_{max}=399 nm; A=0.738; ε_{max}=5539.8 $M^{-1}cm^{-1}$

From the solution with concentrated hydrochloric acid, the absorption data at 399 nm and [B], [A] and pKa were determined as below:

A_{399nm}=0.078;[B]=A/εl=0.078/5539.8*1=1.41*10^{-5} M;

[A]= [C]-[B]=1.33*10^{-4}-1.41*10^{-5}=1.19*10^{-4} M;

pKa=pH-log[B]/[A]=1.5-log[1.41*10^{-5}]/[1.19*10^{-4}]

=1.5-log0.119=1.5-(-0.93)=2.43

(b). Determination of pKa value of 2,6-difluoro-4-[(2,6-diphenyl-4-p-aminophenyl)-N-pyridinio]-phenolate in 1% aqueous methanol solution

Two solutions of the betaine dye were prepared with precise concentration 4.355*10^{-5} M in 1% aqueous methanol solution, but the pH value of one solution was adjusted to 2.2 measured by pH meter by a couple of drops concentrated hydrochloric acid.

From the solution without concentrated hydrochloric acid, the maxium absorption wavelength and molar extinction coefficient of the dye in distilled water were determined as below:

λ_{max}=398.4 nm; A=0.293; ε_{max}=6727.9 $M^{-1}cm^{-1}$

From the solution with concentrated hydrochloric acid, the absorption data at 398.4 nm and [B], [A] and pKa were determined as below:

$A_{398.4nm}$=0.146; [B]=A/εl=0.146/6727.9*1=2.17*10^{-5} M;

[A]= [C]-[B]=4.355*10^{-5}-2.17*10^{-5}=2.185*10^{-5} M;

pKa=pH-log[B]/[A]=2.2-log[2.17*10^{-5}]/[2.185*10^{-5}]

=2.2-log0.993=2.2-(-3.05*10^{-3})=2.20

A average value 2.32 of two values from the distilled water 2.43 and 1% aqueous methanol solution 2.20 was considered as a real pKa value of 2,6-difluoro-4-[(2,6-diphenyl-4-p-aminophenyl)-N-pyridinio]-phenolate.

4.9.2 Determination of pKa value of 2,6-dichloro-4-[(2,6-diphenyl-4-p-aminophenyl)-N-pyridinio]-phenolate in 4% aqueous methanol solution

Two solutions of the betaine dye were prepared with precise concentration 4.016*10^{-5} M in 4% aqueous methanol solution, but the pH value of one solution was adjusted to 4.6 measured by pH meter by a couple of drops concentrated hydrochloric acid.

From the solution without concentrated hydrochloric acid, the maxium absorption wavelength and molar extinction coefficient of the dye in distilled water were determined as below:

λ_{max}=401.6 nm; A=0.461; ε_{max}=11479.1 $M^{-1}cm^{-1}$

From the solution with concentrated hydrochloric acid, the absorption data at 401.6 nm and [B], [A] and pKa were determinated as below:

$A_{401.6nm}$=0.305; [B]=A/εl=0.305/11479.1*1=2.66*10^{-5} M;

[A]= [C]-[B]=4.016*10^{-5}-2.66*10^{-5}=1.36*10^{-5} M;

pKa=pH-log[B]/[A]=4.6-log[2.66*10^{-5}]/[1.36*10^{-5}]

=4.6-log1.956=4.6-0.29=4.31

From the results obtained above, it can be seen that two dyesall have a low pKa value which allowsthem to be applied over a wider pH range.

References:

1. Dimroth, K.; Reichardt, C.; Siepmann, T.; Bohlmann, F. Justus Liebigs Ann. Chem. 1963, 661, 1-37.

2. Reichardt, C. Angew. Chem., Int. Ed. Engl. 1965, 4(1), 29-40.

3. Reichardt, C. Solvent Effects in Organic Chemistry; Verlag Chemie: New York, 1979.

4. Hans Sigrist, Hui Gao and Bernhard Wegmuller, Light-Dependent, Covalent Immobilization of Biomolecules on 'Inert' Surfaces, p. 1026-1028, Bio/Technology, Vol. 10, september, 1992.

5. Louis L. Wood and Gary J. Calton, A Novel Method of Immobilization and Its Use in Aspartic acid Production, p. 1081-1084, Bio/Technology, December, 1984.

6. Jerker PoraiH, General Methods and Coupling Procedures, Methods in Enzymology, Vol. 34, Affinity techniques Enzyme Purification : Part B, Edited by William B. Jakoby and Meir Wilchek.

7. H. H. Weetall and A. M. Filbert, Porous Glass for Affinity Chromatography Application, Methods in Enzymology, Vol. 34, Affinity techniques Enzyme Purification : Part B, Edited by William B. Jakoby and Meir Wilchek.

8. Carl Fredrik Mandenius, Stefan Welin, Bengt Danielsson, Ingemar Lundstrom and Klaus Mosbach, The Interaction of proteins and Cells with Affinity Ligands Covalently Coupled to Silicon Surfaces as monitored by Ellipsomtry, Analytical Biochemistry 137, 106-114 (1984).

9. Alexander M. Klibanov, Review, Enzyme Stabilization by Immobilization, Analytical Biochemistry 93, 1-25 (1979).

10. G. F. Kirkbright, R. Narayanaswamy and N. A. Welti, Analyst, 109, 15 (1984).

11. G. F. Kirkbright, R. Narayanaswamy and N. A. Welti, Analyst, 109, 1025 (1984).

12. M. Bacci, F. Baldini, and S. Bracci, Spectroscopic Behavior of Acid-Base Indicators After Immobilization on Glass Supports, Applied Spectroscopy, Vol. 45, No. 9, 1991, pp1508-1515.

13. A. T. Balaban, W. Schroth and G. Fischer, Pyrylium Salts, in Advances in Heterocyclic Chemistry, Vol. 10, 1969, Edited by A. R. Katritzky and A. J. Boulton.

14. W. Dilthey, J. Prakt. Chem. 94, 53 (1916).

15. W. Dilthey and R. Taucher, Chem. Ber. 53, 252 (1960).

16. W. Dilthey and B. Burger, Ber. Deut. Chem. Ges. 54, 825 (1921).

17. W. Dilthey, G. Frode, and H. Koenen, J. Prakt. Chem. 114, 153 (1926).

18. W. Dilthey and C. Berres, J. Prakt. Chem. 111, 340 (1925).

19. W. Dilthey, Ber. Deut. Chem. Ges. 52, 1195 (1919).

20. W. Dilthey, J. Prakt. Chem. 101, 177 (1921).

21. R. Lombard and J. P. Stephan, Bull. Soc. Chim. France, p.1458 (1958).

22. D. S. Breslow and C. R. Hauser, J. Am. Chem. Soc. 62, 2385 (1940).

23. K. Dimroth, Angew. Chem. 72, 331 (1960).

24. K. Dimroth and K. H. Wolf, "Newer Methods of Preparative Organic Chemistry," Vol. 3, p. 357, Academic Press, New York, 1964.

25. H. Kanai, M. Umehara, H. Kitano, and K. Fukui, Nippon Kagaku Zasshi 84, 432, (1963).

26. J. Pascual Vila and A. Escala, Anales Real Soc. Espan. Fis. Quim. (madrid) 46B, 485 (1950).

27. Johnson, B. P.; Gabrielsen, B.; Matulenko, M.; Dorsey, J. G.; Reichardt, C. Anal. Lett. 1986, 19, 939-962.

28. M. Steven Paley and J. Milton Harris, J. Org. Chem. 1991, 56, 568-574.

29. Entwistle, I. D.; Jackson, A. E.; Johnstone, R. W.; Telford, R. P. J. Chem. Soc. Perkin Trans. 1 1977,443-444.

30. M. S. Paley, E. J. Meehan, C. D. Smith, F. E. Rosenberger, S. C. Howard, and J. M. Harris, J. Org. Chem. 1989, 54, 3432-3436.

31. Manfred A. Kessler and Otto S. Wolfbeis, ET(33), a solvatochromic polarity and Micellar probe for neutral solutions, Chemistry and Physics of Lipids, 50(1989) 51-56.

32. Manfred A. Kessler and Otto S. Wolfbeis, An Improved Synthesis of the Solvatochromic Dye ET-30, Communications, Synthesis, August 1988, pp635-636.

33. Leicester F. Haqmilton, S.B., Stephen G. Simpson and David W. Ellis, Calculations of Analytical Chemistry, Seventh Edition, p316.

Chapter 5

Immobilisation of the conjugated compounds synthesised on solid surface by physical adsorption or by Langmuir-Blodgett film technology and investigation of their optical response to some toxic gases

5.1 Introduction

Attempts were made to obtain orientated layers (monolayer or multilayers) of compounds synthesised in chapter 3 by means of Langmuir-Blodgett film technology. The L-B films formed were detected by uv/vis spectroscopy and FT-IR microspectroscopy. Attempts were also made to align the conjugated compounds at a solid surface using physical adsorption. The response of oriented materials to certain toxic gases was investigated by uv/vis spectroscopy.

5.2 Results and conclusion

5.2.1 Investigation of optical response of 3,3'-dihexyloxacarbocyanine to toxic gases by UV-VIS spectrophotometry

A suitable amount (about 0.5 mg) of 3,3'-dihexyloxacarbocyanine compound was dissolved in 5 ml acetone. The solution was dropped onto a transparent plastic substrate. When solvent was evaporated entirely, it was coated with the compound and ready for use.

The piece of plastic coated with the compound, 3,3'-dihexyloxacarbocyanine was mounted inside a small transparent plastic box through which the gas studied could easily pass. The box was connected to an ordinary balloon filled with the gas. The gas was pushed out to pass through the box by squashing the balloon. The simple diagram of the device is shown in the Fig. 5-1 below. The box was easily mounted inside the compartment of the UV-VIS Spectrophotometer used.

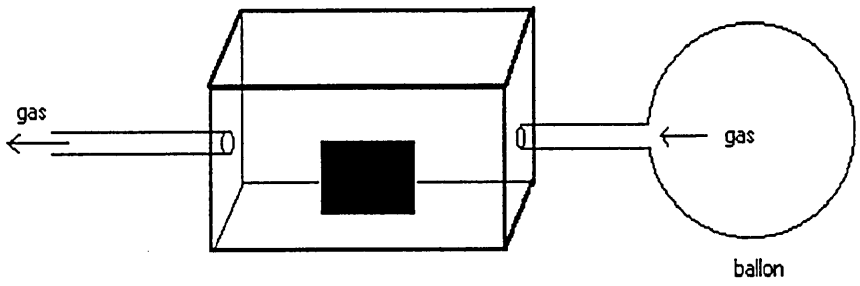

Fig. 5-1 Diagram of the simple device for passing gas

The wavelength maximum, 502 nm, did not change during or following exposure to 9 or 90 ppm NO_2, 100 ppm NH_3, 100 ppm SO_2 or 10 ppm Cl_2. It appeared therefore that 3,3'-dihexyloxacarbocyanine did not respond to the toxic gases, and suggests 3,3'-dihexyloxacarbocyanine is not good for sensing the toxic gases.

5.2.2 Investigation of the optical response of an L-B film of N-alkylquinolinium adduct of TCNQ to toxic gases by UV-VIS spectrophotometry

(i) Preparation of Langmuir-Blodgett film for hexadecyl adduct of TCNQ

A detailed description of the technology of Langmuir- Blodgett (LB) films was given in the Chapter 2. Plotting of a surface pressure versus area (film or per molecule) isotherm is the first step in establishing suitable conditions for building up the L-B film. From the shape of the isotherm, the nature of the film and its degree of packing may be inferred. The stability of a floating monolayer held at a particular surface pressure is another important aspect for producing a good stable film so that constancy of area against time at constant pressure must also be determined before deposition can be achieved.

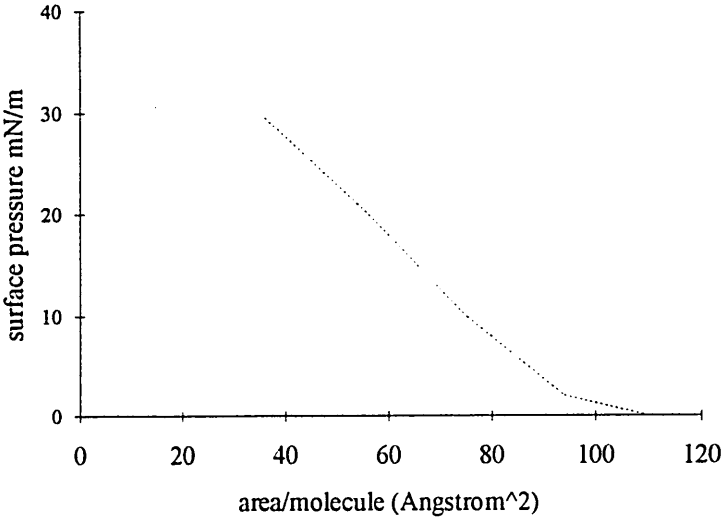

Fig. 5-2 Surface pressure vs. surface area isotherm of hexadecyl adduct of TCNQ

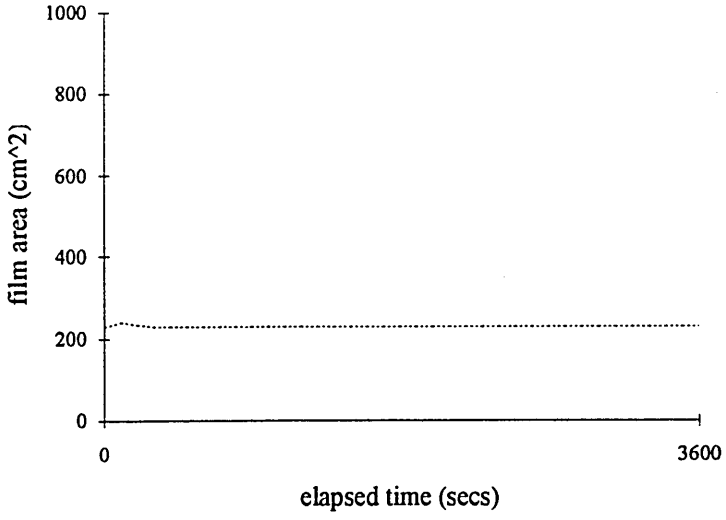

Fig. 5-3 Stability plot for hexadecyl adduct of TCNQ

A plot of a surface pressure versus area per molecule isotherm for hexadecyl adduct of TCNQ prepared was recorded, which is consistent with the results obtained by Ashwell[1] and Bell[2] et al. The plot is showed in Fig. 5-2. It was found that compound formed a monomolecular layer at the air-water interface below 30 mN m^{-1} surface pressure. An area-time stability plot was also recorded (Fig. 5-3) at 25 mN m^{-1} surface pressure, which shows reasonable stability.

Langmuir- Blodgett (LB) films were prepared by depositing a small quantity of a solution of hexadecyl adduct of TCNQ in dichloromethane onto a liquid surface and then allowing time for the organic solvent to evaporate. The material would produce a monomolecular layer film at the air-water surface with the aid of a barrier. The compacted monolayers were transferred at a surface pressure 25 mN m^{-1} by slowly dipping and raising the substrates through the compacted film. Two types of substrates were used. One was a hydrophilic glass slide which was successfully used for deposition of the TCNQ adducts.[2] Another was a glass slide with gold covering. The latter was used for the convenience of detection of the L-B film formed by FT-IR reflectance microspectroscopy.

Although the compacted monolayer was formed and transferred to the substrates, the multilayer L-B film subsequently collapsed. The collapse of the film happened possibly during the course of drying of the film. However, spectral characteristics of the films were still examined using areas of pigment on the slide.

(ii) UV-VIS spectrum and FT-IR microspectroscopy of L-B film of hexadecyl adduct of TCNQ

The L-B film of hexadecyl adduct of TCNQ was found having a maximum

absorption at 612 nm in its uv-vis spectrum, which is different from that of the free adduct in solvent.

The L-B film of a hexadecyl adduct of TCNQ formed on a gold coated glass slide was examined by FTIR reflectance microspectroscopy. A reflectance-transmittance spectrum of the film is shown in Fig. 5-4, which is similar to that of hexadecyl adduct of TCNQ. Two bands at about 2900 cm^{-1} arise from aliphatic C-H stretch (from the long carbon chain), while two bands at 2187 and 2146 cm^{-1} were assigned to C≡N stretch. A broad band found at 3432 cm^{-1} was believed due to water in the film.

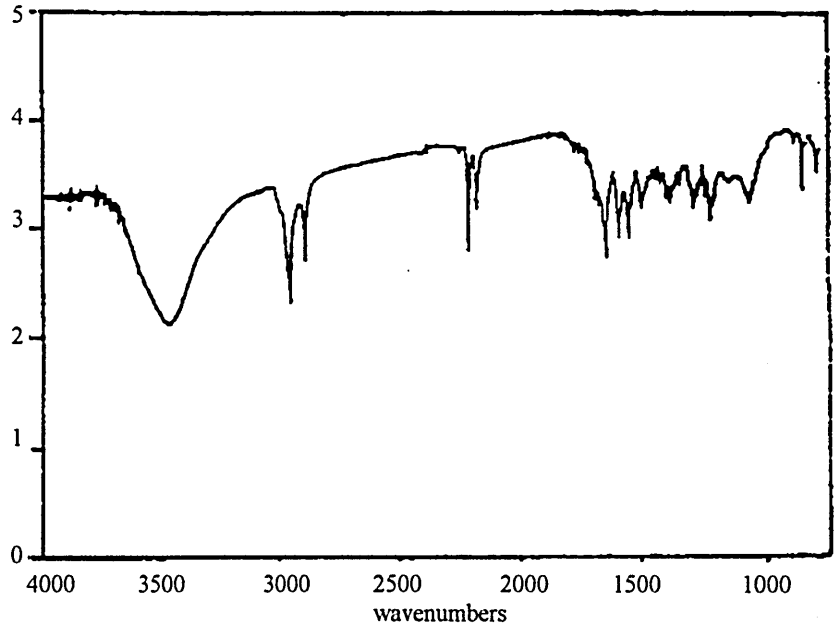

Fig. 5-4 Reflectance transmittance spectrum of the LB film of hexadecyl adduct of TCNQ

(iii) Investigation of optical response of L-B film of hexadecyl adduct of TCNQ to toxic gases by UV-VIS spectrophotometry

The LB film produced was mounted inside a small transparent plastic box.

A simple device used was the same as that showed in Fig. 5-1. Gas responses were investigated by UV-VIS spectrophotometry.

It was reported[3] that the LB film of hexadecyl adduct of TCNQ did respond to NO_2 gas, which resulted in its conductivity increasing, but had no response to NH_3 and SO_2. Similar results were observed for NH_3, SO_2 and Cl_2 gas by UV-VIS spectrophotometry. Only a small change, 2 nm shift in maximum absorption (from 612 to 610 nm) of the LB film of hexadecyl adduct of TCNQ was found for 90 ppm NO_2, but no change was seen for 9 ppm NO_2.

5.2.3 Study of the solvatochromic property of 4-[1-methyl-4(1H)-pyridylidene]-3-phenyl-5(4H)-isoxazolone

The maximum absorptions of the compound in two different solvents were examined. The results are showed in Table 5-1.

Table 5-1

Maximum absorption wavelength of the compound in two different solvent

solvent	dipole moment[4] (D)	λ_{max} (nm)
ethanol	1.69	275
pyridine	2.19	306

From the change in λ_{max}, it is clear that there was a red shift with increase of solvent dipole moment. The λ_{max}, however, were out of the visible range. This is inconvenient for sensor applications. Thus, the structure of this compound was modified by extension of the conjugated system so that its λ_{max} fell into the visible range.

5.2.4 Study of the solvatochromic property of 3-ethyl-5-[1-ethyl-2(1H)-pyridylidene]-rhodanine

Absorption spectra of the compound in six different solvents were studied. This compound was observed to show solvatochromic behaviour. Maximum absorption wavelength for each solvent are listed in Table 5-2.

Table 5-2

Maximum absorption data of 3-ethyl-5-[1-ethyl-2(1H)-pyridylidene]-rhodanine

Solvent	dipole moment[4](D)	λ_{max} (nm)	ε_{max}($dm^3.mol^{-1}.cm^{-1}$)
water	1.87	440	15,107
acetonitrile	3.92	457	15,743
acetone	2.88	460	15,531
methanol	1.70	458	15,342
ethanol	1.69	460	15,126
ether	1.15	466	15,284

A plot of dipole moment of the solvent used versus λ_{max} is given in Fig. 5-5. It can be seen that the increase of solvent dipole moment from ether to acetonitrile produced a slight blue shift in λ_{max} of the compound, but methanol, ethanol and, especially, water do not fit the trend. The reason for this may be due to the formation of hydrogen bonding between these solvents and the compound. In solution the compound would interact with the solvent, normally there are three types of interactions as below:

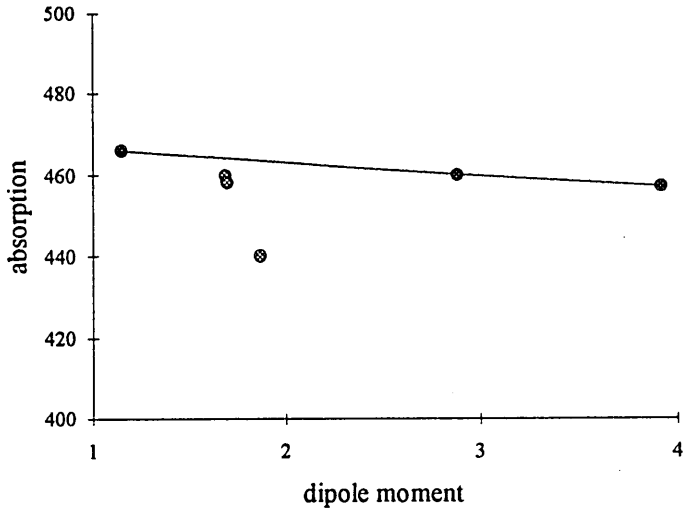

Fig. 5-5 Plot of maximum absorption wavelength of 3-ethyl-5-[1-ethyl-2(1H)-pyridylidene]-rhodanine versus dipole moment of solvent

(a) dipole-induced dipole interaction;

(b) dipole-dipole interaction;

(c) specific association such as hydrogen bonding.

Obviously, methanol, ethanol and especially water can form a hydrogen bond with the compound. The hydrogen bond in some way increases the energy gap between its ground state and excited state thus altering λ_{max}. This phenomenon has been found and confirmed by Suuan.[5]

Because this compound can be dissolved in water, it is difficult to produce a LB film by present LB film technology. Thus a modification of the structure for this compound was carried out and a long carbon chain was successfully attached onto the pyridine ring of this compound instead of the $-C_2H_5$ group.

The solvatochromic properties of the new compounds will be discussed in the following sections. However, the response of 3-ethyl-5-[1-ethyl-2(1H)-pyridylidene]-rhodanine itself to NO_2 gas was still examined by the same device as that used in section 5.2.1, i.e. a suitable amount of the compound (about 0.5 mg) was dissolved in 5 ml acetone and the solution was dropped onto a transparent plastic substrate. When solvent was evaporated entirely, it was coated with the compound and ready for use.

Although the shift in λ_{max} was small, only 3 nm for 90 ppm NO_2 (from 465 to 462 nm) and 2 nm for 9 ppm NO_2 (from 465 to 463 nm), the compound did respond to NO_2 gas. It is expected that if the conjugated chain of the compound is increased, the effect in response to NO_2 gas will increase as well.

5.2.5 Study of the solvatochromic properties of 3-ethyl-5-[1-dodecyl-2(1H)-pyridylidene]-rhodanine and 3-ethyl-5-[1-hexadecyl-2(1H)-pyridylidene]-rhodanine

These two compounds were from the modification of the compound 3-ethyl-5-[1-ethyl-2(1H)-pyridylidene]-rhodanine. They have same structure but different carbon chain lengths, a 12 or a 16 carbon chain. They neither dissolved in water and their maximum absorption data in five solvents are given in Table 5-3.

From Figs. 5-6 and 5-7, it can be seen that there was still a slight trend of λ_{max} for the two compounds in five different solvents, i.e., the λ_{max} shifted towards shorter wavelength with the increase of dipole moment of the solvent used, although this change was small. Methanol and ethanol did not fit this trend, probably because of hydrogen bonding. The results show that attaching a long carbon chain to the compound studied does not affect its solvatochromic

behaviour, which resulted in an opportunity of making a L-B film from this type of compound.

Table 5-3

Maximum absorption data of 3-ethyl-5-[1-dodecyl-2(1H)-pyridylidene]-rhodanine (A) and 3-ethyl-5-[1-hexadecyl-2(1H)-pyridylidene]-rhodanine (B)

solvent	dipole moment[4](D)	A		B	
		λ_{max} (nm)	ε_{max} ($dm^3.mol^{-1}.cm^{-1}$)	λ_{max} (nm)	ε_{max} ($dm^3.mol^{-1}.cm^{-1}$)
acetonitrile	3.92	458.5	16,910	459.5	11,482
acetone	2.88	461.0	22,625	461.0	17,556
methanol	1.70	461.0	20,681	461.0	14,541
ethanol	1.69	461.5	14,931	461.5	10,175
ether	1.15	467.0	20,429	467.0	13,840

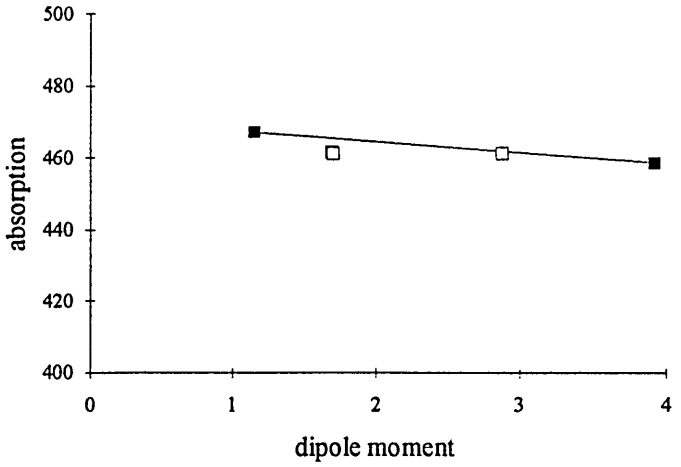

Fig. 5-6 Plot of maximum absorption wavelength of 3-ethyl-5-[1-dodecyl-2(1H)-pyridylidene]-rhodanine versus dipole moment of solvent

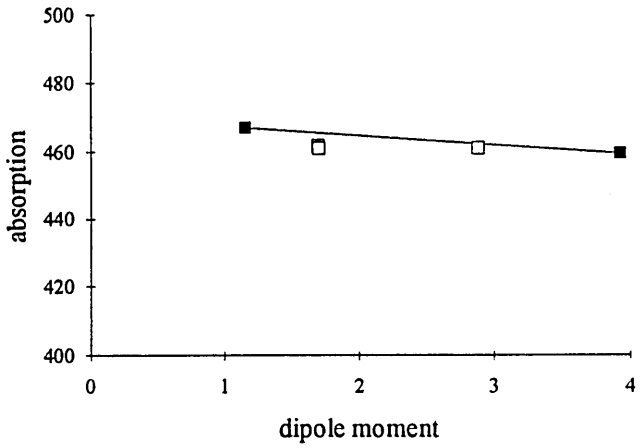

Fig. 5-7 Plot of maximum absorption wavelength of 3-ethyl-5-[1-hexadecyl-2(1H)-pyridylidene]-rhodanine versus dipole moment of solvent

Brooker and his co-workers observed[6] that deviation of λ_{max} increased with conjugated chain length. Therefore, a modification for 3-ethyl-5-[1-dodecyl-2(1H)-pyridylidene]-rhodanine and 3-ethyl-5-[1-hexadecyl-2(1H)-pyridylidene]-rhodanine was carried out in order to enhance solvatochromic properties of this type of compound.

5.2.6 Study of the solvatochromic properties of 3-ethyl-5-{[1-dodecyl-2(1H)-pyridylidene]-ethylidene}-rhodanine and 3-ethyl-5-{[1-hexadecyl-2(1H)-pyridylidene]-ethylidene}-rhodanine and their NO_2 gas response

These two compounds were from the modifications of 3-ethyl-5-[1-dodecyl-2(1H)-pyridylidene]-rhodanine and 3-ethyl-5-[1-hexadecyl-2(1H)-pyridylidene]-rhodanine. The conjugated sections of the two compounds were increased by introducing an ethylidene group.

(i) Solvatochromic properties

Absorption spectra of the two compounds were studied in five different solvents. Maximum absorption data are listed in Table 5-4.

Table 5-4

Maximum absorption data of 3-ethyl-5-{[1-dodecyl-2(1H)-pyridylidene]-ethylidene}-rhodanine (A) and 3-ethyl-5-{[1-hexadecyl-2(1H)-pyridylidene]-ethylidene}-rhodanine (B)

solvent	dipole moment[4](D)	A		B	
		λ_{max} (nm)	ε_{max} ($dm^3.mol^{-1}.cm^{-1}$)	λ_{max} (nm)	ε_{max} ($dm^3.mol^{-1}.cm^{-1}$)
acetonitrile	3.92	524.0	45,828	525.0	47,495
acetone	2.88	544.5	76,831	544.5	72,329
methanol	1.70	542.0	68,472	542.0	59,699
ethanol	1.69	542.5	51,003	542.5	53,707
ether	1.15	584.0	38,428	584.0	26,740

It can be seen that maximum absorptions of the two compounds did have a significant shift (about 60 nm from ether to acetonitrile), and their molar absorption coefficients also increased remarkably. An apparent trend of maximum absorption shift can be seen from Fig. 5-8 and Fig. 5-9 for two modified compounds. All these changes were only due to the increasing in the length of conjugated chain of the compounds. It was expected that these changes might result in enhanced response of these two compounds to NO_2 gas.

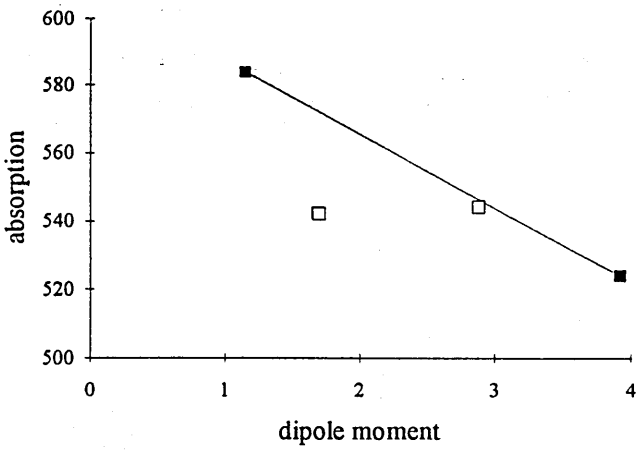

Fig. 5-8 Plot of maximum absorption wavelength of 3-ethyl-5-{[1-dodecyl-2(1H)-pyridylidene]-ethylidene}-rhodanine versus dipole moment of solvent

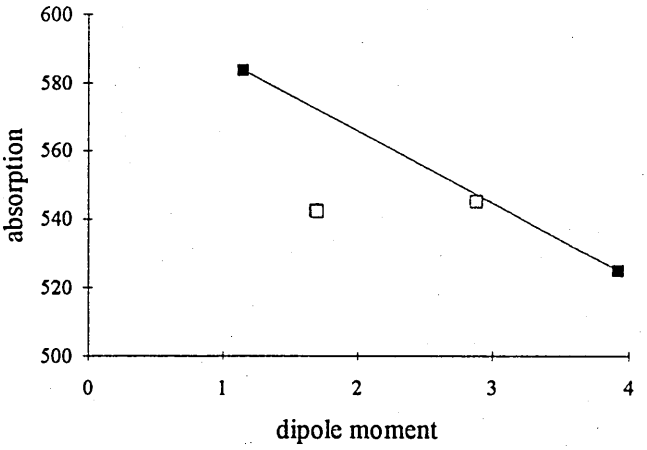

Fig. 5-9 Plot of maximum absorption wavelength of 3-ethyl-5-{[1-hexadecyl-2(1H)-pyridylidene]-ethylidene}-rhodanine versus dipole moment of solvent

(ii) Preparation of L-B films of 3-ethyl-5-{[1-dodecyl-2(1H)-pyridylidene]-ethylidene}-rhodanine and 3-ethyl-5-{[1-hexadecyl-2(1H)-pyridylidene]-ethylidene}-rhodanine

L-B films of the two compounds were prepared by depositing 0.1 ml of a solution in chloroform, 0.59 mg/ml for 3-ethyl-5-{[1-dodecyl-2(1H)-

pyridylidene]-ethylidene}-rhodanine and 0.63 mg/ml for 3-ethyl-5-{[1-hexadecyl-2(1H)-pyridylidene]-ethylidene}-rhodanine, onto a pure water subphase (18 MW Milli-Q). When the chloroform had evaporated, the compacted monolayers were transferred at a surface pressure of 25 mN m^{-1} by slowing dipping and raising the substrates through the compacted film. Hydrophilic glass slides and gold coated glass slides were used as substrates.

Plots of surface pressure versus area isotherms for the two compounds are given in Fig. 5-10 and Fig. 5-11. It can be seen that the two compounds formed monomolecular layers at the air-water interface below 30 mN m^{-1} surface pressure. Area-time stability plots were recorded for the two compounds at 25 mN m^{-1} surface pressure and are given in Fig. 5-12. The stability plots for both materials seem to be typical of most films and show a reasonable stability.

The same problem was found for preparation of multilayer films of the two compounds as for previous multilayer films, i.e. the films collapsed. This was observed by the uneven colour distribution seem when the slides were examined under a microscope.

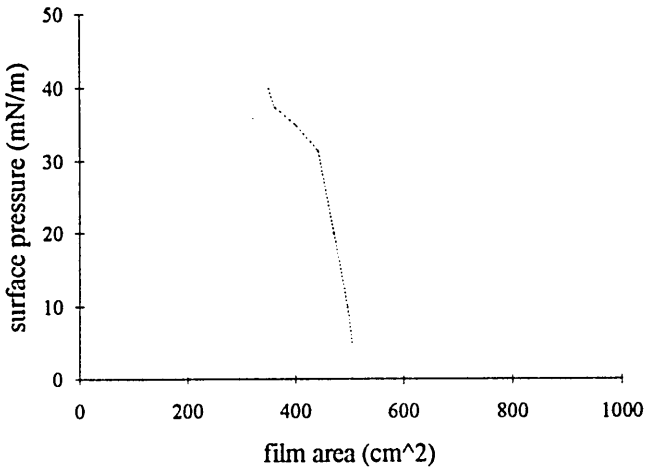

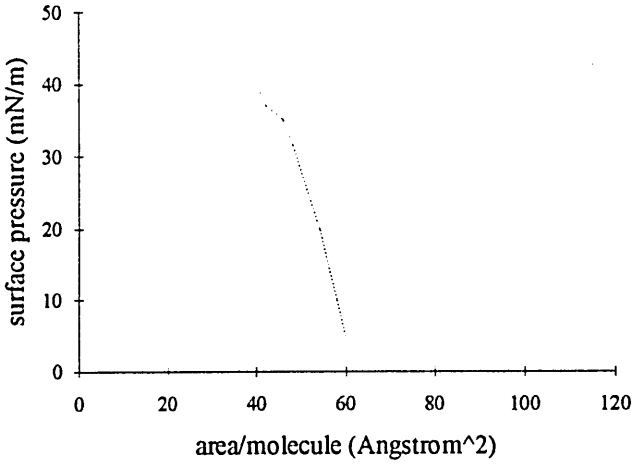

Fig. 5-10 Plots of surface pressure versus film area/area per molecule isotherms for 3-ethyl-5-{[1-dodecyl-2(1H)-pyridylidene]-ethylidene}-rhodanine

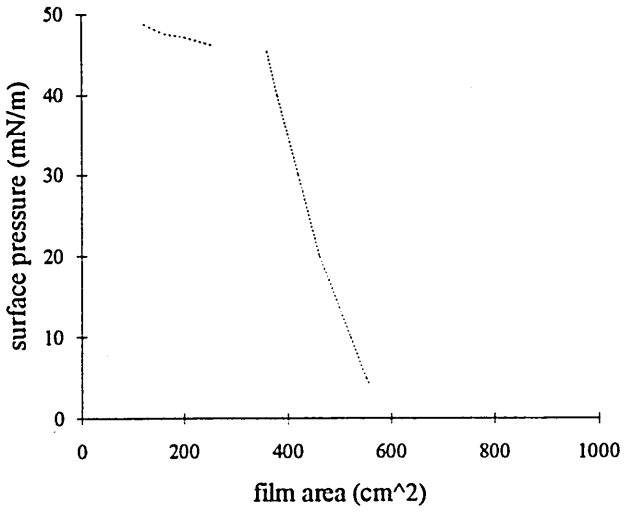

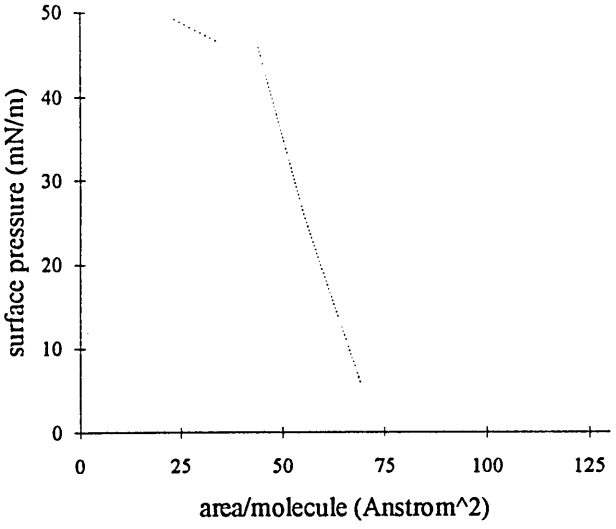

Fig. 5-11 Plots of surface pressure versus film area/area per molecule isotherms for 3-ethyl-5-{[1-hexadecyl-2(1H)-pyridylidene]-ethylidene}-rhodanine

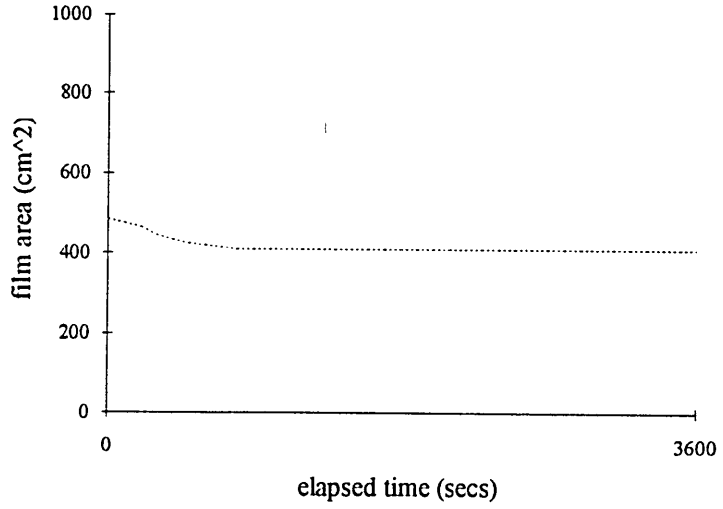

A: 3-ethyl-5-{[1-dodecyl-2(1H)-pyridylidene]-ethylidene}-rhodanine

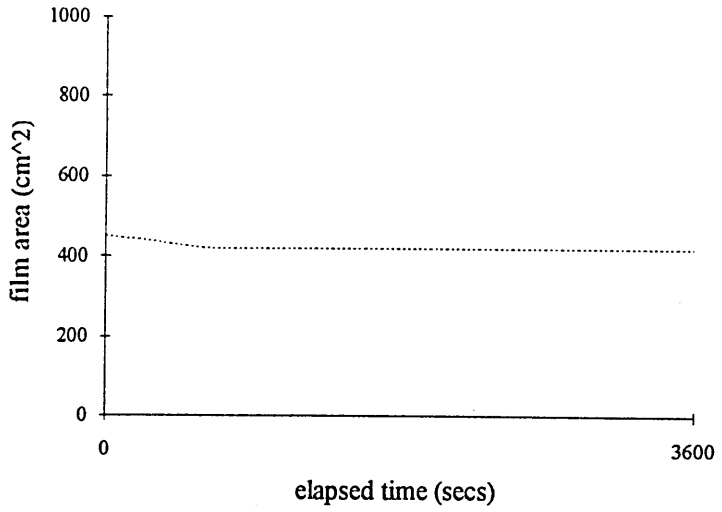

B: 3-ethyl-5-{[1-hexadecyl-2(1H)-pyridylidene]-ethylidene}-rhodanine

Fig. 5-12 Area-time stability plots for two compounds

(iii) UV-VIS spectrum and FT-IR microspectroscopy of the LB films of 3-ethyl-5-{[1-dodecyl-2(1H)-pyridylidene]-ethylidene}-rhodanine and 3-ethyl-5-{[1-hexadecyl-2(1H)-pyridylidene]-ethylidene}-rhodanine

UV-VIS spectra of the LB films of the two compounds were studied and it was found that the film of 3-ethyl-5-{[1-dodecyl-2(1H)-pyridylidene]-ethylidene}-rhodanine had a maximum absorption at 615 nm and the film of 3-ethyl-5-{[1-hexadecyl-2(1H)-pyridylidene]-ethylidene}-rhodanine at 623 nm. The data are different from those of the free dyes in solvent.

Reflectance-transmittance spectra of the two L-B films of the two compounds are given in Fig. 5-13 and Fig. 5-14. Typical aliphatic C-H stretch bands at about 2900 cm^{-1} were found for both the films, and a broad weak band at about 3500 cm^{-1} was found for both the films, possibly due to trapped water.

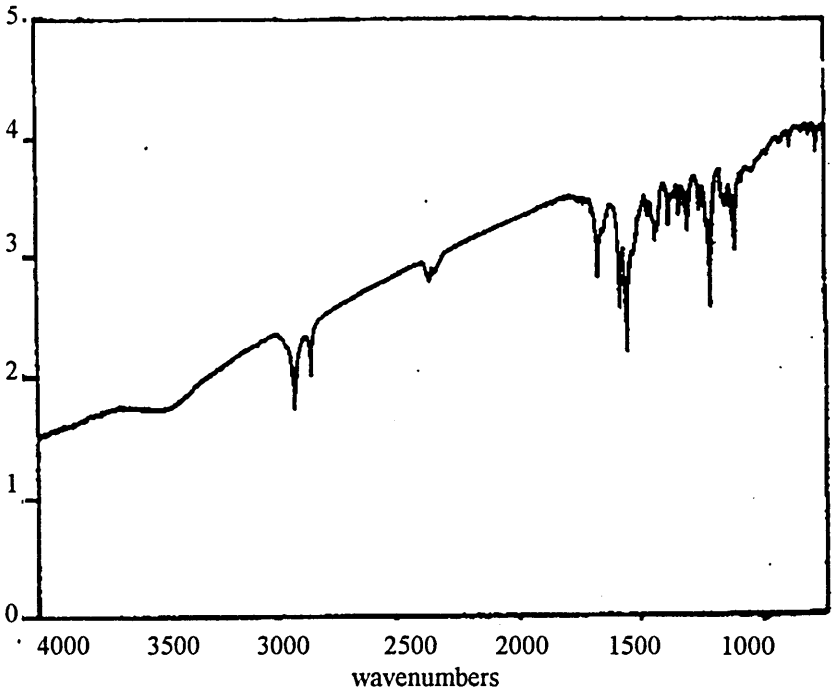

Fig. 5-13 Reflectance-transmittance spectrum of the LB film of 3-ethyl-5-{[1-dodecyl-2(1H)-pyridylidene]-ethylidene}-rhodanine

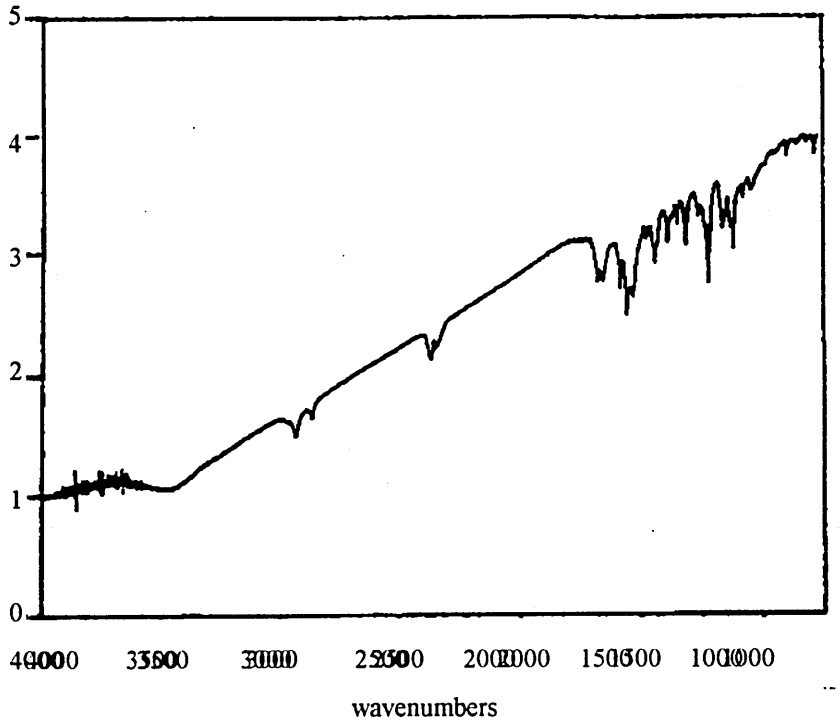

Fig. 5-14 Reflectance-transmittance spectrum of the LB film of 3-ethyl-5-{[1-hexadecyl-2(1H)-pyridylidene]-ethylidene}-rhodanine

(iv) Investigation of optical response of the LB films prepared to NO_2 gas

The simple device used in section 5.2.1 was used for holding the LB films and passing NO_2 gas.

Results:

(a) LB film of 3-Et-5-[(1-dodecyl-2(1H)-pyridylidene)-ethylidene]-rhodanine

90 ppm NO_2 gas:

before passing NO_2 gas, λ_{max}=615 nm;

passing NO_2 gas, λ_{max}=620 nm;

after passing NO_2 gas, λ_{max}=615 nm.

(b) LB film of 3-Et-5-[(1-hexadecyl-2(1H)-pyridylidene)-ethylidene]-rhodanine

90 ppm NO_2 gas:

before passing NO_2 gas, λ_{max}=623 nm;

passing NO_2 gas, λ_{max}=627 nm;

after passing NO_2 gas, λ_{max}=623 nm.

From the results above, it was observed there was a gas response for the two L-B films, but it was only 3-4 nm shift in maximum absorption. This shift is still too small to be of practical use for detection of low concentrations of NO_2.

5.2.7 Study of the solvatochromic property of 1-hexadecyl-4-[(4-oxocyclohexadienylidene)-ethylidene-1,4-dihydropyridine and its response to NO_2 gas

(i) Solvatochromic property

Absorption spectra of the compound were obtained in four different solvents, methanol, ethanol, acetone and acetonitrile. It was found that the compound did not dissolve in ether. Spectral data are given in Table 5-5.

A change in maximum absorption was observed. An overall trend of λ_{max} change can be seen from Fig. 5-15, that is, λ_{max} moved towards direction of longer wavelength with decrease of solvent dipole moment. Methanol and ethanol which have ability to form hydrogen bonding, did not fit this trend.

Table 5-5

Maximum absorption data of 1-hexadecyl-4-[(4-oxocyclohexadienylidene)-ethylidene-1,4-dihydropyridine

Solvent	dipole moment[4](D)	λ_{max} (nm)	ε_{max}($dm^3.mol^{-1}.cm^{-1}$)
acetonitrile	3.92	571.0	21,097
acetone	2.88	588.0	23,232
methanol	1.70	394.0	25,897
ethanol	1.15	401.0	30,335

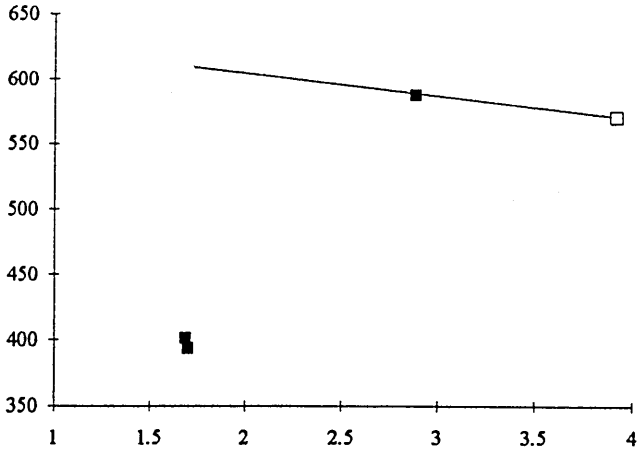

Fig. 5-15 Plot of maximum absorption wavelength of 1-hexadecyl-4-[(4-oxocyclohexadienylidene)-ethylidene-1,4-dihydropyridine versus dipole moment of solvent

Absorption spectra of the compound in mixtures of methanol and acetone were also examined. Results are given in Table 5-6.

Table 5-6

Maximum absorption data of 1-hexadecyl-4-[(4-oxocyclohexadienylidene)-ethylidene-1,4-dihydropyridine in mixture solvent of methanol and acetone

acetone%(MeOH%)	0 (100)	10 (90)	20 (80)	30 (70)	40 (60)	50 (50)	60 (40)	70 (30)	80 (20)	90 (10)	100 (0)
λ_{max} (nm)	393.0	393.0	393.0	393.0	393.0	393.0	393.5	393.5	394.0	532.0	588.5

From the data above, it can be seen that only 10% methanol resulted in 56.5nm change in λ_{max} for the compound in pure acetone. This suggests that the compound may be used as an indicator of purity for solvent and also used to respond to concentration changes of electrolyte in liquid systems.

(ii) Preparation of L-B film of 1-hexadecyl-4-[(4-oxocyclohexa-dienylidene)-ethylidene]-1,4-dihydropyridine

A plot of surface pressure versus area isotherm for 1-hexadecyl-4-[(4-oxocyclohexa-dienylidene)-ethylidene-1,4-dihydropyridine is given in Fig. 5-16 and a stability plot for the compound at 25 mN m^{-1} surface pressure is shown in Fig. 5-17. The plots show that 1-hexadecyl-4-[(4-oxocyclohexadienylidene)-ethylidene]-1,4-dihydropyridine can form a monomolecular layer at the surface pressure below 30 mN m^{-1} with a reasonable stability.

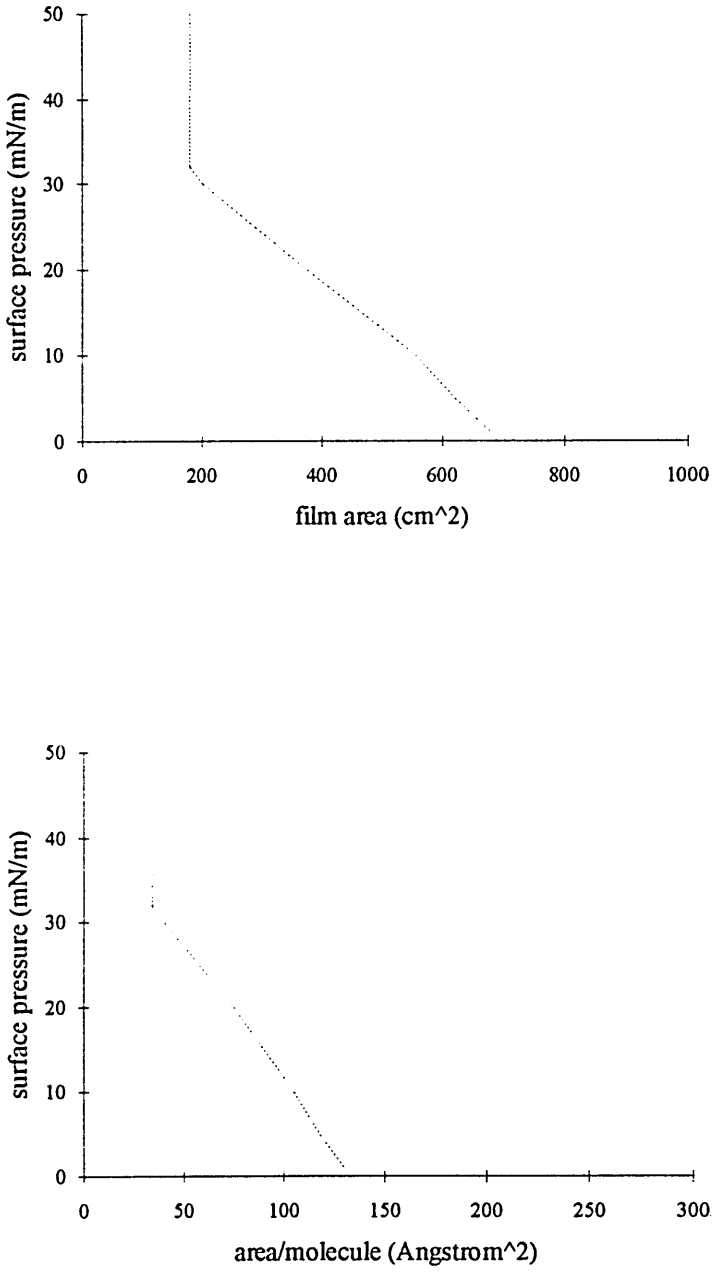

Fig. 5-16 Plots of surface pressure versus film area/area per molecule isotherms for 1-hexadecyl-4-[(4-oxocyclohexa-dienylidene)-ethylidene-1,4-dihydropyridine

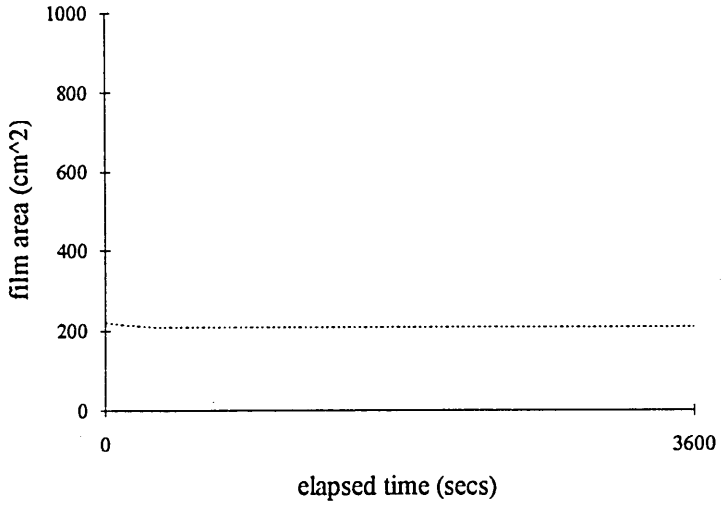

Fig. 5-17 Area-time plot for for 1-hexadecyl-4-[(4-oxocyclohexa-dienylidene)-ethylidene-1,4-dihydropyridine

An L-B film of the compound was prepared by depositing 0.08 ml of the compound solution in chloroform, 0.22 mg/ml, onto a pure water subphase (18 MAW Milli-Q). Surface pressure was controlled at 25 mN m^{-1}. Similar substrates were used to those for previous work.

The same problem, collapse of the multilayer L-B film, was found for this compound.

(iii) UV-VIS spectrum and FT-IR microspectroscopy of the L-B film of 1-hexadecyl-4-[(4-oxocyclohexadienylidene)-ethylidene]-1,4-dihydropyridine

Maximum absorption in the UV-VIS spectrum of the L-B film of 1-hexadecyl-4-[(4-oxocyclohexadienylidene)-ethylidene]-1,4-dihydropyridine was found at 385 nm. This is different from that of the free dye in the solution.

A reflectance-transmittance spectrum of the L-B film was recorded and given in Fig. 5-18. The spectrum is similar to that of the compound, 1-hexadecyl-

4-[(4-oxocyclohexadienylidene)-ethylidene]-1,4-dihydropyridine. The broad band at about 3450 cm^{-1} was believed due to the influence of trapped water.

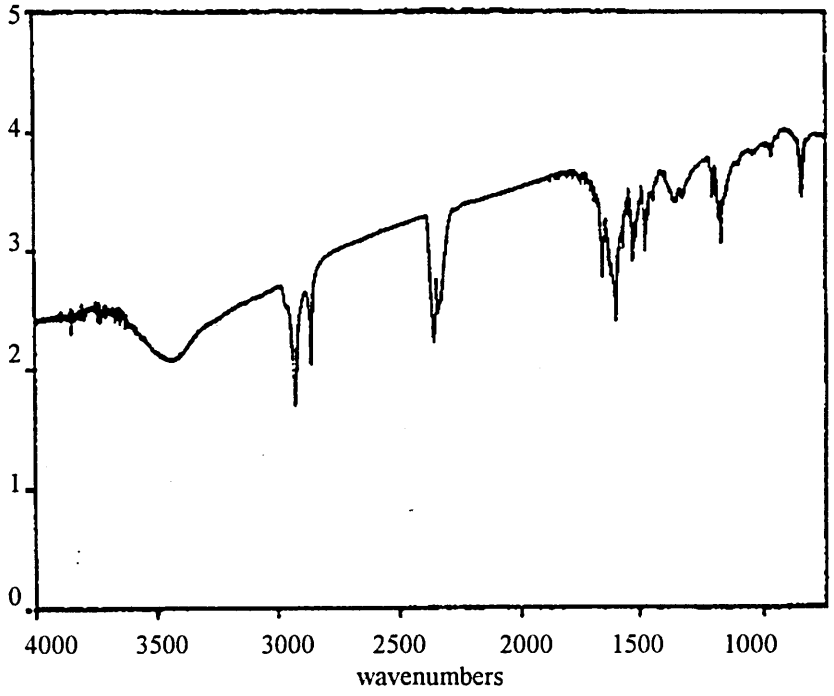

Fig. 5-18 Reflectance-transmittance spectrum of the LB film of 1-hexadecyl-4-[(4-oxocyclohexadienylidene)-ethylidene]-1,4-dihydropyridine

(iv) Gas Response

Although an ideal multilayer LB film was difficult to obtain, the film produced was used to examined its response to NO_2 gas as a rough guide. The same device used in section 5.2.1 was employed for holding the LB film and passing NO_2 gas.

Results:

90 ppm NO_2 gas:

before passing NO_2 gas, λ_{max}=385 nm;

passing NO_2 gas, λ_{max}=383 nm;

after passing NO_2 gas, λ_{max}=385 nm.

A small change in λ_{max} between before and passing NO_2 gas was observed. Although the change is so small, it suggests that the compound does respond to NO_2 gas.

From the description above it can be seen that λ_{max} position of the compounds in a LB film were greatly different from those of the compounds in different solvents. Similar phenomena in TCNQ adducts were observed by Ashwell et al..[1,2] They thought that this λ_{max} change between LB film and solution was due to alignment change of the molecules of the compound when it was forming a LB film, which resulted in a transition change from intermolecular to intramolecular transition.

A problem met in all preparations of the L-B films was to obtain ideal thickness of multilayers for LB film, because the multilayer films collapsed, possibly during the course of drying. Reasons for this are unknown.

References:

1. G.J. Ashwell, Emma J.C. Dawnay, A.P. Kuczynskl, M. Szablewskl and Ian M. Sandy, Martin R. Bryce, Andrew M. Grainger and Masihul Hasan, J. CHEM. SOC. FARADY TRANS., 1990, 86(7), 1117-1121.

2. Norman A. Bell, Richard A. Broughton, John S. Brooks, T. Alwyn Jones, Stephen C. Thorpe and Geoffrey J. Ashwell, J. CHEM. SOC., CHEM. COMMUN., 1990, 325-326.

3. P. Carr, May, 1990, Gas detection using adducts of TCNQ, A report on the final year project, Sheffield City polytechnic.

4. a. Streitweiser Jr. and C. H. Heathcock, 'Introduction to Organic Chemistry' (2nd ed.), Collier MacMillan publishers, London, 1981.

5. J. Suppan, J. Chem. Soc. (A), 3125 (1968).

6. L. G. S. Brooker, G. H. Keyes, R. H. Sprague, R. H. VanDyke, E. VanLare, G. VanZandt, F. L. White, H. W. J. Cressman, and S. G. Dent, J. Am. Chem. Soc. 73, 5332 (1951).

Chapter 6

Covalent binding of compounds with a functional group to a solid support

6.1 Introduction

Applications of covalent binding technology in biotechnology

Immobilisation Technology has been widely used in biotechnology, for example, proteins have been immobilised on a wide variety of solid supports for applications including analysis, separation, synthesis, and detection.[1,2,3] Attachment of a compound to a solid support may be made in two ways. One is by physical adsorption or entrapment and another is by a chemical reaction that links the compound to the support matrix by a covalent bond. Covalent binding, far superior due to the strong, stable linkage that is formed, is generally the preferred method. A number of review articles on covalent binding methods and procedures have been published.[4,5,6] Generally, the component attached to the solid support is called a ligand. In most of cases, ligands are covalently linked to the solid matrix containing hydroxylic or amino groups by means of bifunctional reagents, X-R-Y, where X and Y are 'connector' groups that react with the functional groups in both the solid support and ligand, respectively. X and Y may be identical. Normally the linkage is carried out in two steps. One is an activation step and another is a coupling step, as follows:

Activation step:

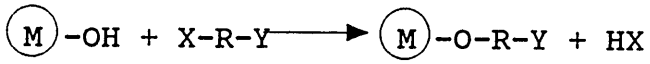

Coupling step:

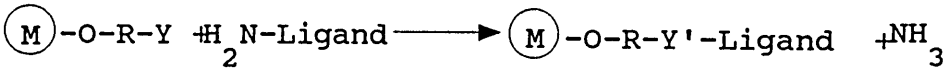

Activation may also include several steps. A number of covalent attachment techniques were introduced by Weetall.[7] Methods for preparation of the carriers with a functional group are well described in his paper. These techniques are described below.

I. Silane coupling techniques

This technique has been successful used for introducing a functional group to a solid support such as porous glass, which can be used further to link with ligands. Silanization of a solid material can be performed in two different ways. One is aqueous silanization and another is organic silanization. Aqueous silanization appears to couple a monolayer of silane across the solid support surface and organic solvent techniques give higher amine loadings. In the field of biology, experience has shown that greater solid carrier durability with slightly lower enzyme loadings are achieved by aqueous silanization. A simple scheme for silanization is shown in Fig. 6-1. Based on silanized materials, a number of techniques can be used to link an enzyme, which will be in turn introduced.

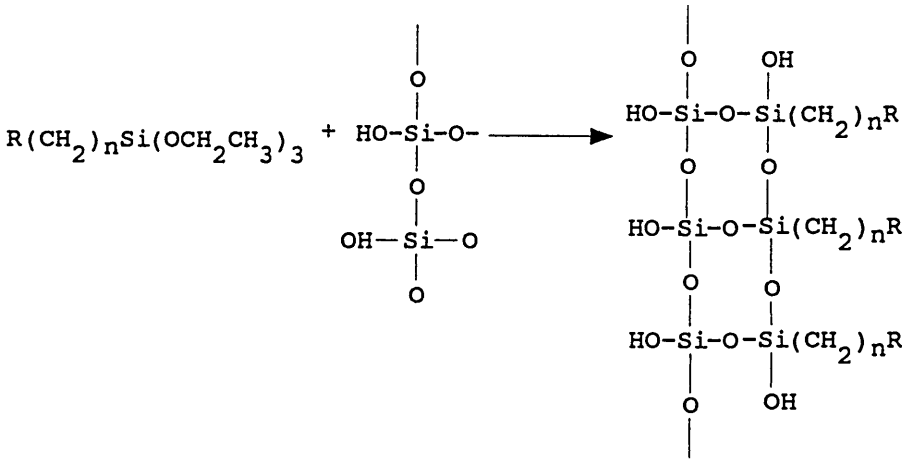

where R represents an organic functional group,

in most of cases, R=NH_2

Fig. 6-1 Silanization of the surface of glass

II. Preparation of carrier with a carbonyl group

This technique uses glutaraldehyde to react with an alkyl amine material from the amino alkyl silanization of a solid support. A carrier with a carbonyl group can be easily prepared by this way (Fig. 6-2):

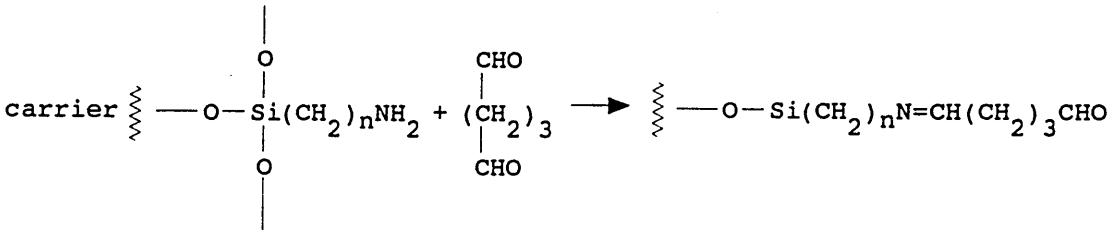

Fig. 6-2 Preparation of the carrier with a carbonyl group

The carrier produced can be used to link with an enzyme, but it is important to remove all excess glutaraldehyde before adding the enzyme, otherwise cross-linking will occur between the enzymes through glutaraldehyde.

III. Preparation of the carrier with an isothiocyanate (-NCS) group

This method provides a carrier with an isothiocyanate group, which can be linked with an enzyme. A simple scheme is shown in Fig. 6-3 as below.

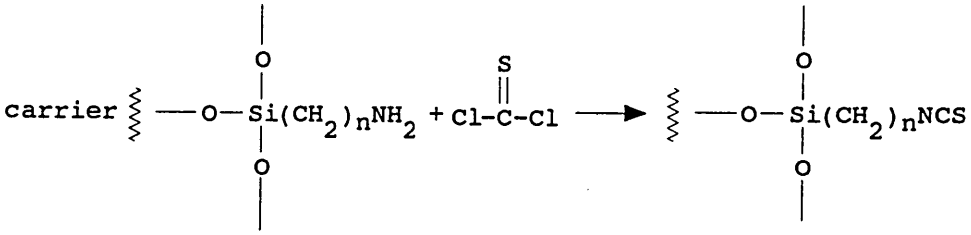

Fig. 6-3 Preparation of the Isothiocyanate carrier

Using this method one must be very careful because of the nauseous and toxic nature of the thiophosgene used. All work must be carried out in a fume cupboard. The carrier generated should be used as soon as possible for coupling to a ligand.

IV. Preparation of the pseudourea of a carboxyl derivative

This carrier is prepared in two steps. The carrier produced can be used to link with an enzyme in both acidic and basic conditions. The reaction steps are shown in Fig. 6-4.

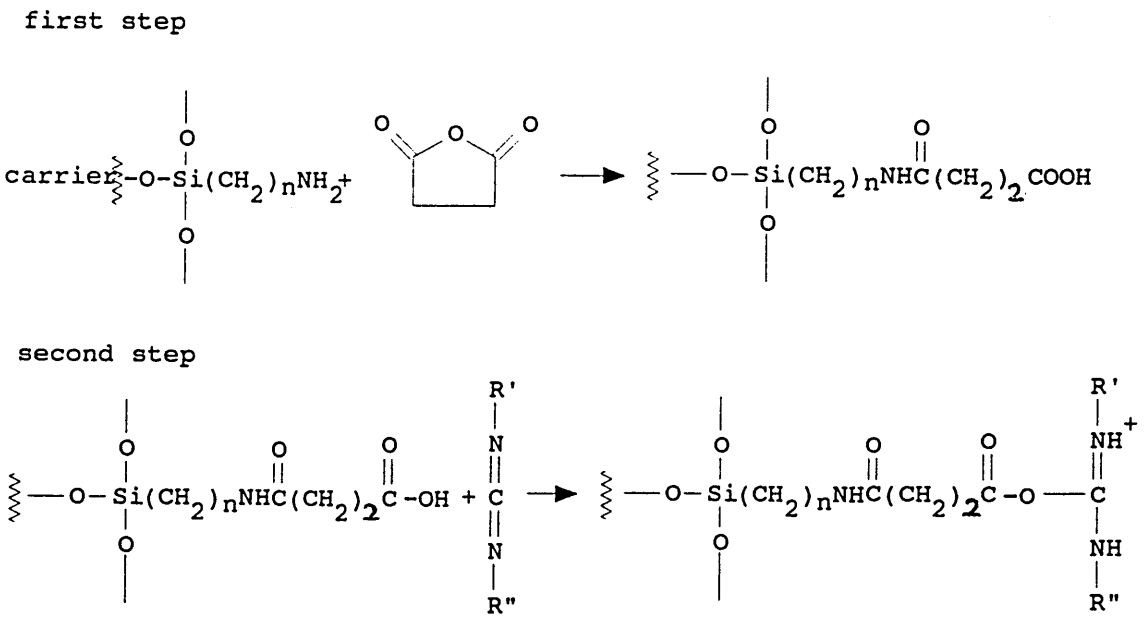

Fig. 6-4 Preparation of the pseudourea of a carboxyl derivative

In the first step, the alkylamine carrier from the silanization of a solid support reacts with succinic anhydride to produce a carboxyl derivative. Then it reacts with a carbodiimide compound to produce a carrier which can be used to link an enzyme directly.

Porath[5] (1974) also reviewed three methods of coupling which are briefly described below.

1. The cyanogen bromide method of coupling

Solid materials containing hydroxyl groups can be activated by cyanogen bromide to form the reactive intermediates containing imino carbonate ester groups. These reactive materials can be used for coupling with ligands having amino groups, as below.

Activation step:

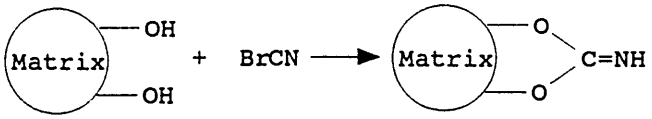

Coupling step:

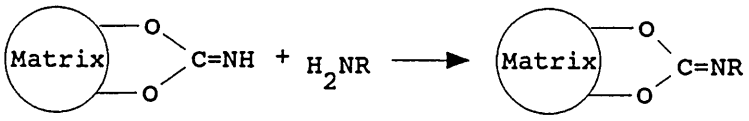

2. Bisoxirane coupling

Bisoxirane (bisepoxides) are very useful reagents for linking low molecular weight ligands with amino or hydroxyl groups.[8] Coupling reactions take place in the following way:

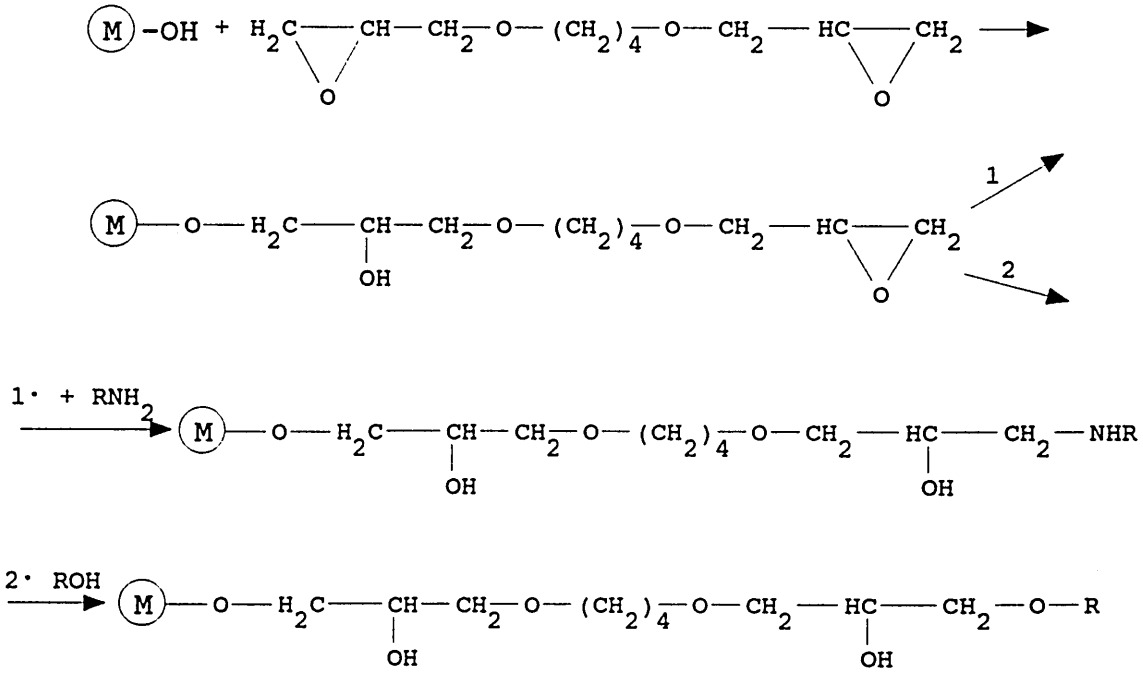

As seen from above, one of the oxirane groups of the reagent is allowed to react with the hydroxyl on the solid matrix first, leaving the other group to couple with the amino or hydroxyl group in the ligand.

3. Divinylsulfone coupling

Divinylsulfone can be used in similar fashion to bisoxiranes,[9] as below:

$$M\text{-}OH + CH_2{=}CH\text{-}SO_2\text{-}CH{=}CH_2 \text{ ------> } M\text{-}O\text{-}CH_2\text{-}CH_2\text{-}SO_2\text{-}CH{=}CH_2$$

(M: solid matrix)

In this step, one of vinyl group of the reagent reacts with the hydroxyl group of the solid material. The vinyl groups introduced onto the solid matrix are more reactive than are the oxirane groups. They can couple with amines, alcohols and phenols at low temperature and at low pH. This method is well suited for the attachment of hydroxylic compounds, R-OH, to form products presumably containing the following structure:

$$M\text{-}O\text{-}CH_2\text{-}CH_2\text{-}SO_2\text{-}CH_2CH_2\text{-}OR$$

However, the products are unstable in alkaline solution (the amino link above pH 8 and the hydroxyl link at about pH 9 or 10).

Other methods exist to link a compound covalently to a solid support, mainly used in the biological and biomedical fields to link an enzyme or an antibody to a solid matrix. Few examples have been found in chemical sensors. Although some studies of immobilised materials as optical-fiber chemical sensors have been reported, in particular regarding indicators for pH[10,11,12,13] and oxygen[14,15] determination, physical adsorption techniques have generally been used. One example of covalent linkage in a chemical system is that of pH indicators based on immobilisation of dyes on controlled pore glass.[16]

The purpose of the present work is to immobilise solvatochromic dyes with a functional $-NH_2$ linkage group, on a chosen solid support without destroying the optical characteristics of the dyes. The techniques used are based on those which have been successfully used in biological and biomedical work.

6.2 Applications of the covalent binding techniques for the dye compounds synthesised in the present work

6.2.1 Covalent binding between 2,6-dimethyl-4-[(2,6-diphenyl)-4-(p-aminophenyl)-N-pyridinio]-phenolate and 1,1'-carbonyldiimidazole activated-agarose (called Reacti-Gel^{R} (6X) CDI support)

This involved immobilisation of the dye, 2,6-dimethyl-4-[(2,6-diphenyl)-4-(p-aminophenyl)-N-pyridinio]-phenolate, to CDI gel support through the reaction of an N-nucleophile with the imidazolyl carbamate of the CDI gel support to form a stable N-arylcarbamate linkage (Fig. 6-5):

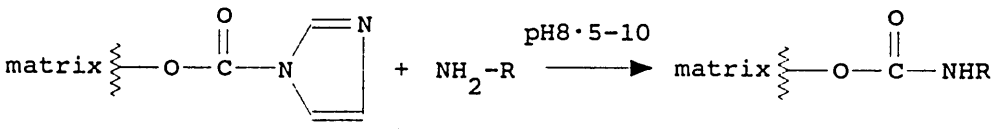

Where R-NH_2 represents the dye used

Fig. 6-5 Immobilisation of the Dye with CDI Gel

The Reacti-GelR (6X) support is 6% cross-linked beaded agarose, which has been derivatized with 1,1'-carbonyldiimidazole (CDI), producing a highly activated imidazolyl-carbamate matrix. The imidazolyl-carbamate group couples most efficiently to free amino-containing ligands in a pH range of 9-11. This technique had been well applied to biological work.[17,18]

Procedures of immobilisation:

Two methods were used to immobilise the dye on the gel. One followed the procedures used in biomedical systems[19] i.e. in aqueous solution while the other used an organic solvent.

a) acetone was removed from 1 ml of gel (PIERCE, supplied stabilised in acetone slurry) with a 3 ml Buchner funnel under vacuum (do not dry gel completely), washing quickly with 0.1 M borate + 0.9% NaCl buffer solution (pH 8.5).

b) the gel cake was added to 4 ml of borate buffer solution (or an organic solvent for immobilisation in organic solvent) containing 1 mg of dye, 2,6-dimethyl-4-[(2,6-diphenyl)-4-(p-aminophenyl)-N-pyridinio]-phenolate or 2,6-dichloro-4-[(2,6-diphenyl)-4-(p-aminophenyl)-N-pyridinio]-phenolate.

c) the mixture solution was left for two days under stirring at room temperature to allow the coupling complete.

d) the dye coupled gel was washed with 2 M Tris buffer (pH 8.0) to block remaining active sites until the washings became colourless (for organic immobilisation, an organic solvent was used to wash the gel), and the dye coupled gel was dried under vacuum. A light yellow colour solid gel was formed.

Because the dyes used have very poor solubility in aqueous solution, this might limit the loadings of the dye on the gel. Therefore, an attempt was tried to immobilise the dye on the gel in organic solution. Two organic solvents, acetone and acetonitrile were used.

The dyes coated on the gel did not respond to polarity changes of solvents. Possible reasons for this are: not having enough dyes coated on the gel, that the solvatochromic property of the dyes was destroyed by the carbamate linkage, or that the multiple hydroxyl groups in the gel matrix interacted with the dye more strongly than the solvent.

6.2.2 Silane methods for coating the dyes on a) cover slips; b) quartz; c) glass slides

These methods use a silanized carrier to link with the dye. The silanized carrier is obtained by treating a solid support such as a cover slip or a quartz slide with an organosilane containing an organic functional group at one end and a silylalkoxy group at the other. Coupling of the silane to the solid support is through the surface silanol or oxide groups to the silylalkoxy groups.[20] The resulting product is a carrier having available organic functional groups.

Several methods of linking the dyes by using silanized carrier are available.

6.2.2.1 Use of thiol-terminal silane and heterobifunctional crosslinker for immobilisation of the dye synthesised on silica surfaces

Using this type of immobilisation technique, antibodies were successfully coupled with silica surfaces by Bhatia et al.[21] Immobilisation of flavoproteins on silicon was successfully done too by Rusin et al.[22] They also found that there were different effects with different heterobifunctional cross-linker reagents, i.e. EMCS (N-succinimidyl 6-maleimidocaproate)-immobilised protein was four times more active than GMBS (N-succinimidyl 4-maleimidobutyrate)-immobilised protein. It was desired to use this technique for attachment of the

dyes synthesised onto the surface of silica. The reaction sequence is schematically represented as in Fig. 6-6 with 3-mercaptopropyl trimethoxysilane and N-succinimidyl 6-maleimidocaproate (EMCS).

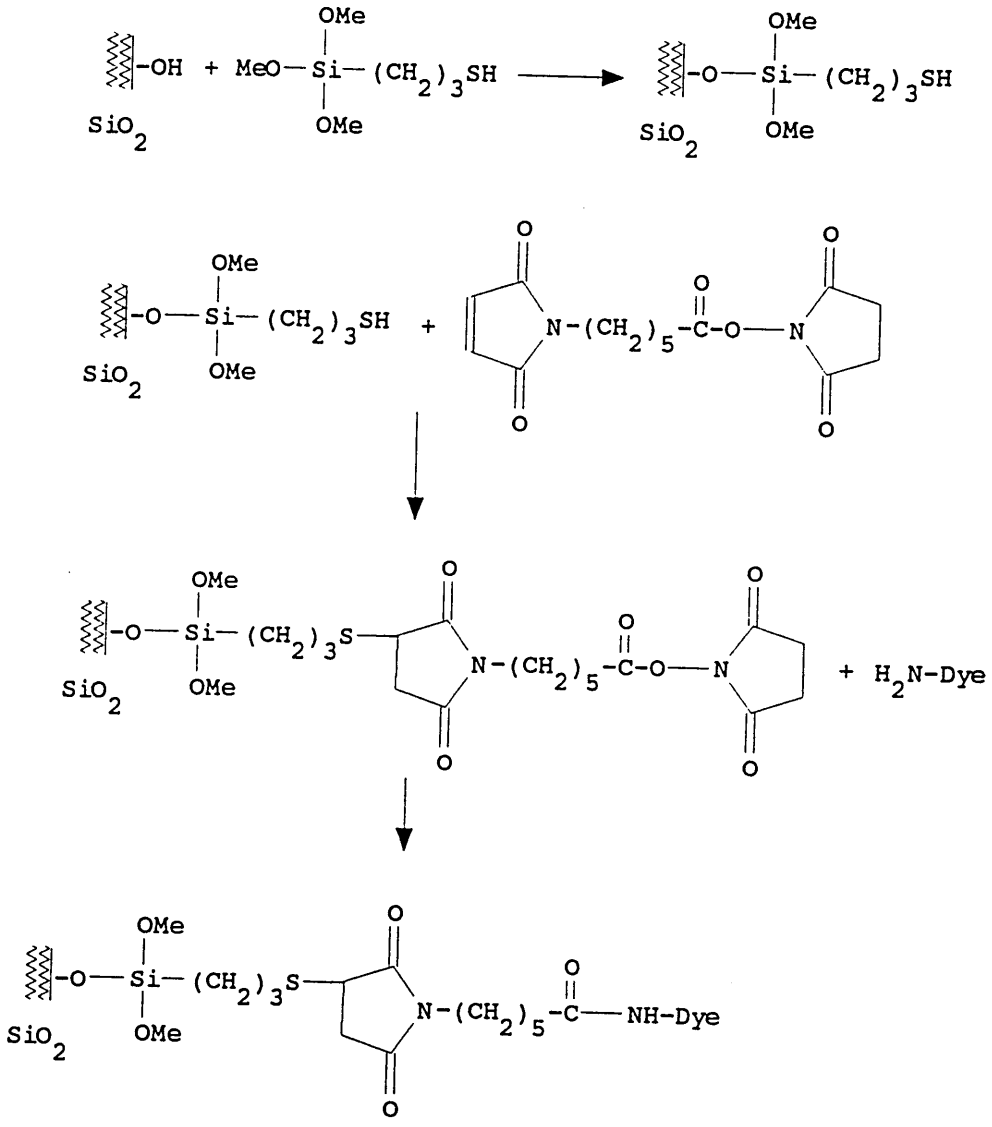

Fig. 6-6 Immobilisation procedure for covalent attachment of dye to a silica surface

Procedures of immobilisation:

a) Cleaning of silica surfaces:

Three substrates, glass cover slips, glass slides and quartz slides were used. The substrates were first acid-cleaned by immersion in a 1:1 mixture of concentrated hydrochloric acid and methanol for one hour followed by rinsing several times with distilled deionized water, and then placed in concentrated sulphuric acid for one hour. After a thorough water rinse, the substrates were boiled in distilled deionized water for 30 mins. Finally, the substrates were removed from water and allowed to air dry.

b) Silanization of the substrates

The cleaned substrates were placed in a 2% solution of 3-mercaptopropyl trimethoxysilane prepared in dry toluene under a nitrogen atmosphere for 2 hours. The substrates were removed from the solution, rinsed in dry toluene, and allowed to air dry.

c) Treatment of silanized substrates with a heterobifunctional cross linker reagent EMCS

The organic cross linker reagent EMCS (Fluka) was firstly dissolved in a minimum amount of dimethylformamide (DMF) and then diluted with 0.1 M phosphate buffer solution to a final concentration of 2 mM. The silanised substrates were placed in this solution for one hour and then rinsed with phosphate buffer solution.

d) Immobilisation of the dye

The substrates coated with silane and cross linker were placed in a 0.05 mg/ml solution of 2,6-diphenyl-4-[(2,6-diphenyl)-4-(p-aminophenyl)-N-pyridinio]-phenolate, prepared in dry acetone. The mixture was left overnight to allow the coupling reaction to complete. Then the substrates were removed from the solution and washed thoroughly with dry acetone.

The substrates after the series of treatments shown no difference from the original substrates in terms of IR spectra. It appeared that little or no dye had been coated on the surfaces of substrates or that having not enough dye was coated on the surfaces of the substrates. The reason for this is uncertain.

6.2.2.2 Use of amino-terminal silane and bifunctional cross linker glutaraldehyde for immobilisation of the dye on silica surfaces

Glutaraldehyde is a very popular bifunctional reagent used widely in biological and biomedical systems for the cross-linking of proteins.[23] Amino-terminal silane is also a popular silane used for preparation of silanised carrier. For example, a fibre-optic evanescent wave biosensor of oligonucleotides was successfully made by means of 3-aminopropyl triethoxysilane (APTS) and glutaraldehyde by Graham et al.[24] This method was tried for coupling of the dyes synthesised in the present work on substrates including glass cover slips, glass slides and quartz slides. A simple reaction scheme (Fig. 6-7) is showed as follows:

Procedures of immobilisation:

a) Cleaning of silica surface

The method used for cleaning silica surfaces was the same as that used in 6.2.2.1.

b) Purification of glutaraldehyde

Commercial glutaraldehyde is a mixture of the monomeric dialdehyde and indeterminate amounts of impurities, mainly polymerization products of dialdehyde.[25]

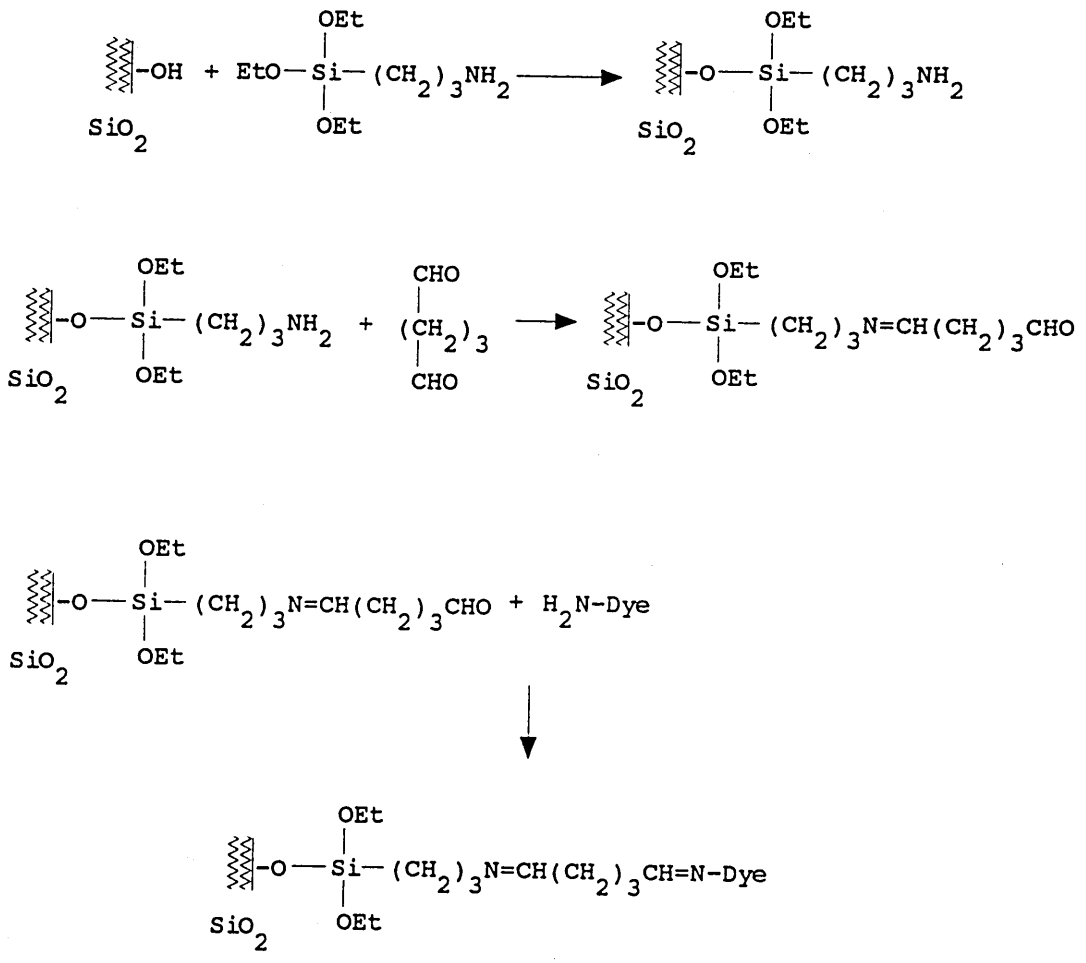

Fig. 6-7 Coupling reaction for covalent attachment of dye to a silica surface by amino-terminal silane and glutaraldehyde

Pure glutaraldehyde has an absorbance at 280 nm while polymeric impurities absorb at 235 nm.[26] Because only pure glutaraldehyde can be used as cross-linking reagent, it is necessary to purify it before use. There are many methods to purify glutaraldehyde. The method used[25] involved shaking the

commercial glutaraldehyde (Aldrich, 25%) with active charcoal (about 5% w/v) and subsequent filtration. This was repeated until the UV absorbance spectrum showed absorbance only at 280 nm.

c) Silanization of the Substrates

The silanizations were carried out in two different ways. One was in organic solvent and the other was in aqueous solution.

I. Silanization of the substrates in aqueous solution[9]

The substrates (glass cover slips, glass slides and quartz slides) were immersed in a 10% (v/v) aqueous solution of 3-aminopropyl triethoxysilane (APTS, Aldrich). The pH of the solution was controlled to between pH3 and 4 with 6 M HCl. The neutralisation of the basic silane solution caused heating. After pH adjustment, the mixture was placed in a 75 °C water bath for 3 hr. Then the substrates were removed from the solution and washed thoroughly with distilled water. The substrates were allowed to air dry.

II. Silanization of the substrates in organic solvent[24]

The substrates were immersed in a 2% (v/v) solution of APTS in dry acetone for 24 hr. at room temperature, then washed with dry acetone thoroughly, and finally allowed to air dry.

d) Treatment of silanized substrates with the bifunctional reagent glutaraldehyde[9]

The silanized substrates were immersed in a 2.5% solution of glutaraldehyde (Aldrich) prepared with 0.05 M Na_2HPO_4 buffer solution adjusted to pH 7.0. The mixture was left for at least 1 h. at room temperature to

allow the reaction to complete. Then the substrates were washed exhaustively with distilled water and allowed to air dry.

e) Immobilisation of the dyes

Two dyes, 2,6-dimethyl-4-[(2,6-diphenyl)-4-(p-aminophenyl)-N-pyridinio]-phenolate and 2,6-dichloro-4-[(2,6-diphenyl)-4-(p-aminophenyl)-N-pyridinio]-phenolate, were linked with the substrates treated with silane and glutaraldehyde.

The substrates coated with APTS and glutaraldehyde were immersed in a 0.05 mg/ml solution of dye mentioned above, prepared in dry acetone. The mixture was left for a week to allow the reaction complete. The substrates were removed from the solution and washed exhaustively with dry acetone.

The substrates after the series of treatments shown above had no obvious difference from the original ones in IR spectra. The situation was similar to that found in section 6.2.2.1, that is, little or no dye had been coated on the surfaces of the substrates or having not enough dye was coated on the surfaces of the substrates.

6.2.3 Covalent binding between the dyes synthesised and amberlite IRA-93 through glutaraldehyde

Amberlite IRA-93 is a weakly basic anion exchanger. It was thought that the amino groups on the surface of Amberlite IRA-93, might react with glutaraldehyde (Fig. 6-8) to produce a carrier for coupling with the dyes synthesised, as follows:

Procedures of immobilisation:

a) Amberlite IRA-93 (Sigma) was ground into fine powder (white) by means of a mortar, washed with plenty of distilled water, and finally dried by filtering with a Buchner funnel under vacuum.

b) To 2 g clean fine powder of Amberlite IRA-93, was added 50 ml of a 2.5% solution of purified glutaraldehyde prepared in 0.05 M Na_2HPO_4 buffer solution adjusted to pH 7.0. The mixture was stirred for 24 hr. at room temperature to complete the reaction. The resulting white powder was filtered off, and washed thoroughly with distilled water. Finally it was dried by a Buchner funnel under vacuum.

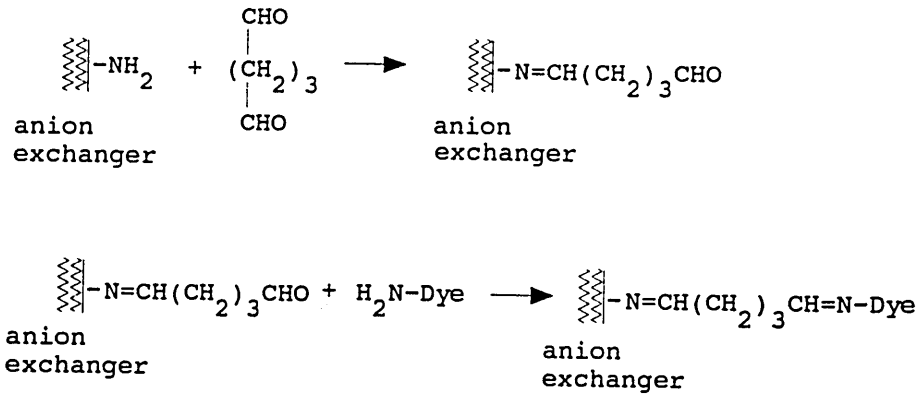

Fig. 6-8 Coupling reaction for covalent attachment of dye to amberlite IRA-93

c) Amberlite IRA-93 (1.0 g) treated with purified glutaraldehyde was mixed with a 1% solution of the dye synthesised (two dyes, 2,6-difluoro-4-[(2,6-diphenyl)-4-(p-aminophenyl)-N-pyridinio]-phenolate or 2,6-dichloro-4-[(2,6-diphenyl)-4-(p-aminophenyl)-N-pyridinio]-phenolate) in dry ethanol. The

mixture was stirred at room temperature for a week. Then the solid powder was filtered off, washed exhaustively with dry ethanol, and dried under vacuum.

The resulting solid powder was still colourless. It appeared that the dye had not been coated on the surface of Amberlite IRA-93. Possible reasons for this are that the density of amino groups on the resin is very low, or that the activation chemistry was faulty.

6.2.4 Covalent binding between the dyes synthesised and NH_2 aminopropyl sorbent through glutaraldehyde

NH_2 aminopropyl sorbent is a type of silica sorbent used in solid phase extraction. The silica surface is modified and its main structure is shown in Fig. 6-9 as below:

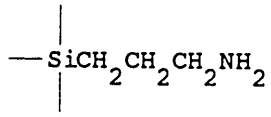

Fig. 6-9 The structure of NH_2 aminopropyl sorbent

The aim was to use the amino groups on the surface of NH_2 aminopropyl sorbent, to react with glutaraldehyde and produce a carrier for the dyes synthesised in the present work.

Procedures for immobilisation:

a) Treatment of NH_2 aminopropyl sorbent by glutaraldehyde

To 0.5 g of NH_2 Aminopropyl Sorbent (Varian Sample Preparation Products), add 15 ml of a 2.5% solution of glutaraldehyde in (a) 0.05 M Na_2HPO_4 buffer adjusted to pH 7.0; (b) pH=1.5 diluted hydrochloric acid

solution; (c) ultra pure water. The reaction was allowed to continue for three hours at room temperature under stirring. During this time a colour change to amagenta or tan was observed. [tan in (b), magenta in (a) and (c), but the colour in (a) was stronger than that in (c)]. The material was wash exhaustively with distilled water first and then organic solvent. Three coloured products were obtained after filtering and drying. This result was the same as that found in the reaction between alkyl amine carrier produced from silanization of a porous material with glutaraldehyde.[9] This showed that NH_2 aminopropyl sorbent did react with glutaraldehyde, and resulted in a carrier with the structure shown in Fig. 6-10. This carrier should react with the dye to achieve the covalent binding.

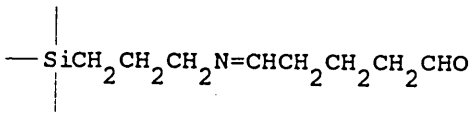

Fig. 6-10 The structure of the carrier

However, the carriers produced from the reaction mentioned above all have a strong colour. This is not desirable, because it will overlap the colour of the dye coated on the carriers so that the measurement of maxima absorption of the coated dye will be affected.

b) Coupling the dyes synthesised with NH_2 aminopropyl sorbent treated with glutaraldehyde

2,6-diphenyl-4-{[4-(4-aminophenyl)-2,6-diphenyl]-N-pyridinio}-phenolate and 2,6-dimethyl-4-{[4-(4-aminophenyl)-2,6-diphenyl]-N-pyridinio}-phenolate, were linked with the carriers produced from step a).

To the NH_2 aminopropyl sorbents treated with glutaraldehyde, was added 0.0010g/1ml of dye solution dry chloroform. As little solution as possible was used to allow just cover the sorbent. The mixture was left for a week to complete the coupling reaction. The solid powder was washed with plenty of dry chloroform, filtered off and dried under vacuum. The colour of the products were not any difference from the carrier. It was also difficult to see colour response of the coated dyes in different solvents.

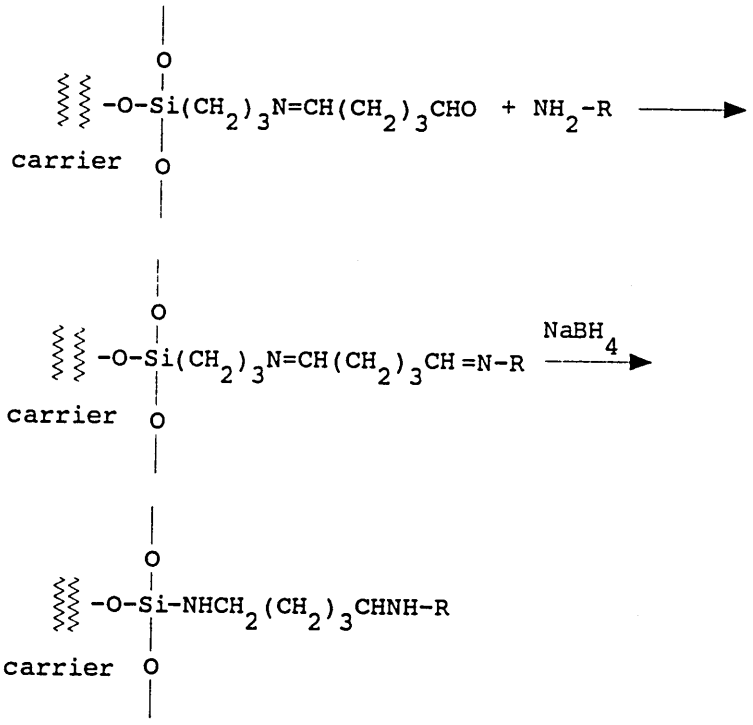

Fig. 6-11 The covalent coupling of a protein with the aldehyde derivative followed by reduction with sodium borohydride

The colour of the carriers, probably due to the vinyl amine double bond or cyclic structure formation, might be masking the colour response of the coated dyes in different solvents, so an attempt was made to reduce the colour of the carriers, according to the method (Fig. 6-11) mentioned by Weetall.[27] A 1.0 % solution of sodium borohydride was used to reduce the vinyl amine double bond in the

material generated from a reaction between a carrier treated with glutaraldehyde and the dye.

Unfortunately, the attempt was unsuccessful. The colour of the material disappeared after treatment with sodium borohydride. Although the real reason for this is not clear, obviously, sodium borohydride did not only react with vinyl amine double bond, but also reacted with the coated dyes. The situation was the same after reducing the concentration of sodium borohydride.

6.2.5 Immobilisation of the dyes synthesised on NH_2 aminopropyl sorbent through a thiourea linkage

As mentioned in the introduction to this chapter, an alkylamine carrier may be converted to an isothiocyanate and then covalently linked to a free amine group through a thiourea linkage. This method was successfully applied to immobilise an enzyme by Wide et al.[28, 29] This method was also chosen to immobilise the dyes synthesised in the present work (Fig. 6-12).

Procedures of immobilisation:

a) Treatment of NH_2 aminopropyl sorbent by thiophosgene

To 1 g of NH_2 aminopropyl sorbent was added 80 ml of 10% solution of thiophosgene (Aldrich) in chloroform (v/v). All work was carried out in a fume cupboard due to the nauseous and toxic nature of the thiophosgene. The reaction mixture was refluxed overnight and then the solid sorbent was filtered off and washed with dry chloroform thoroughly. A white solid was obtained after dryness under vacuum. The resulting solid derivative was used as soon as possible for coupling with the dyes.

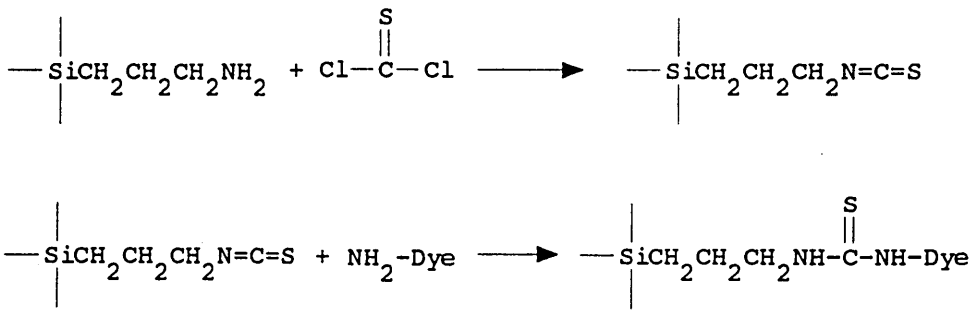

Fig. 6-12 Immobilisation reaction of NH_2 aminopropyl sorbent with the dyes synthesised through a thiourea linkage

b) Immobilisation of the dyes

The dyes used for immobilisation are listed as below:

(A) 2,6-dimethyl-4-[(2,6-diphenyl)-4-(p-aminophenyl)-N-pyridinio]-phenolate;

(B) 2,6-diphenyl-4-[(2,6-diphenyl)-4-(p-aminophenyl)-N-pyridinio]-phenolate;

(C) 2,6-difluoro-4-[(2,6-diphenyl)-4-(p-aminophenyl)-N-pyridinio]-phenolate;

(D) 2,6-difluoro-4-[(4,6-diphenyl)-2-(p-aminophenyl)-N-pyridinio]-phenolate;

(E) 2,6-dichloro-4-[(2,6-diphenyl)-4-(p-aminophenyl)-N-pyridinio]-phenolate;

(F) 2,6-dichloro-4-[(4,6-diphenyl)-2-(p-aminophenyl)-N-pyridinio]-phenolate;

The procedures for immobilisation are described as follow.

The isothiocyanate derivative (0.5 g) from previous step a) was added to a chloroform solution (5 ml) of the dye studied (0.0020 g/5 ml). As soon as they were mixed, the colour of the solution became earth yellow from dark green. The mixture was allowed to continue the reaction at room temperature under stirring for 2 days. The resulting coloured solid dye coated materials were filtered off, washed with plenty of dry chloroform, and dried under vacuum. The resulting materials from the dyes (A) was very pale yellow in colour, almost colourless. A possible reason for this was that the dye was changed to its protonated form

during the course of linking, which resulted in it becoming colourless. The materials from the dyes (B), (C), (D), (E) and (F) were deeply coloured.

6.2.6 Immobilisation of the dyes on transparent substrates treated by silane agent APTS through thiourea linkage

It seemed that the dyes were coated on the NH_2 aminopropyl sorbent satisfactorily by thiourea linkage, so an attempt was made to covalently link the dyes onto transparent substrates including glass cover slips, glass slides and quartz slides, because transparent substrates are easier to use for UV-VIS spectroscopy.

Substrates silanized with APTS (see the previous section 6.2.2.2) were used to link the dyes via thiophosgene. The procedures used were the same as those used for the NH_2 aminopropyl sorbent. However, the resulting substrates were still colourless and it seemed that no dye was coated on.

The lack of success in this and previous attempts may be due either to poor Silanization of the surfaces, or to the amount deposited being too small to be visible. The aminopropyl sorbent has a large surface area and is known to be derivatised over about 1% of the surface area.

6.2.7 Immobilisation of the dyes on NH_2 aminopropyl sorbent through amide linkage

As described in the introduction to this chapter, a pseudourea of a carboxyl derivative can be used to couple both aryl and alkyl amines. This method has been used in biological and biomedical systems successfully.[9,27] This

method of coupling the dyes synthesised in the present work to a solid surface was investigated. A simple reaction scheme is showed in Fig. 6-13.

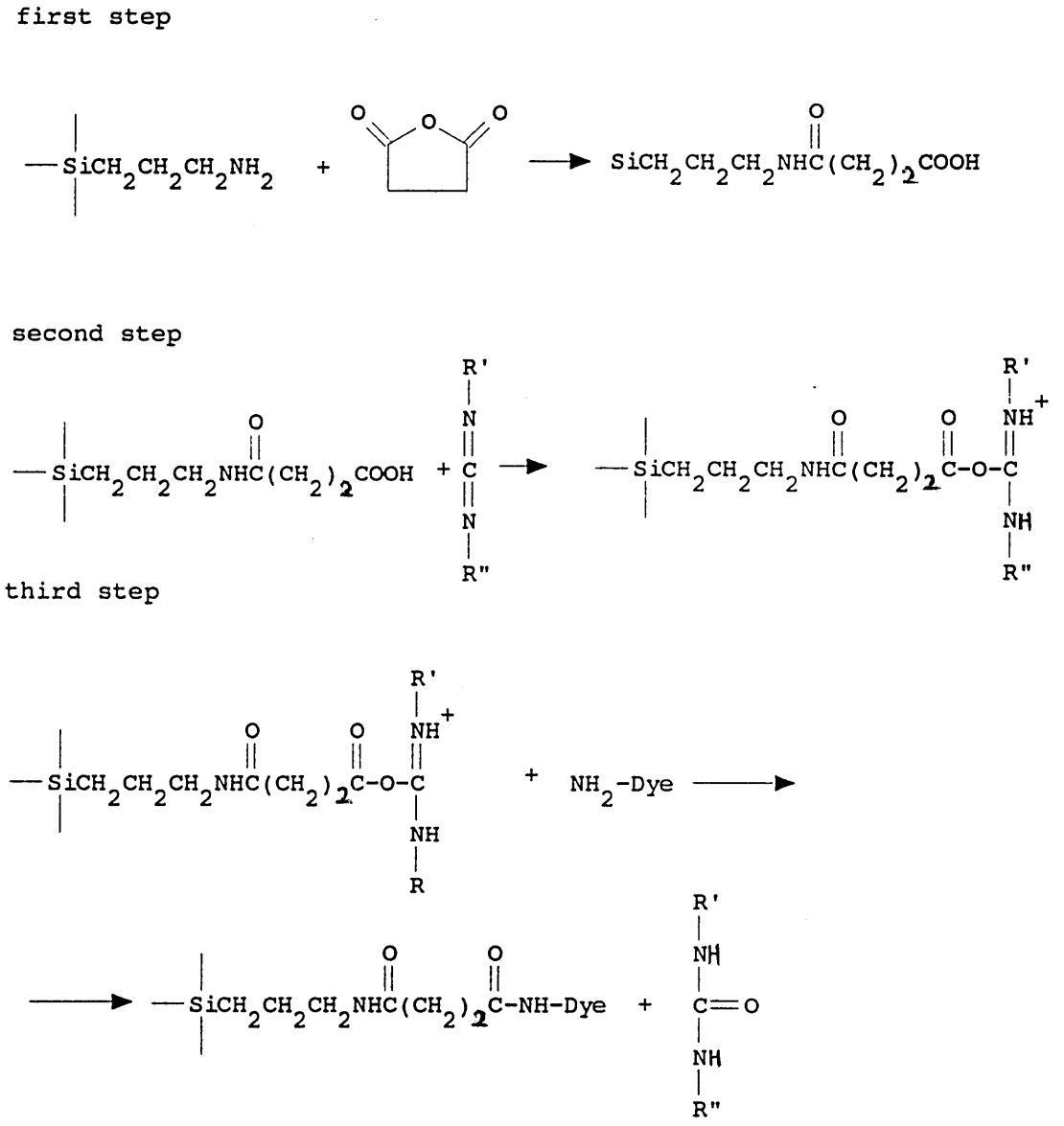

Fig. 6-13 Reactions for immobilisation of the dyes on NH_2 aminopropyl sorbent through an amide linkage

Procedures of immobilisation:

a) Preparation of carboxylic derivative

The carboxylic derivative can be prepared by the reaction of the NH_2 aminopropyl sorbent with succinic anhydride.[9]

Succinic anhydride (1.0 g) and NH_2 aminopropyl sorbent (1 g) were placed in a 25 ml of 0.05 M phosphate buffer solution adjusted to pH 6.0. The mixture was stirred at room temperature with pH adjustment as necessary over the first few hours. The reaction was allowed to continue for 24 hours under stirring and at room temperature. The white solid product was filtered off, washed thoroughly with distilled water, and dried under vacuum. The final product was stored for the next step.

b) Treatment of the carboxylic derivative with carbodiimide agent

1-cyclohexyl-3-(2-morpholinoethyl)-carbodiimide (100 mg) was dissolved in deionized water. The carboxylated sorbent (0.5 g) generated from the previous step a) was added to the solution. The mixtures were allowed to react at room temperature for at least two hours and the pH of the reaction solution was controlled at 10. The white pseudourea was washed with plenty of deionized water and dried under vacuum.

c) Immobilisation of the dyes

The dyes used for immobilisation were:

(A) 2,6-dimethyl-4-[(2,6-diphenyl)-4-(p-aminophenyl)-N-pyridinio]-phenolate;

(B) 2,6-diphenyl-4-[(2,6-diphenyl)-4-(p-aminophenyl)-N-pyridinio]-phenolate;

(C) 2,6-difluoro-4-[(2,6-diphenyl)-4-(p-aminophenyl)-N-pyridinio]-phenolate;

(D) 2,6-difluoro-4-[(4,6-diphenyl)-2-(p-aminophenyl)-N-pyridinio]-phenolate;

(E) 2,6-dichloro-4-[(2,6-diphenyl)-4-(p-aminophenyl)-N-pyridinio]-phenolate;

(F) 2,6-dichloro-4-[(4,6-diphenyl)-2-(p-aminophenyl)-N-pyridinio]-phenolate;

The carrier (0.5 g) from step b) above was added to 10 ml of dye solution (0.0050 g/10 ml) prepared in acetone. The mixture was stirred for two days to allow the coupling reaction complete. The resulting coloured solid dye coated materials were filtered off, washed thoroughly with dry acetone, and dried under vacuum. The resulting materials were similar to those from thiourea linkage in section 6.2.5. The materials from the dye (A) was very pale yellow colour, and the materials from the dyes (B), (C), (D), (E) and (F) were with a deep colour.

6.2.8 Immobilisation of the dyes on transparent substrates treated by silane agent APTS through amide linkage

The methods described above in section 6.2.7 was used to couple the dyes synthesised on a number of different transparent substrates including a. glass slide; b. glass slip; c. quartz slide and d. fresh glass slide made from melted glass beads, but the results were not successful. All substrates used were colourless, which further confirmed that either the surface area on the substrates were not enough to coat enough silane agent, or that the Silanization procedure was ineffective.

6.3 Results of reflectance spectra of the dye coated materials

It was expected that the solvatochromic properties of dyes would be changed by covalent binding, but it was hoped that they would still keep solvatochromic properties after covalent linkage, to probe the polarities of different solvents.

Because the materials obtained were all not transparent, their solvatochromic properties were investigated by means of reflectance measurements. For easier comparison, the reflectance measurements are

expressed in an analogous way to those for absorbance (A'= log1/R, where R is the diffuse reflectance), and transition energies are also expressed in an analogous way ET'(kJ/mol)= 1.1959 * ν (cm^{-1}).

Measurements of reflectance spectra of covalent immobilised dyes were carried out in PYE UNICAM SP 800 spectrophotometer, using the original reflectance unit. The sample of the coated dye material was made as a hard disc, just like a KBr i.r. sample disc, in order to provide a smooth surface for reflectance measurement. The sample disc was put in a small, thin transparent container with the solvent. Then the container was placed in the reflectance unit for measurement. After every measurement, the solvent was changed and sample disc was dried by a hair-drier or allowed to air dry before the next measurement.

Reflectance peaks and transition energies of dye (B) coated on NH_2 aminopropyl sorbent by thiourea linkage and by amide linkage are shown in Table 6-1, together with the free dye (B) and standard ET(30) values in different solvents. Like the free dye (B), the covalently coated dyes (B) are negatively solvatochromic, i.e., polar solvents shift the reflectance peak to shorter wavelengths and nonpolar solvents shift it to longer wavelengths. Although the solvatochromic shifts (50.1 kJ/mol in thiourea linkage and 42.5 kJ/mol in amide linkage) were reduced compared with the free dye (B) (112.1 kJ/mol) in going from MeOH to THF, an apparent solvatochromic shift trend can still be identified, as seen in Fig. 6-14 and Fig. 6-15. Two plots of the ET values of the coated dye (B) versus those of the standard dye ET(30) are given in Fig. 6-16 and Fig. 6-17 for the two different linkage methods. Both demonstrate good correlation. Also, the presence of small amount of water in nonpolar solvent benzene caused a

Table 6-1

Reflectance peak positions and transition energies of coated dye (B) on aminopropyl sorbent by thiourea and amide linkages, together with the values of the free dye (B) and ET(30)

solvent	coated dye (B) by thiourea linkage		coated dye (B) by amide linkage		free dye (B)		ET (30)	
	λ_{max} (nm)	ET (kJ/mol)	λ_{max} (nm)	ET (kJ/mol)	λ_{max} (nm)	ET (kJ/mol)	λ_{max} (nm)	ET (kJ/mol)
water	430.0	277.9	430.0	277.9	.....	.....	453.0	264.0
methanol	460.0	259.8	460.0	259.8	428.0	279.2	515.0	232.2
ethanol	470.0	254.3	470.0	254.3	432.0	276.6	551.0	217.0
acetonitrile	510.0	234.3	510.0	234.3	588.0	203.2	622.0	192.3
DMF	.....	.....	.....	.....	612.8	195.0	653.0	183.1
acetone	530.0	225.5	520.0	229.8	636.0	187.9	677.0	176.6
dichloro-methane	540.0	221.3	530.0	225.5	658.9	181.4	696.0	171.8
chloroform	560.0	213.4	540.0	221.3	661.6	180.6	731.0	163.5
THF	570.0	209.7	550.0	217.3	715.2	167.1	764.0	156.5
benzene	590.0	202.6	570.0	209.7	.....	.....	834.0	143.3
benzene (0.02% H_2O)	569.0	210.0	553.0	216.1	.....	.....		.....

Dye (B): 2,6-diphenyl-4-[(2,6-diphenyl)-4-(p-aminophenyl)-N-pyridinio]-phenolate.

significant shift (21 nm for thiourea linkage and 17 nm for amide linkage in the benzene with 0.02% H_2O) in the reflectance peak for both linkages (Table 6-1). This suggests that the coated dye (B) might be useful for the spectrophotometric determination of water in nonpolar solvents.

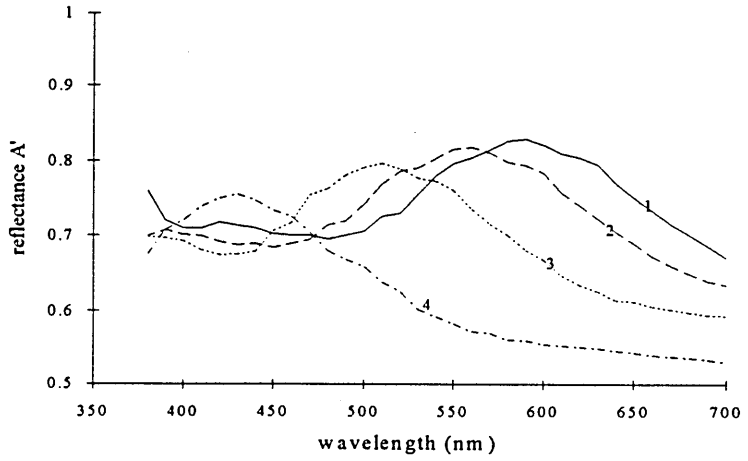

1. with C_6H_6; 2. with $CHCl_3$; 3. with MeCN; 4. with H_2O

Fig. 6-14 Reflectance spectra of immobilised dye (B) on aminopropyl silica by thiourea linkage

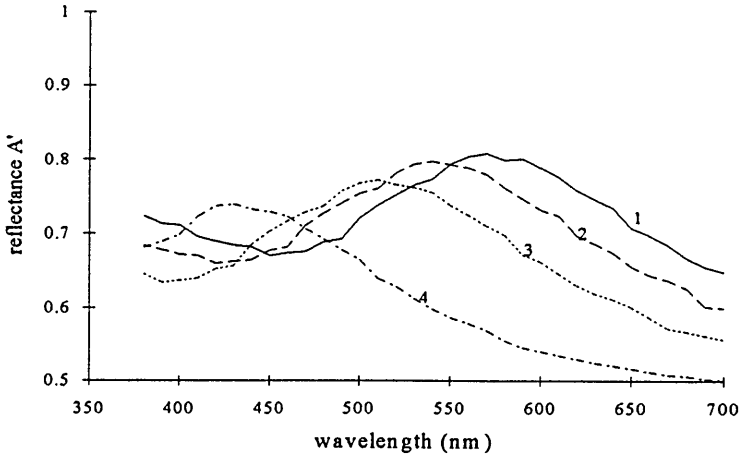

1. with C_6H_6; 2. with $CHCl_3$; 3. with MeCN; 4. with H_2O

Fig. 6-15 Reflectance spectra of immobilised dye (B) on aminopropyl silica by amide linkage

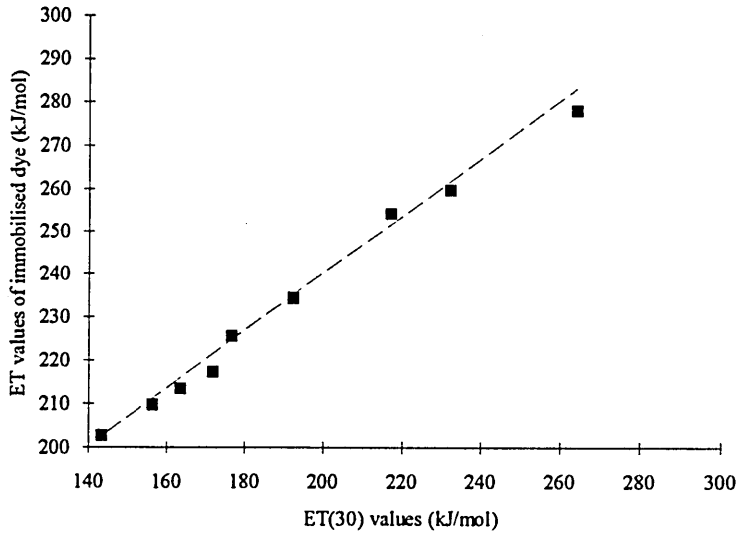

Fig. 6-16 Plot of ET values of immobilised dye (B) by thiourea linkage versus standard ET(30) values in different solvents showed in Table 6-1

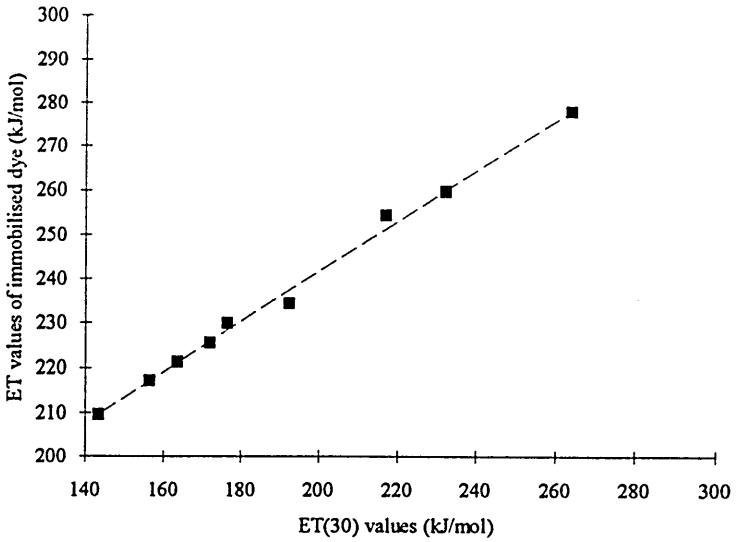

Fig. 6-17 Plot of ET values of immobilised dye (B) by amide linkage versus standard ET(30) values in different solvents showed in Table 6-1

Immobilised dyes (C), (D), (E), and (F) on aminopropyl sorbent by thiourea or amide linkage have the same properties as the immobilised dye (B). Their reflectance peaks and transition energies are given in Table 6-2, 6-3, 6-4, and 6-5, together with the values of their free dyes and standard ET(30) in different solvents. They all show a negative solvatochromism. An apparent solvatochromic shift trend can be identified for the four immobilised dyes, and the plots of their ET values versus standard ET(30) values all demonstrate good correlation, which can be seen from Fig. 6-18 to Fig. 6-33. Similarly, the presence of a small amount of water in the nonpolar solvent benzene caused a shift in reflectance peak for the four immobilised dyes.

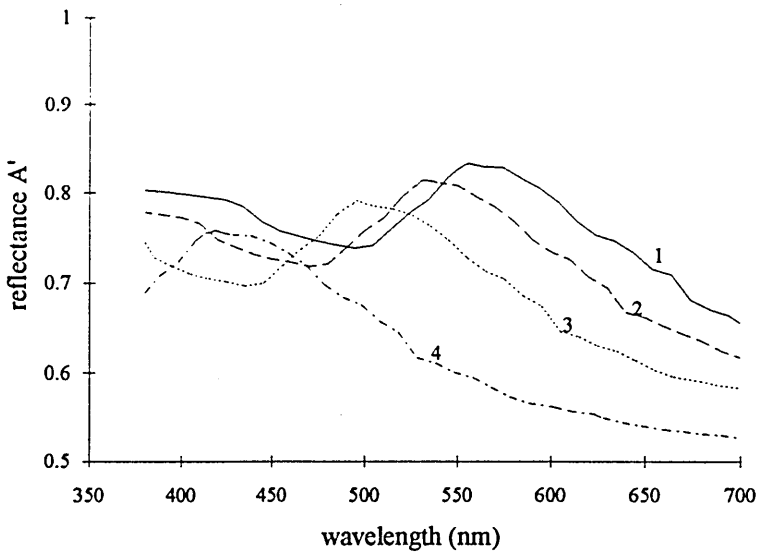

1. with C_6H_6; 2. with $CHCl_3$; 3. with MeCN; 4. with H_2O

Fig. 6-18 Reflectance spectra of immobilised dye (C) on aminopropyl silica by thiourea linkage

Table 6-2

Reflectance peak positions and transition energies of coated dye (C) on aminopropyl sorbent by thiourea and amide linkages, together with the values of the free dye (C) and ET(30)

solvent	coated dye (C) by thiourea linkage		coated dye (C) by amide linkage		free dye (C)		ET (30)	
	λ_{max} (nm)	ET (kJ/mol)	λ_{max} (nm)	ET (kJ/mol)	λ_{max} (nm)	ET (kJ/mol)	λ_{max} (nm)	ET (kJ/mol)
water	418.0	285.9	415.0	288.0	399.0	299.5	453.0	264.0
methanol	448.0	266.8	442.0	270.4	428.4	279.0	515.0	232.2
ethanol	460.0	259.8	454.0	263.2	435.2	274.6	551.0	217.0
acetonitrile	495.0	241.4	484.0	246.9	500.0	239.0	622.0	192.3
DMF	.....	.....	.....	.....	517.8	231.2	653.0	183.1
acetone	510.0	234.3	500.0	239.0	523.0	228.5	677.0	176.6
dichloro-methane	518.0	230.7	507.0	235.7	526.9	227.2	696.0	171.8
chloroform	532.0	224.6	521.0	229.4	538.0	222.1	731.0	163.5
THF	544.0	219.7	533.0	224.2	588.0	203.2	764.0	156.5
benzene	556.0	214.9	545.0	219.3	.....	.....	834.0	143.3
benzene (0.02% H_2O)	540.0	221.3	530.0	225.5	.....	.....		.....

Dye (C): 2,6-difluoro-4-[(2,6-diphenyl)-4-(p-aminophenyl)-N-pyridinio]-phenolate.

Table 6-3

Reflectance peak positions and transition energies of coated dye (D) on aminopropyl sorbent by thiourea and amide linkages, together with the values of the free dye (D) and ET(30)

solvent	coated dye (D) by thiourea linkage		coated dye (D) by amide linkage		free dye (D)		ET (30)	
	λ_{max} (nm)	ET (kJ/mol)	λ_{max} (nm)	ET (kJ/mol)	λ_{max} (nm)	ET (kJ/mol)	λ_{max} (nm)	ET (kJ/mol)
water	430.0	277.9	425.0	264.4	.....	.....	453.0	264.0
methanol	458.0	260.9	450.0	249.7	393.0	304.1	515.0	232.2
ethanol	470.0	254.3	463.0	242.7	406.0	294.4	551.0	217.0
acetonitrile	506.0	236.2	498.0	225.6	495.0	241.4	622.0	192.3
DMF	.....	.....	.....	.....	550.0	217.3	653.0	183.1
acetone	520.0	229.8	510.0	220.3	553.0	216.1	677.0	176.6
dichloro-methane	531.0	225.1	521.0	215.7	.....	.....	696.0	171.8
chloroform	544.0	219.7	533.0	210.8	561.0	213.0	731.0	163.5
THF	556.0	214.9	543.0	206.9	610.0	195.9	764.0	156.5
benzene	566.0	211.1	552.0	203.6	.....	.....	834.0	143.3
benzene (0.02% H_2O)	551.0	216.9	540.0	208.1	.....	.....		.....

Dye (D): 2,6-difluoro-4-[(4,6-diphenyl)-2-(p-aminophenyl)-N-pyridinio]-phenolate.

Table 6-4

Reflectance peak positions and transition energies of coated dye (E) on aminopropyl sorbent by thiourea and amide linkages, together with the values of the free dye (E) and ET(30)

solvent	coated dye (E) by thiourea linkage		coated dye (E) by amide linkage		free dye (E)		ET (30)	
	λ_{max} (nm)	ET (kJ/mol)	λ_{max} (nm)	ET (kJ/mol)	λ_{max} (nm)	ET (kJ/mol)	λ_{max} (nm)	ET (kJ/mol)
water	420.0	284.5	423.0	282.5	400.0	298.8	453.0	264.0
methanol	450.0	265.6	450.0	265.6	428.1	279.2	515.0	232.2
ethanol	460.0	259.8	460.0	259.8	433.6	275.6	551.0	217.0
acetonitrile	490.0	243.9	489.0	244.4	480.0	249.0	622.0	192.3
DMF	.....	.....	.....	.....	500.0	239.0	653.0	183.1
acetone	510.0	234.3	499.0	239.5	516.0	231.6	677.0	176.6
dichloro-methane	520.0	229.8	510.0	234.3	536.8	222.6	696.0	171.8
chloroform	540.0	221.3	525.0	227.6	544.2	219.6	731.0	163.5
THF	550.0	217.3	538.0	222.1	602.0	198.5	764.0	156.5
benzene	560.0	213.4	551.0	216.9	.....	.....	834.0	143.3
benzene (0.02% H_2O)	543.0	220.1	536.0	223.0	.....	.....		.....

Dye (E): 2,6-dichloro-4-[(2,6-diphenyl)-4-(p-aminophenyl)-N-pyridinio]-phenolate.

Table 6-5

Reflectance peak positions and transition energies of coated dye (F) on aminopropyl sorbent by thiourea and amide linkages, together with the values of the free dye (F) and ET(30)

solvent	coated dye (F) by thiourea linkage		coated dye (F) by amide linkage		free dye (F)		ET (30)	
	λ_{max} (nm)	ET (kJ/mol)	λ_{max} (nm)	ET (kJ/mol)	λ_{max} (nm)	ET (kJ/mol)	λ_{max} (nm)	ET (kJ/mol)
water	430.0	277.9	425.0	281.2	.....	.....	453.0	264.0
methanol	469.0	254.8	460.0	259.8	398.0	300.3	515.0	232.2
ethanol	480.0	249.0	470.0	254.3	409.0	292.4	551.0	217.0
acetonitrile	514.0	232.5	505.0	236.7	490.0	243.9	622.0	192.3
DMF	.....	.....	.....	.....	536.0	223.0	653.0	183.1
acetone	525.0	227.6	518.0	230.7	545.0	219.3	677.0	176.6
dichloro-methane	535.0	223.4	530.0	225.5	561.0	213.0	696.0	171.8
chloroform	550.0	217.3	543.0	220.1	569.0	210.0	731.0	163.5
THF	561.0	213.0	555.0	215.3	625.0	191.2	764.0	156.5
benzene	572.0	208.9	568.0	210.4	.....	.....	834.0	143.3
benzene (0.02% H_2O)	557.0	214.5	554.0	215.7	.....	.....		.....

Dye (F): 2,6-dichloro-4-[(4,6-diphenyl)-2-(p-aminophenyl)-N-pyridinio]-phenolate.

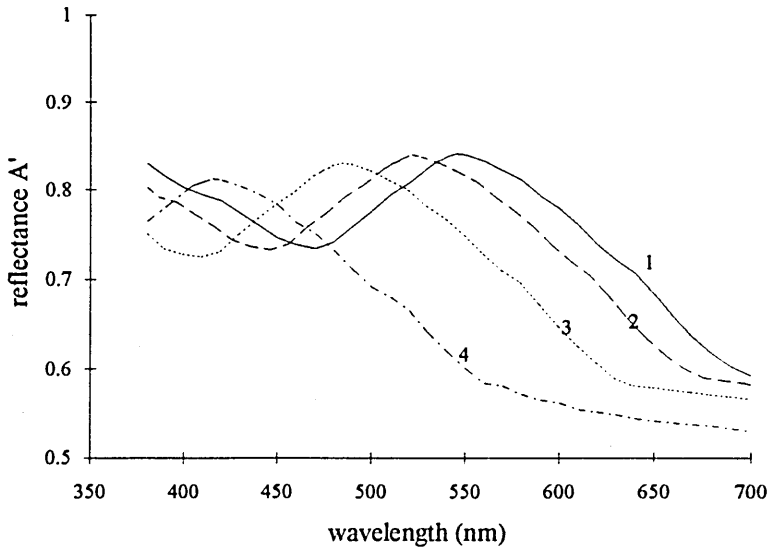

1. with C_6H_6; 2. with $CHCl_3$; 3. with MeCN; 4. with H_2O

Fig. 6-19 Reflectance spectra of immobilised dye (C) on aminopropyl silica by amide linkage

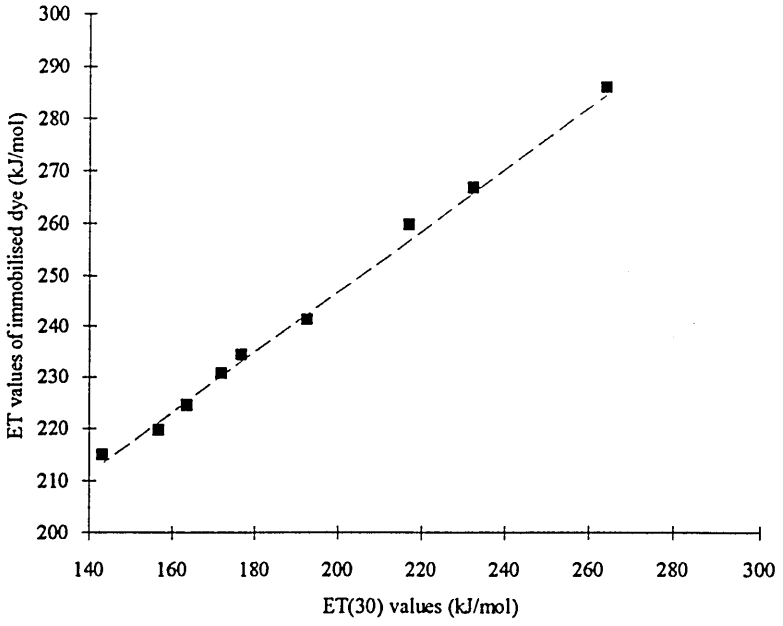

Fig. 6-20 Plot of ET values of immobilised dye (C) by thiourea linkage versus standard ET(30) values in different solvents showed in Table 6-2

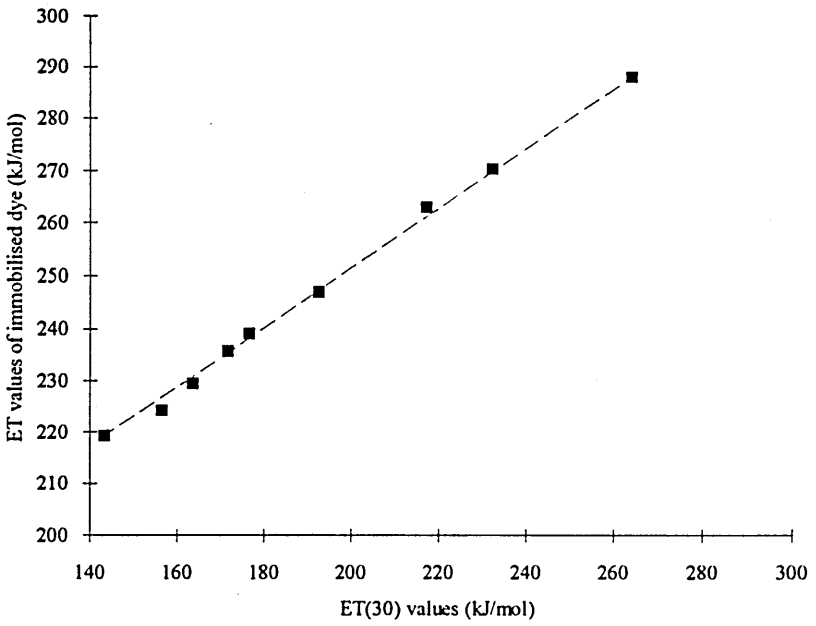

Fig. 6-21 Plot of ET values of immobilised dye (C) by amide linkage versus standard ET(30) values in different solvents showed in Table 6-2

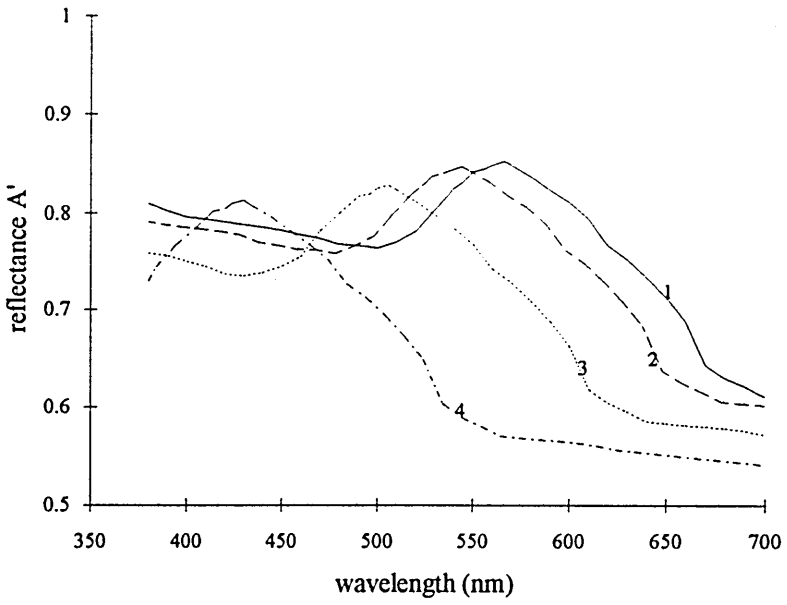

1. with C_6H_6; 2. with $CHCl_3$; 3. with MeCN; 4. with H_2O

Fig. 6-22 Reflectance spectra of immobilised dye (D) on aminopropyl silica by thiourea linkage

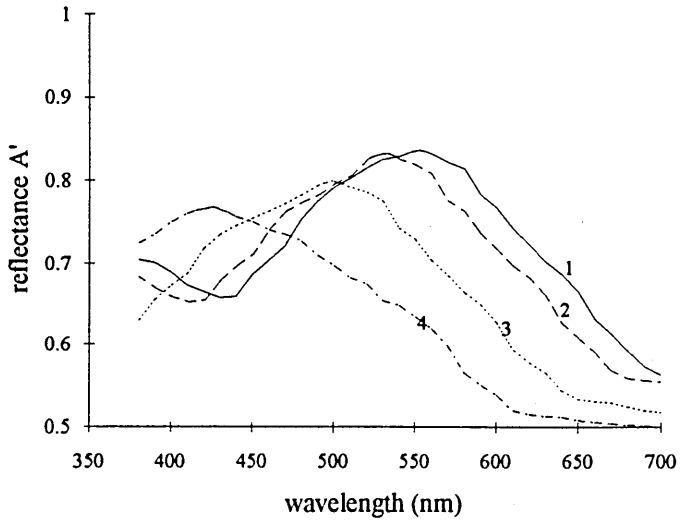

1. with C_6H_6; 2. with $CHCl_3$; 3. with MeCN; 4. with H_2O

Fig. 6-23 Reflectance spectra of immobilised dye (D) on aminopropyl silica by amide linkage

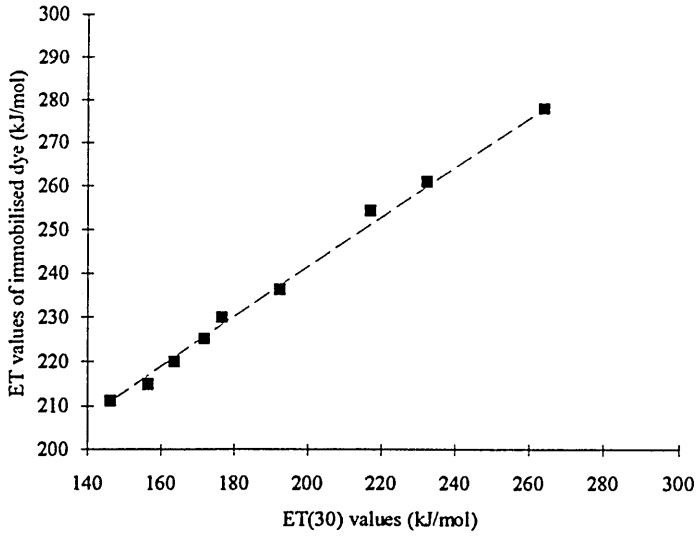

Fig. 6-24 Plot of ET values of immobilised dye (D) by thiourea linkage versus standard ET(30) values in different solvents showed in Table 6-3

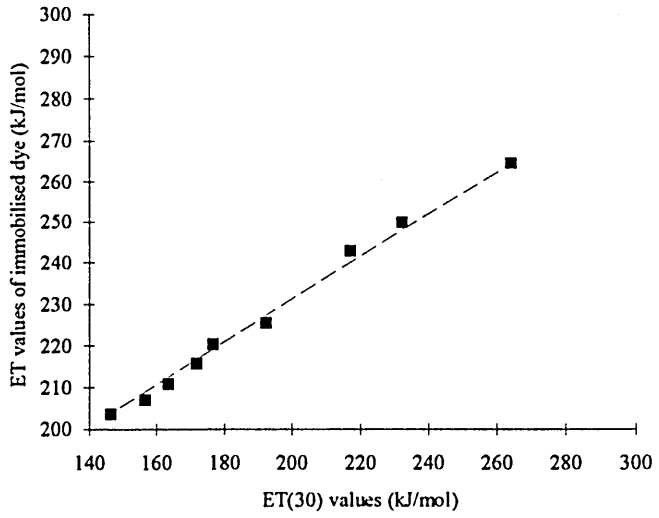

Fig. 6-25 Plot of ET values of immobilised dye (D) by amide linkage versus standard ET(30) values in different solvents showed in Table 6-3

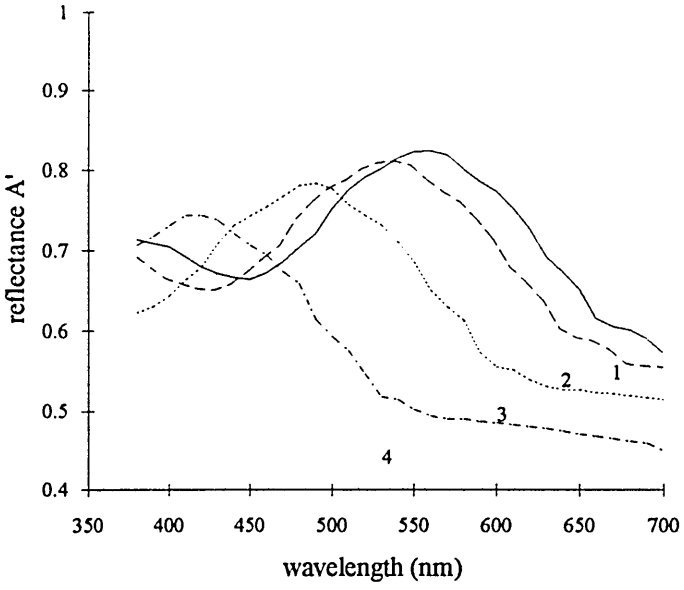

1. with C_6H_6; 2. with $CHCl_3$; 3. with MeCN; 4. with H_2O

Fig. 6-26 Reflectance spectra of immobilised dye (E) on aminopropyl silica by thiourea linkage

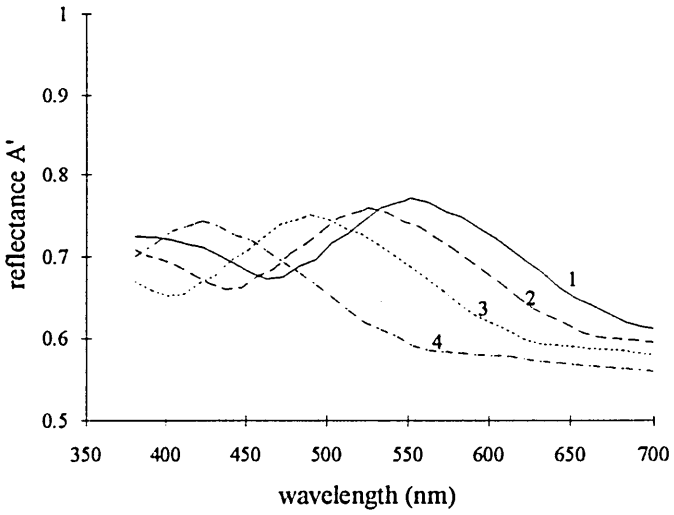

1. with C_6H_6; 2. with $CHCl_3$; 3. with MeCN; 4. with H_2O

Fig. 6-27 Reflectance spectra of immobilised dye (E) on aminopropyl silica by amide linkage

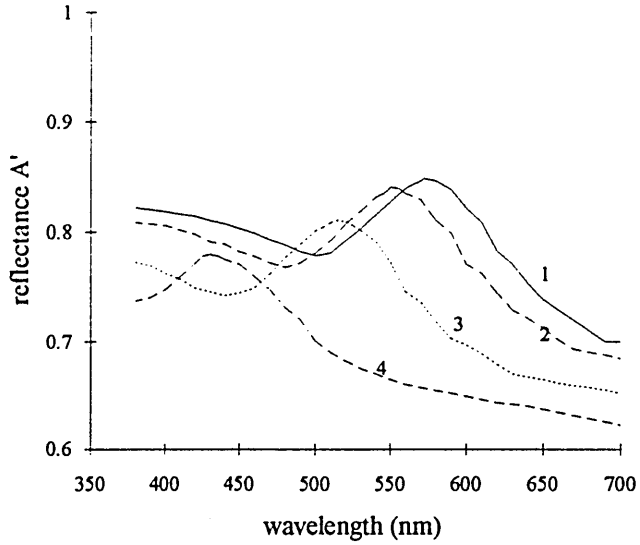

1. with C_6H_6; 2. with $CHCl_3$; 3. with MeCN; 4. with H_2O

Fig. 6-28 Reflectance spectra of immobilised dye (F) on aminopropyl silica by thiourea linkage

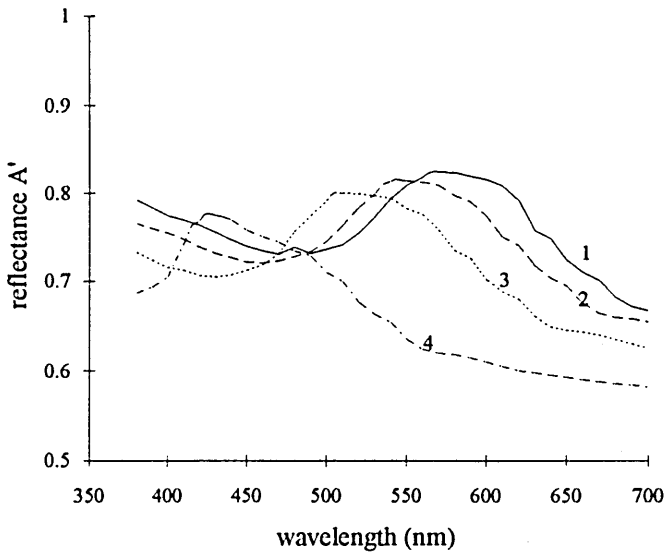

1. with C_6H_6; 2. with $CHCl_3$; 3. with MeCN; 4. with H_2O

Fig. 6-29 Reflectance spectra of immobilised dye (F) on aminopropyl silica by amide linkage

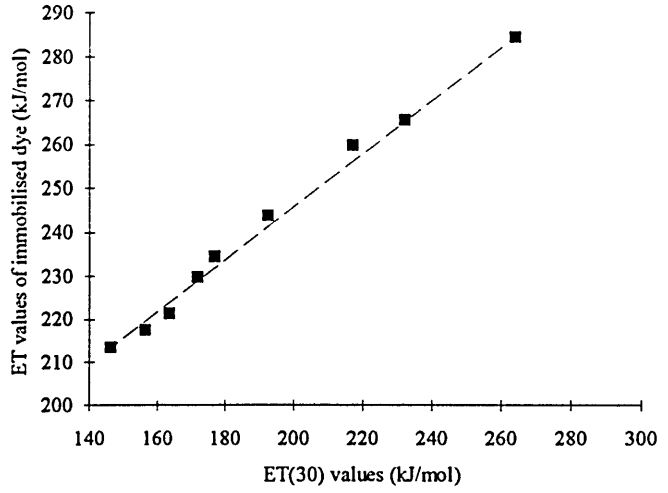

Fig. 6-30 Plot of ET values of immobilised dye (E) by thiourea linkage versus standard ET(30) values in different solvents showed in Table 6-4

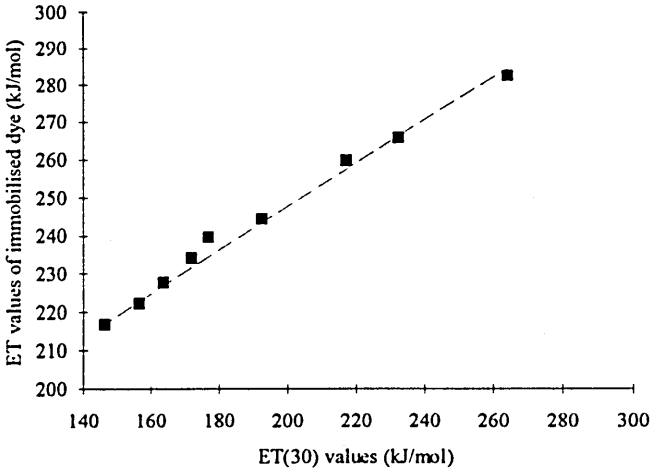

Fig. 6-31 Plot of ET values of immobilised dye (E) by amide linkage versus standard ET(30) values in different solvents showed in Table 6-4

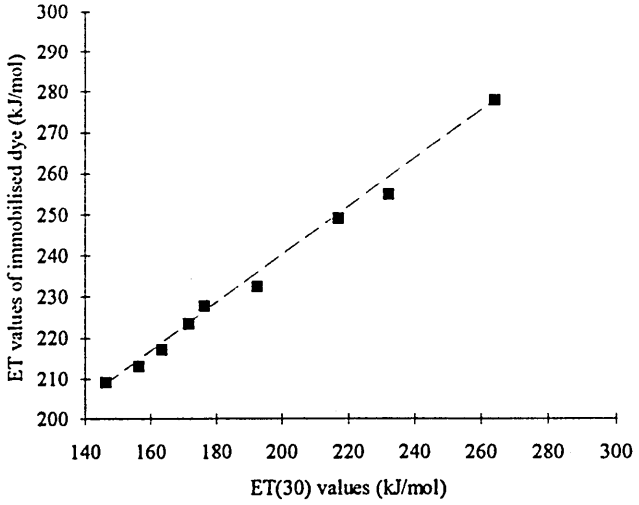

Fig. 6-32 Plot of ET values of immobilised dye (F) by thiourea linkage versus standard ET(30) values in different solvents showed in Table 6-5

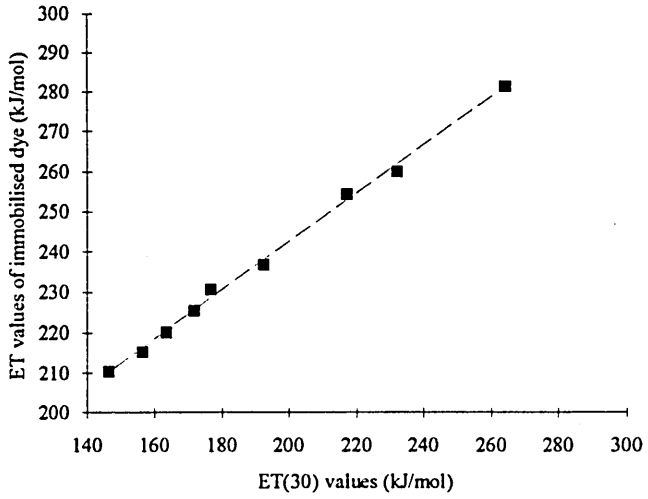

Fig. 6-33 Plot of ET values of immobilised dye (F) by amide linkage versus standard ET(30) values in different solvents showed in Table 6-5

References:

1. Mosbach, K. (1988), Methods in Enzymology Vol. 137, Academic Press, New York.

2. Wingard, L. B., Jr., Katchalski-Katzir, E., and Goldstein, L. (1976) Immobilized Enzyme Principles, Academic Press, New York.

3. Cuatrecasas, P. (1971) in Biochemical Aspects of Reactions on Solid Supports, (Stark, G. R., Ed.), pp.79-109, academic Press, New York.

4. Cuatrecasas, P. 36, 29 (1972), Advan. Enzymol. Relat. Areas Mol. Biol.

5. Porath, J. (1974), Methods in Enzymology Vol. 34, pp13-30, General Methods and Coupling Procedures, Academic Press, New York.

6. Inman, John K. (1974), Methods in Enzymology Vol. 34, pp30-58, Covalent Linkage of Functional Groups, Ligands, and Proteins to polyacrylamide Beads, Academic Press, New York.

7. Weetall, H. H. (1976), Methods in Enzymology Vol. 44, pp134-148, Covalent Coupling Methods for Inorganic Support Materials, Academic Press, New York.

8. Porath, J. and Sundberg, L. 18, 401 (1970), Protides Biol. Fluids, Proc. Colloq.

9. Porath, J. and Sundberg, L. 238, 261 (1972), Nature (London).

10. R. Narayanaswamy and F. Sevilla III, Anal. Chim. Acta 189, 365 (1986).

11. O. S. Wolfbeis and H. Marhold, Frezenius Z. Anal. Chem. 327, 347 (1987).

12. M. Bacci, F. Baldini, and A. M. Scheggi, Anal. Chim. Acta 207, 343 (1988).

13. F. Baldini, M. Bacci, and S. Bracci, Proc SPIE, Chemical, Biochemical, and enviromental Fiber Sensors II, R. A. Liebermann and M. T. Wlodarczyk, Eds. (SPIE, Bellingham, Washington, 1991), Vol. 1368, p210.

14. O. S. Wolfbeis and F. M. Carlini, Anal. Chim. Acta 160, 301 (1984).

15. E. D. Lee, T. C. Werner, and W. R. Seitz, Anal. Chem. 59, 279 (1987).

16. M. Bacci, F. Baldini, and S. Bracci, Applied Spectroscopy Vol. 45, No. 9, 1991.

17. Hissey, P. H., et al. (1985) J. Immunol. Meth. 78, 211-216.

18. Cook, J. H., et al. (1984) Biochem. 23, 899-904.

19. ImmunoTechnology Catalog & Handbook, 1992 (PIERCE) B14-15.

20. W. Haller, Nature (London) 206, 693 (1965).

21. Suresh K. Bhatia, Lisa C. Shriver-Lake, Kimberly J. Prior, Jacque H. Georger, Jeffrey M. Calvert, Reinhard Bredehorst, and Frances S. Ligler, Analytical Biochemistry 178, 408-413 (1989).

22. Karin M. Rusin, Thomas L. Fare & Joseph Z. Stemple, Biosensors & Bioelectronics 7 (1992) 367-373.

23. P. M. Hardy, A. C. Nicholls, and H. N. Rydon, Chemical Communications, 1969, 565-566.

24. C. R. Graham, D. Leslie & D. J. Squirrell, Biosensors & Bioelectronics 7 (1992) 487-493.

25. Knud-Erik Rasmussen and John Albrechtsen, Histochemistry 38, 19-26 (1974).

26. A. H. Korn, S. H. Feairheller, and E. M. Filachione, J. Mol. Biol. (1972) 65, 525-529.

27. Weetall, H. H. and Filbert (1974), Methods in Enzymology Vol. 34, pp59-72, Porous Glass for Affinity Chromatography Applications, Academic Press, New York.

28. L. Wide, R. Axen, and J. Porath, Immunochem. 4, 381 (1967).

29. L. Wide and J. Porath; Biochim. Biophys. Acta 130, 257 (1967).

7.1. Conclusion and discussion

The results show that the dyes synthesised in this work are solvatochromic, some of them having strong solvatochromism.

For some of the materials, it was proved that solvatochromic property of the compounds would increase with the increase of conjugated chain length.

It was found that the LB films made from some of the dyes synthesised in this work did respond to NO_2, which resulted in a shift in maximum absorption, although the response was small.

However, the response of the LB films made from the conjugated compounds in Chapter 3 to the toxic gases was not as good as expected. Except for the properties of the compounds themselves used, a possible reason is the thickness of the films. It was found that the multimolecular layers collapsed. This is a common problem in LB film preparation at present. The main limitation on the Langmuir-Blodgett technique at the moment is the difficulty of building up thick multilayers of sufficient quality. The thickness of the LB films made in this work might not be enough to produce efficient signal for gas sensing.

A functional NH_2 group was introduced to a series of pyridinium N-phenoxide betaine dyes without destroying their solvatochromic properties.

Several of the pyridinium N-phenoxide betaine dyes synthesised were successfully linked covalently to a solid support, aminopropyl silica sorbent, through two different methods, thiourea linkage and amide linkage.

Reflectance spectra of the immobilised dyes indicated that they still showed good solvatochromism, and their ET values demonstrated a good correlation with the standard ET(30) values, proving that the immobilised dyes could be used as probe for polarity of solvents.

Several methods were used to attempt immobilisation of the pyridinium N-phenoxide betaine dyes onto planar solid supports such as glass and quartz slabs, but without apparent success. The reasons for this might be that the methods used were inadequate, or simply that the surface area of the substrates was too low for efficient detection of bound dye. The flat surfaced slides have much lower surface area than microporous materials such as the silica sorbents. The percentage surface coverage in the sorbent is probably only a few percent. If the percentage coverage on the planar slabs is also low, then the total amount of dye bound to the slabs will be so low that detection would be difficult.

7.2. Future work

The most important step in the future is to improve the properties of the surface of the substrates used for immobilisation in order to increase the amount of dye that can be bound. Other immobilisation methods and other substrates should be used to try to immobilise the dyes synthesised in this work.

An investigation of the LB films should be performed to find the reasons for the collapse of the films.

Finally, more extensive synthetic work on solvatochromic materials should be carried out to find more suitable materials, to modify the betaine dyes described here, to increase their molar absorptivity, and to find better linkage groups for immobilisation.